Durability of Reinforced Concrete Incorporating Recycled Concrete as Aggregate (RCA)

By

Ramtin Movassaghi

A thesis
presented to the University of Waterloo
in fulfilment of the
thesis requirement for the degree of
Master of Applied Science
in
Mechanical Engineering

Waterloo, Ontario, Canada, 2006

I hereby declare that I am the sole author of this thesis. This is a true copy of the thesis, including any required final revisions, as accepted by my examiners.

I understand that my thesis may be made electronically available to the public.

Ramtin Movassaghi

Abstract

The interest in using recycled construction materials is derived from the growth in construction and demolition waste due to rehabilitation and natural and technological disasters. The driving force for recycling concrete is three-fold: preserving natural resources, utilizing the growing waste and saving energy and money. While some waste concrete is currently being crushed and used for grading and base material for highways, it has not been used as the aggregate in new concrete in Canada, largely because of the plentiful supply of good quality virgin material. However, crushed concrete is being used in new concrete in other parts of the world where the local aggregate is inferior, and there is now a push within the Canadian cement and concrete sector to improve the industry sustainability, one aspect of which is recycling of materials.

The research done to date has emphasized the influence of recycled concrete aggregate (RCA) on the workability and strength of the new concrete with little attention being paid to the behaviour in service. In contrast, the present study is focused on the durability of concrete containing RCA in reinforced structures. Since the most common cause of failure of reinforced concrete structures in this part of the world is corrosion of the reinforcement by de-icing salts, the focus of the project is on this aspect of durability. The project involves a comparative study of the durability of three concrete mixtures containing, as coarse aggregate:

1) new clean recycled concrete aggregate (NC-RCA) obtained by crushing the excess concrete returned to the ready mix yard;
2) old de-icing salt contaminated, recycled concrete aggregate (OC-RCA) from a demolished bridge over Highway 401 in Ontario;

3) natural aggregate as a control material.

These three materials were crushed and sieved to give the same grading for each mix. Natural sand was used as fine aggregate. The mixes were adjusted to account for the different water absorption characteristics of the aggregates but were otherwise identical. Prism specimens with a centrally placed reinforcing bar, cylindrical specimens and non-reinforced slabs were cast from each of the concretes. After curing, the reinforced prisms were exposed to a saturated de-icing salt solution for two of every four weeks. For the second two week period, they were allowed to dry in the laboratory atmosphere or, to accelerate the process, dried at 32°C in a low humidity (18%) chamber.

The electrochemical corrosion behaviour of the steel was monitored using linear polarization resistance and cyclic polarization techniques. In addition, the physical properties of the materials were assessed. For the aggregates, water absorption, chloride content and susceptibility to abrasion were determined. For the concretes, compressive strength, salt scaling resistance and chloride permeability were measured and microscopic observation of the interfacial zones between the aggregate and the new cement paste were conducted.

On the basis of the results, it is concluded that the durability and the strength of the RCA concrete is very dependent on the age of the RCA aggregate. Water and chloride permeability, and, salt scaling and reinforcing steel corrosion resistance of concrete made with a very well hardened old RCA were comparable with or better than those of in normal concrete. Concrete incorporating new RCA exhibited inferior properties and consequently, it is recommended that, the OC-RCA concrete can be used as a sustainable material in structural applications.

Acknowledgments

My special thanks to Professor Hansson for her contribution towards my research and thesis. She is an admirable teacher and I have learned from her many things that I will take with me into my future work.

I thank Dr.Corbin and Dr.West for taking the time to review my thesis and providing me with their valuable comments. I acknowledge the financial support by the Development Cement Association of Canada; and The Ontario Research and Challenge fund and the technical assistance of Dufferin concrete division ready mix yard located in Kitchener and Capital Paving Inc.

I appreciate the emotional support that my colleagues gave me for the past two years. I am particularly grateful to Dr. L. Mammoliti for her contributions to my research, Amir Poursaee for taking the time to help me when it was required and Shahzma Jaffar for her support.

I would like to thank the Mechanical and Civil engineering technical staff. I am very grateful for the friendly service and the valuable assistance provided by Fred Bakker, Rob Kaptein, Jorge Cruz in the engineering machine shops and John Potzlold in the student shop. Also, the administrative assistance of the Graduate Studies office and the Mechanical engineering Department, particularly, Marlene Dolson and Jian Zou is very much appreciated.

I would like to thank my friends Dan Cluff, Mohammad Amin Eshraghim, Arash Tajik and Samtin Anousheh for keeping me company and creating an open and enjoyable working environment. My deepest thanks to my family for their constant support, understanding and love they have provided me during the past years.

This thesis is dedicated to

My Mother

and

in loving memory of my father

and

All those who believe in the richness of learning

List of Tables

List of Figures

Chapter 1

Introduction

The wide availability of concrete components, the relatively low level of manufacturing technology, and the variety of applications provided by concrete material have been made concrete as the most commonly used constructional material in the world [1, 2].

The global concrete industry uses approximately 10 billion tonnes of sand and rock annually, which makes it the largest consumer of natural resources in the world [2]. Mining, processing, and transportation of cement-making raw materials and concrete aggregates consume a great deal of energy. Also, cement production alone contributes approximately 5% of global emissions through the combustion of fossil fuels and the decomposition of limestone. It is generally accepted that production of one tonne cement is equal to one tonne of carbon dioxide (CO_2) emission, half of it coming from fuel combustion and the other half from limestone decomposition. Since 6% of global cement production is in North America, the cement and concrete industry is involved in a challenge to reduce the carbon dioxide emission in this part of the world [1].

According to the world commission on environment and development, sustainability means “Meeting the needs of the present without compromising the ability of the future generations to meet their own needs” [3]. A sensible use of natural resources, achieved by the use of waste materials and reduced natural aggregate extraction, and a lower environmental impact, achieved through reduced carbon emission, represent two main activities aimed at meeting the requirements of sustainable concrete construction development [3].

Recycled construction materials derived from construction and demolition waste, rehabilitation, natural and technological disasters are an example of construction material in harmony with this concept. Equals 10% of the global sand and rock consumption is the

amount of construction and demolition waste generated each year that about half of the waste has potential for recycling [2,4].

The search for alternative resources instead of existing natural resources, the continuing shortage of landfill sites due to rapid urbanization, the sharp increase in transportation and disposal costs and severe environmental pollution and regulation control have raised a new challenge to planners and engineers to recycle construction and demolition waste (C&D) material [2, 3, 4, and 12]. Table1-1, gives a rough estimation of construction and demolition (C&D) waste generated in countries using the most percentage of recycled concrete as aggregates (RCA) [2, 4, 17, 20, 34, and 52].

Table 1-1, Global consumption of construction and demolition wastes as aggregates.

Country	C & D waste (million tonnes/ year)	Percentage of C&D waste Recycling,%	Recycled concrete (million tonnes/year)
United State	650	20-30	150
Europe	200	28	50
Japan	85	85	35
Hong Kong	14	50	3.5
Canada	11	21	2.3
Australia	3	50	1.5

The table indicates that in countries which are suffering from a lack of natural resources and landfills, such as Japan and Hong Kong, the percentage of construction and demolition waste recycling is high (about 85% and 50%). While, in countries that possess a plentiful supply of high-quality natural sands and rocks, such as Canada, recycled waste construction materials are mostly used for grading and backfill materials for highways and pavements. However, using recycled crushed concrete as aggregate in

new concrete structures can improve the sustainability of the concrete industry in which recycling of material is counted as one of the most effective factors.

In order to promote the application of recycled aggregate to concrete structures, it is necessary to provide a suitable balance between quality, cost-effectiveness and environmental impact [5]. From the view point of life-cycle assessment (LCA), the cost of recycled concrete as aggregate would be more efficient if its quality is competitive with that of natural aggregates while improves the environmental conditions [6]. Figure 1-1, shows the required optimum balance between the demand quality, cost effectiveness and environmental impact of recycling concrete as aggregates [5].

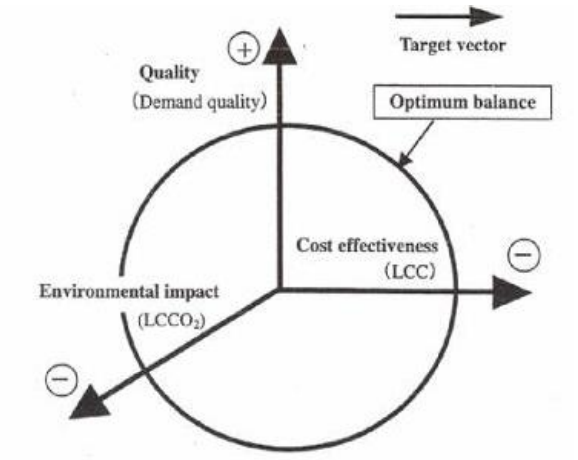

Figure 1-1, Evaluation of demolished and waste concrete recycling [5].

The objective of this experimental work is to study the durability of reinforced concrete made with old, contaminated and new, clean recycled aggregate. For this purpose, a comparative study has been made of the physical and mechanical properties of RCA and of hardened concrete incorporating RCA. The tests include porosity, water absorption, chloride permeability, abrasion resistance, salt scaling resistance, reinforcement corrosion and compressive strength.

Chapter 2

Literature Review

2.1- Production of recycled concrete as aggregates (RCA)

RCA concrete is concrete made with crushed RCA used as partial or full replacement of conventional coarse or fine aggregate in new concrete. Since RCA come from different sources and occupies around 75% of the volume of concrete, it is necessary to maintain the high quality of aggregate during the entire course of recycling system. This requires a preliminary survey prior to demolition along with advanced processing techniques using special facilities to control the quality of recycled aggregate [1, 4, and 5].

Recycled aggregate refining and replacing methods are two recycling methods which are currently being used for production of aggregate from demolished concrete [1, 5]. Aggregate refining method is a closed-loop concrete recycling system in which the adhered cement in RCA is made fragile by a thermal treatment to about 300˚ C and is removed selectively from original aggregate by rubbing crushed concrete. The retained coarse and fine aggregates can be applied to concrete mix. The by-product powder, which has a large specific surface area, can be used as clinker raw material, cement production and deep or shallow ground improvement as a partial substitute for cement. Figure 2-1, shows the schematic diagram of the close-loop concrete recycling system [1].

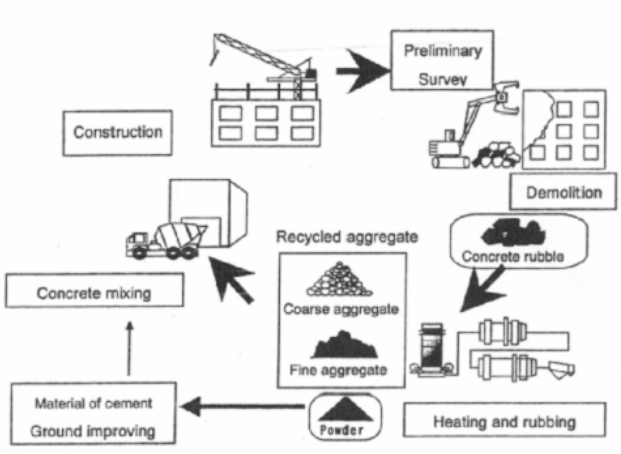

Figure 2-1, Closed-loop concrete system [1].

It is believed that this method provides the highest quality control throughout the process, from aggregate production to concrete placement, while the original coarse aggregate does not lose its integrity and has equivalent quality to natural coarse aggregate. The literature reviewer believes that although removing the hardened porous adhered mortar by further processing of crushing can contribute to improve the strength of recycled concrete, defects in original aggregates, in the form of cracks and voids could be considered as a destructive mechanical effect as well.

Refining method would contribute to preserve natural resources and to decrease carbon dioxide emissions of cement production. However, it needs more energy and advanced facilities to remove the original cement and reuse of recycled fine aggregate and fine powder by-products [5].

For this reason, the aggregate replacing method, which does not remove the original mortar, is more effective. In this manufacturing process, the demolished original concrete undergoes crushing with a jaw crusher and foreign materials such as steel reinforcement are separated magnetically. The aggregate with larger size than 20 mm goes through secondary crushing with an impact crusher and after impurity removal by human power, coarse and fine recycled aggregates are separated based on the their sizes. The ratio of original coarse aggregate replacement by recycled coarse aggregate is determined by relative quality value method according to the desired construction specifications. The remaining fine recycled aggregates can be used for manufacturing of precast concrete products. The advantages of this system are simple manufacturing process with mobile and general-purpose facilities. Figure 2-2, shows a schematic of recycling system for aggregate replacing method [5].

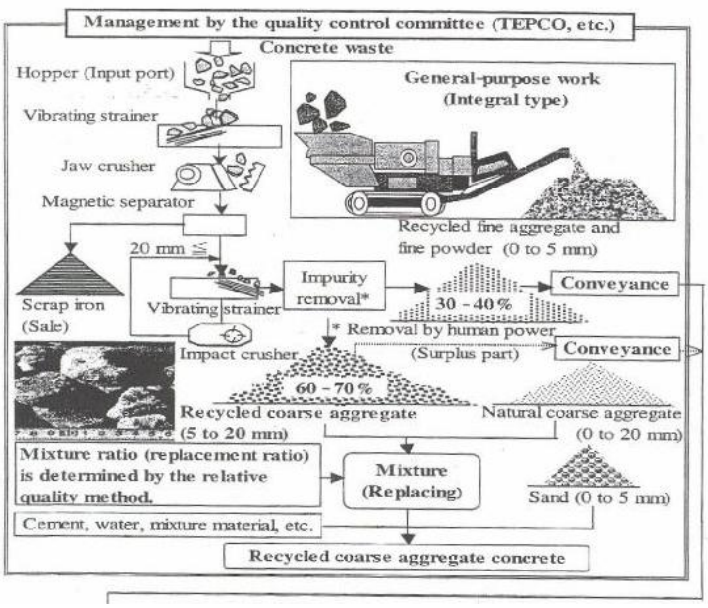

Figure 2-2, Aggregate replacing method [5].

2.2- Effect of physical properties of recycled aggregate on fresh concrete

In Portland cement concrete, 60% to 75% of the concrete volume and 70 – 85% of the mass is made up of aggregates. The most important feature of RCA concrete is the presence of adhered mortar in RCA. Due to the higher porous nature of adhered mortar, the physical and mechanical properties of RCA and concrete made with this aggregate are significantly different from ordinary concrete. For instance, the workability of fresh concrete decreases with increase in the surface area of recycled aggregate. In turn, the surface area is influenced by grading, shape, texture and maximum size of the recycled aggregate [7, 8]. Therefore, for the successful use of RCA in fresh concrete production, the properties of RCA must be accurately determined.

2.2.1- Grading and size of recycled aggregate

Grading of recycled aggregates can influence the mix proportioning, workability, porosity, durability and strength of concrete.Gradation of recycled aggregates is

determined from sieve analysis in which the aggregates are passed through a series of superimposed wire-mesh sieves with square opening arranged in decreasing sizes. The maximum size of coarse aggregate is defined as the smallest sieve opening through which the entire particular aggregate passes.

In practice it is common to use a nominal maximum size, which is the smallest sieve opening that most (not all) of the aggregate pass through [8, 9, and 10]. The choice of the nominal maximum size of an aggregate used in reinforce concrete depends on the size and shape of the concrete member and the amount and distribution of reinforcing steel. The ASTM and CSA standards limit the maximum size of coarse aggregate for different applications. For example, in reinforced concrete, the maximum aggregate size should not exceed three-fourths of the minimum clear distance between the bars or one-half of the specified cover depth for concrete exposed to chlorides [9].

A particle-size distribution curve is obtained by plotting the logarithm of the sieve opening size on the x-axis, and the percentage of particle, by weight, coarser than or finer than the particular sieve on the y-axis. A linear shape (dense) of curve shows a good gradation recommended by the standard. A horizontal or vertical shift away from the linear shape shows missing or using more a percentage of one size.

In Gap-graded aggregate one or more aggregate sizes are intentionally missing. The small aggregates, which can block the voids between the larger aggregates, are omitted in open-graded aggregates. In a one-sized distribution, the large part of aggregates is made up of the same size and causes a vertical drop in the curve. In Figure 2-3, typical aggregate grain size distribution curves are illustrated [10].

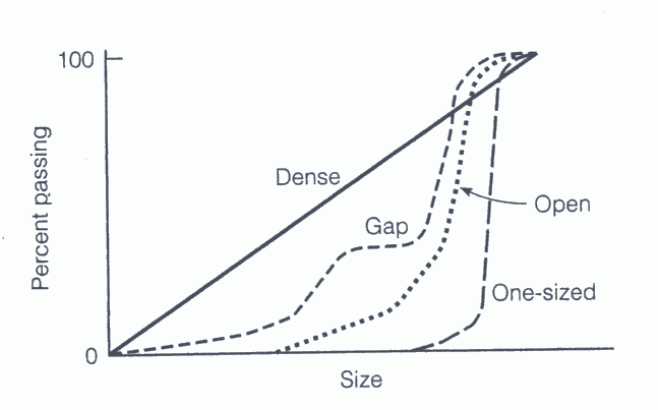

Figure 2-3, Types of particle-size distribution curves [10].

The specific gravity and water absorption of recycled aggregate varies with the size, the age, the strength and the cement content of adhered mortar. The specific gravity decreases progressively as particle size decreases. The smaller the size of RCA, the higher values of adhered mortar .As a result, a wrong choice of the fine recycled aggregate percentage can lead to segregation or higher water demand of concrete mixture due to the high porosity of adhered mortar [11, 12]. Therefore, replacement of fine aggregates with recycled concrete results in higher water absorption and water-cement ratio of concrete than for natural fine aggregate. Consequently, assessment to an optimal mixture with the highest amount of coarse aggregate and the lowest fine recycled aggregate content is the final goal of mixture design. The mix of coarse RCA and natural sand provides an intermediate to high performance of RCA concrete in compare to concrete incorporating natural aggregates [7].

2.2.2- Particle shape and surface texture of recycled aggregate

Crushing demolished concrete produces angular particles with a rough surface texture. Thus, RCA has a larger surface area than round natural aggregate and may provide better interlock and adhesion to cement paste [10].

In terms of workability of fresh concrete during mixing and placing, the inter-particle friction in concrete incorporating RCA might more increase than that of in concrete made with rounded natural aggregate. Also, in addition to high porosity, the angular shape of RCA increases the void content between aggregate particles. So, the fresh concrete mix incorporating recycled concrete as aggregate may require more water and cementitous material than those of normal fresh concrete mix to produce a workable concrete [7, 8, and13].

2.2.3- Bulk Specific gravity and bulk density of recycled aggregate

In comparison to natural aggregates, a recycled concrete aggregate has higher water absorption and a lower specific gravity due to adhered mortar content. Since recycled aggregate are porous, the volume of pores should be considered in the measurement of total volume.

The bulk specific gravity of RCA is an essential parameter for concrete mix design because it is representative of the unit volume of aggregate containing both permeable and impermeable pores. The fresh unit weight and the workability of concrete decrease with increasing the amount of RCA [7]. According to the report made by cement association of Japan [14], the density of the coarse recycled concrete is between 2120 kg/m^3 and 2430 kg/m^3 while the density of the recycled concrete made with fine recycled aggregate is between 1970 kg/m^3 and 2140 kg/m^3 . As the proportion of recycled concrete aggregate increases, the density and unit weight decrease in the hardened concrete. Through the research performed by Topcu et al. [15], it was observed that, the unit weight of concrete incorporating 50% of waste concrete as aggregate was higher

(2301 kg/m^3) than the one for concrete made with whole waste concrete aggregate which was 2251 kg/m^3 .

2.2.4- Porosity and water absorption of recycled concrete aggregate

Higher volume of porosity in adhered mortar of RCA makes it more susceptible to absorb water than natural aggregate. The mix design of RCA concrete is carried out based on water-cement ratio and considering the higher water absorption of RCA. Hence, it is necessary to increase the proportion of water to compensate the high water absorption of recycled aggregate. Although the workability of concrete mixture can be improved in this way, the increase in the water content enhances the volume of capillary pores and the permeability and reduces the compressive strength of hardened concrete [16, 17, 18, 19, and 20].

The amount of water absorbed by aggregate pores does not participate in the cement hydration and, therefore, does not contribute to the workability of the fresh concrete mix. The potential of water absorption and adsorption for recycled coarse (16-32 mm maximum nominal size) is typically lower than recycled fine (4-8mm maximum nominal size) aggregates [13]. Degree of RCA fineness and its effect on decreasing the workability is another aspect that should be considered. Greater surface area and higher water absorption of the fine fraction of RCA provide more potential for higher water demand leading to decreasing the workability. Mukai [21], determined that using RCA concrete made with coarse RCA and natural sand had less slump value (10%) than that of in concrete using both coarse and fine RCA concrete.

Through one effort made with Lin et al. [22], for obtaining an optimal mixture for recycled concrete, the following results were achieved. When water-cement ratio was 0.5

and volume percentage consisted of dried coarse RCA of 42% and 100% natural sand, the concrete had slump of 180mm and 30.17 MPa compressive strength at 28 days

Limbachia [23], found a reduction in workability of the concrete with increase in RCA proportion beyond 30% in the mix, although the slump remained within the allowable tolerance of 25 mm. The mixes with high proportions of RCA were found to be less consolidated and displayed slight bleeding. Using a mineral admixture such as fly ash as filler material in mix made a significant improvement of the workability, consolidation and reducing the bleeding properties [23]. ACI 555-01 report lists an appropriate guideline for mixture proportioning of recycled concrete aggregates [16].

2.2.5- Abrasion resistance of recycled aggregate

The resistance of aggregates to degradation caused by loads, stockpiling, mixing, placing and compacting of fresh mixed concrete is defined as abrasion resistance [10]. Any literature about abrasion resistance of RCA could not find. However, recycled concrete as aggregate has lower strength compared to natural aggregate due to the presence of weak mortar adhered to the aggregate particles. Accordingly, the assessment of abrasion loss in mass of recycled aggregate indicates general characteristic of its quality particularly when it is subjected to wear or impact during the mixing or after concrete placement.

The mechanical wearing of recycled aggregate surface caused by friction during mixing can increase the presence of silt on the surface of aggregate. This, in turn, can lower the bond characteristics, increase the water demand of concrete mix and increase scaling off the concrete during the finishing. The Los Angeles [24] and Micro-Deval [25, 26, and 27] abrasion tests evaluate the toughness and abrasion resistance of aggregates.

2.3- Properties of hardened RCA concrete

Properties of concrete made with recycled aggregates can be defined depends on the performance requirements and property specifications. For instance, the waste concrete applied for grading and base material for road and highway pavement should possess little movement under the load impacts, while the recycled concrete used for a highway bridge should contain appropriate strength, sufficient rigidity and adequate durability.

Research indicates that recycled concrete may present some benefits such as comparable physical and mechanical properties with normal concrete [6, 11, 22, 38, 39, and 41]. However, the behaviour in service of recycled concrete is still not very well understood because of limited and contradictory obtained results [14, 15, 32, 36, 43, 44, and 47]. To evaluate the performance of reinforced recycled concrete structure for a particular application, the properties of hardened recycled concrete need to be studied individually.

2.3.1- Porosity and its effect on permeability of RCA concrete

Concrete incorporating recycled concrete as aggregate can be considered to be more porous concrete with lower general strength, and two to five times more permeable (depending on water-cement ratio) than those of in normal concrete. Permeability is a significant factor that has a major effect in the durability of hardened concrete. A permeable concrete allows water and aggressive agents such as chloride ions to penetrate into concrete and, in turn, decreases the resistance of concrete structure to freezing and thawing, chemical aggregate reactivity and corrosion of reinforcing steel. Therefore, evaluating of water absorption of concrete is the first essential step to study the durability of concrete made with recycled aggregate.

Characteristically, entrained air voids in cement paste and pores in natural aggregate are not interconnected and, therefore, do not affect permeability. However, the capillary pores that influence on permeability of hardened concrete are resulting from evaporation of excess mixing water which is not used for hydration of cement. As a result, increasing the water-cement ratio near the surface of concrete can strongly increase distribution, size and interconnection between the capillary pores which, in turn, has influence on permeability of hardened concrete [28].

2.3.1.1- Permeability improvement of RCA concrete

In addition to preserving the quality of recycled aggregates (namely cohesive mortar) and the water-cement ratio at the desired level, curing conditions and using mineral admixtures have a significant impact on permeability of the recycled concrete [29, 30, 31, 32, 33, and 34].

The rate of hydration in freshly mix concrete is rapid immediately after placing and finishing but continues slowly for an indefinite period of time. Disproportionate loss of water by evaporation at the surface of concrete can delay or prevent early hydration. If loss of water from evaporation is not compensated by moist curing, concrete shrinks and the internal tensile stresses caused by drying shrinkage can result in surface cracking and increasing the air and water flow content of concrete [24]. There is one investigation [29], which studied the effects of various curing conditions of cylindrical samples made with six types of concrete:

Three types of recycled aggregate concrete (RAC1, RAC2 and RAC3), one type of concrete mixed of coarse recycled and fine natural aggregate concrete (MAC), and two types of normal concrete (NAC1 and NAC2) made with ordinary aggregates.

Different curing methods were considered as short (1 day in the mould), extended (3 days in the mould), favorable (28 days in the mould), and water curing (1 day in the mould followed by 27 days in water at 20°C). A non-destructive and easy surface permeability test method (Figure 2-4) was performed to evaluate the effects of curing and mix design.

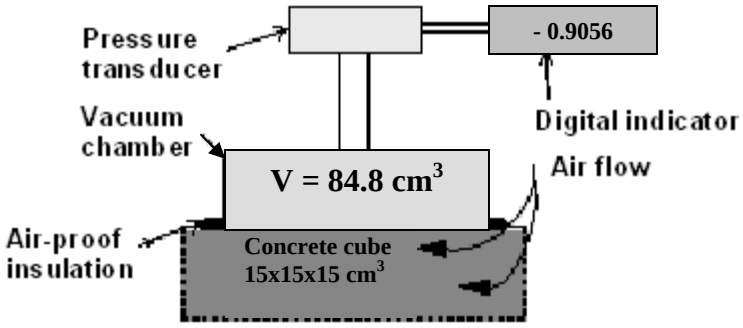

Figure 2-4, Surface permeability test, experimental arrangement [29].

In this test, applying an initiated vacuum (P_{ini} = -1.0 bar), created in a chamber, induces a pressure gradient that forces airflow through the concrete with a specific rate and time (t). Response time (T), the time to re-establish the atmospheric pressure (P) in the chamber, is used as a permeability-measuring factor. This time obeys this equation (2-1):

$$T = - t / \ln (P/P_{ini}) \quad (2\text{-}1)$$

The shorter response time indicates greater permeability of concrete. Also the relation between surface permeability and water-cement ratio is defined by equation (2-2), while T is response time and a, b are the experimental parameters:

$$T = b (W/C)^{a} \quad (2\text{-}2)$$

Since the response time is well correlated with physical properties such as density and porosity (Figures 2-5 and 2-6), the surface permeability can be used as an aggregate

replacement indicator and correlated with water sorptivity and carbon dioxide diffusivity which directly can affect durability of recycled concrete (Figures 2-7 and 2-8).

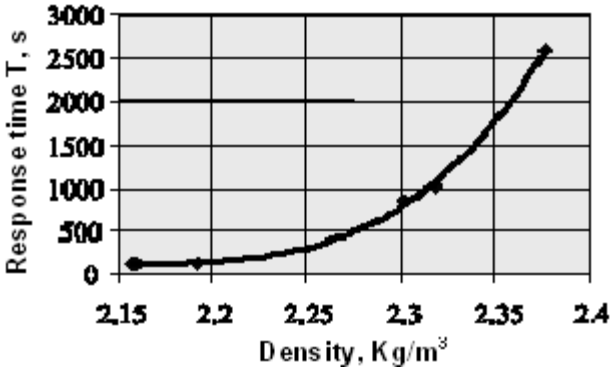

Figure 2-5, Relationship between surface permeability and density of concrete [29].

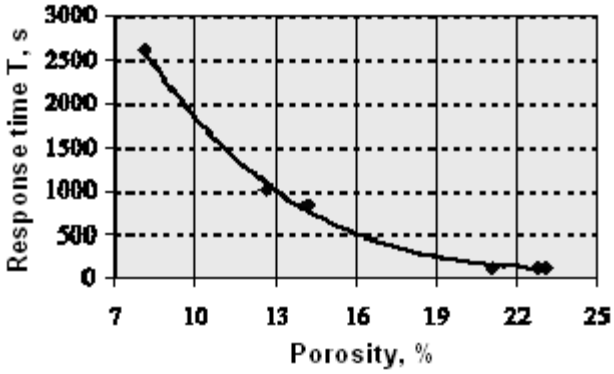

Figure 2-6, Relationship between surface permeability and porosity of concrete [29].

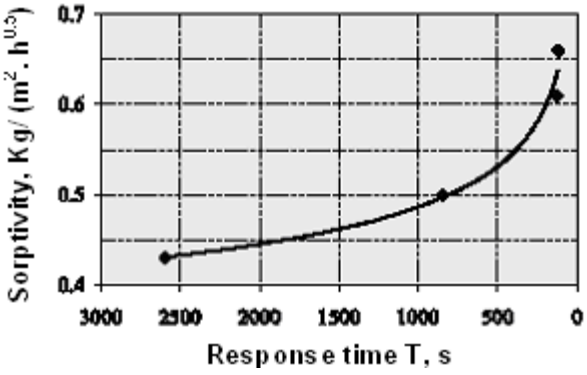

Figure 2-7, Relationship between surface permeability and water sorptivity [29].

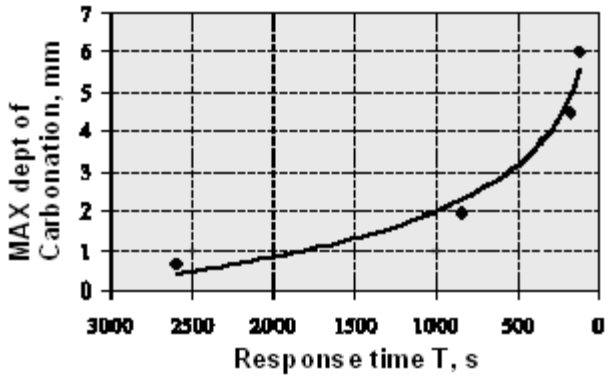

Figure 2-8, Relationship between surface permeability and carbonation [29].

The study indicated that, the permeability of recycled concrete depends more on aggregate mix proportions and curing conditions than other physical parameters. RAC types were more permeable than normal concrete types (NAC), while replacing only coarse aggregate (not fine aggregate) with recycled concrete aggregate resulted in producing a concrete with higher permeability. Also, increasing the water curing time to 28 days and maintaining the concrete water-cement ratio at lower level produced a concrete with lower porosity volume and surface permeability, compared to the other methods of curing. Figure 2-9, shows the effect of coarse recycled aggregate replacement with natural aggregates and extending the curing time at the moist environment on surface permeability of different concretes.

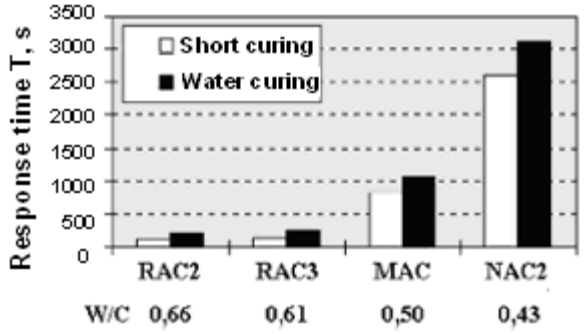

Figure 2-9, Surface permeability in accordance to the type of curing [29].

Another study achieved by Levy et al. [30] was showed that, permeability aspects of recycled concrete could be affected by the cement composition and mineralogy of aggregates. Since RCA contains adhered mortar, a higher cement content in the mixture is required to obtain an appropriate strength and durability level of concrete. This, results in higher alkaline reserve of concrete, in turn, the concrete surface can be protected properly from the oxygen diffusion and carbonation attack [30].

Adding a mineral admixture is another way to improve permeability. Moriconi [31], believed that adding fly ash at the high volume, could contribute to a reduction of chloride ion and carbon dioxide penetration into concrete made with recycled concrete aggregates. He considered four different types of mixtures to compare the effects of fly ash on durability of RCA concrete which completely made by coarse and fine RCA: natural aggregate with w/c = 0.6 (NAT-0.6), recycled aggregate with w/c=0.3 (REC-0.3), recycled aggregate with water reducer admixture at a dosage of 1.0% by weight of cement and w/c=0.3 (REC-WRA-0.3) and RCA with namely w/c = 0.6 (REC-FA-0.6) in which a high amount of fly ash (as much as cement) was replaced to the fine aggregate fraction to remain the value of water-cement ratio at 0.3 .

After demoulding the cubic concrete specimens at one day and exposing to air, a linear relationship (equation 2- 3) was found between the carbonation depth (X, in mm) and square root of time (t, in days) for all concretes.

$$X = k \cdot t^{1/2} \qquad (2\text{-}3)$$

Comparison of NAT-0.6 and REC-FA-0.6 shows that the carbonation depth is reduced by adding more fly ash to the mixture in recycled concrete (Figure 2-10).

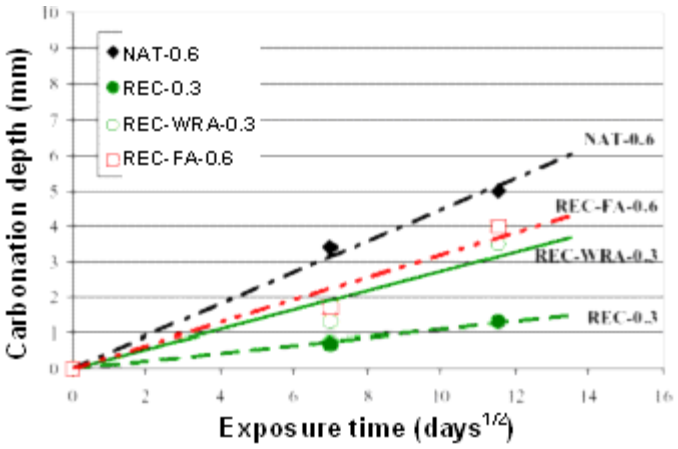

Figure 2-10, Carbonation depth as a function of the time of exposure to air [31].

After 1 year exposing the specimens (cured for one week wet and three weeks in air) to a 10% NaCl aqueous solution, chloride penetration was measured and results in Table 2 -1 were obtained [31].

Table 2-1, Diffusion coefficient of chloride ions into different concretes [31].

Mixture	NAT-0.6	REC-0.3	REC-WRA-0.3	REC-FA-0.6
D($cm^2 . s^{-1}. 10^{-8}$)	1.90	0.87	0.72	0.46

By comparing the diffusion coefficient of chloride ions in REC-0.3 and REC-FA-0.6, the significant improvement effect of adding fly ash to the mixture can be observed (Figure2-11) [31].

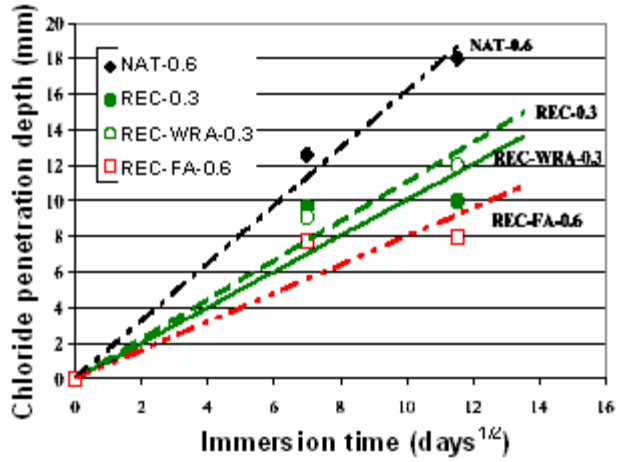

Figure 2-11, Chloride penetration as a function of exposure time to 10% NaCl [31].

According to these results, RCA concrete can provide better carbonation and chloride penetration resistance if the water-cement ratio is remained at the low level by simultaneously adding the fly ash to the mixture as much as cement [31]. Fly ash, through the pozzolanic reaction, reduces the amount of calcium hydroxide which can react with carbon dioxide in the paste [28].

In addition, the effects of adding admixtures in the forms of blast furnace slag and fly ash as a replacement for cement [32, 33], and silica fume, in the form of slurry coated on the RCA [34], on performance of concrete made with RCA have been investigated. All of them have showed excellent results on improvement of water and air permeability.

2.3.2- Mechanical properties of RCA concrete

It has been demonstrated that replacement of natural aggregates with RCA which has lower strength than that of natural aggregate causes a reduction in mechanical properties such as compressive, tensile and flexural strengths of RCA concrete. In table 2-2 the mechanical properties of concrete made with recycled concrete aggregate (RCA) and natural aggregates are compared [35].

Table 2-2, Concrete relative properties made with natural and RCA [35].

Concrete property	RCA concrete compared to natural aggregate concrete
Slump control	Higher water demand in RCA
Flexural strength	RCA comparable to NAC
Compressive strength at equal w/c	Less than 90% of NAC
Strength development to 7 days	RCA comparable with NAC
Modulus of elasticity	RCA generally lower than NAC
Drying shrinkage	RCA generally higher than NAC
Expansion	TCA comparable with NAC

Of the major mechanical properties, the compressive strength is considered as the most significant property because reinforced concrete structures are mostly required to bear against compressive loads and the other strength properties of concrete constructions are dependent to compressive strength [24].

Basically, a number of studies have evaluated the strengths of concrete with RCA and most of researchers believe that the compressive strength of concrete is lower than that of concrete with natural aggregate [8, 12, 16, 36, 37, and 38].

2.3.2.1- Effect of mix proportion on strength of RCA concrete

Hansen et al. [36] found that the compressive strength of RCA concrete can be reduced from 5 to 24% in comparison with ordinary concrete. However, it can be increased to the same or even higher level than in normal concrete if the water-cement ratio of the RCA concrete remains at the lower or constant level of that in normal concrete [13].

Topcu [14], performed compressive tests on cylindrical samples at 7 and 28 days age with water-cement ratio of 0.6.The results showed an inverse relationship between concrete compressive strength and using waste concrete as aggregate (Figure 2-12).

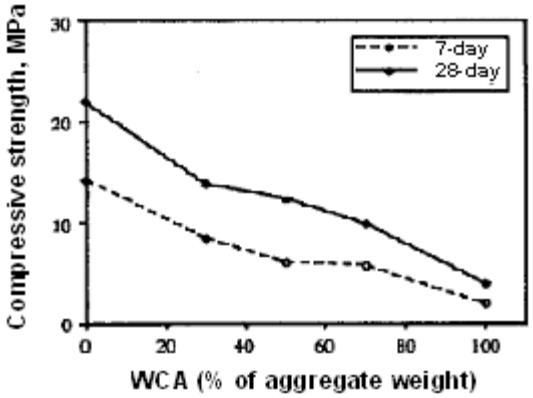

Figure 2-12, Changes in compressive strength with the amount of WCA [14].

However, the compressive strength of recycled concrete could reach to 85-95% of normal concrete if it is produced with coarse recycled and fine natural aggregates [14, 15].

Partially replacement of up to 20% natural coarse aggregate with RCA did not have any influence on the compressive strength reduction of concrete cube samples which Limbachia investigated, while there was a gradual reduction in strength with increasing the recycled concrete aggregate content [23].

2.3.2.2- Effect of crushing age on strength of RCA concrete

The shorter time gap between crushing a recent cast concrete (1 to 3 days) and using crushed aggregates in new concrete, can improve the strength of concrete due to the additional hydration of the old cement in new RCA concrete [39, 40]. The concrete products which are rejected or returned from the manufacturing process may contain some unhydrated cement. The partially hydrated waste concrete aggregate could influence on the properties (such as strength) of the new concrete made with it. A very well hydrated cement paste with a finer pore structure is stronger than an unhydrated paste containing coarser pore structure. But in spite of RCA strength, the cementing potential of the unhydrated cement remaining in the recycled concrete aggregates might improve the strength of new concrete as well. According to the results of Katz [40], the 3-days crushed cast concrete used as RCA was combined the advantages of both strength and cementing capability which could produce a stronger RCA concrete compared to the concretes made with crushed recycled concrete aggregates at age 1 or 28 days .

2.3.2.3- Effect of RCA porosity on strength of RCA concrete

Using mercury intrusion porosimetry (MIP), it has been demonstrated that, physical properties such as absorption and permeability of concrete made with RCA, have a linear

correlation with total porosity while mechanical properties were better fitted with quadratic-type equations (Table 2-3) [17].

Table 2-3, Correlation between total porosity and other properties of the RCA [17].

Property	Equation[a]	R^2
Absorption (%)	$y = 0.3501x + 4.0460$	0.7641
Porosity to water(%)	$y = 0.571x + 11.036$	0.7000
D_s (t/m^3)	$y = -0.0165 x + 2.3514$	0.7267
D_{sss} (t/m^3)	$y = -0.0191 x + 2.5836$	0.7745
Permeability (cm) average	$y = 0.1564 x – 1.3955$	0.7652
Permeability (cm) maximum	$y = 1.0006 x – 1.3819$	0.6076
f_t (MPa)	$y = 0.0185 x^2 – 0.6527 x + 8.9077$	0.5727
f_c (MPa)	$y = 0.3744 x^2 – 12.906 x + 141.05$	0.7350
E (GPA)	$y = 0.1984 x^2 – 6.395 x + 77.316$	0.6510
$\varepsilon_{xh\ drying}$ (mm/m)	$y = 2 E^{-0.8} z^2 – 9E^{-0.5} + 0.4607$	0.8367
φ ($90_{\ days}$, t_0)	$y = -3 E^{-0.7} z^2 + 0.0019 z + 1.0833$	0.9347

The quadratic equation shows that other factors such as the interfacial transition zone and variations in pore size distribution could affect the mechanical properties of RCA concrete. Another (MIP) test was done to compare the influence of different aggregates derived from normal strength concrete (NC), high performance concrete (HPC) and normal concrete with natural aggregates (NA), on the strength of new concrete cured for 28 days . The correlation between mercury intrusion and pore size of these three concretes is shown in Figure 2-13 [20].

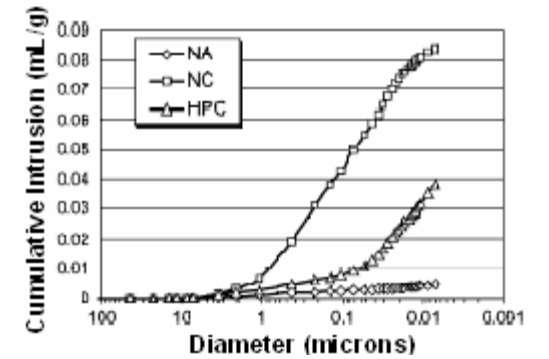

Figure 2-13, Cumulative pore distribution curves of normal and RCA concrete [20].

These data indicate that, RCA concrete incorporating recycled normal strength aggregates has higher porosity and lower strength than normal concrete due to the presence of more adhered mortar content. It can be assumed that, less distribution of pores in concrete made with recycled HPC as aggregate is due to the presence of less capillary pores or mineral admixtures in RCA which has already improved the new and old interfacial transition zone (ITZ) [20].

Also, according to another study on the mechanical properties of HPC made from moderate or high strength (40-70 MPa) recycled concrete as aggregate, better results were achieved on compressive (over 80 MPa using RCA from normal concrete about 60 MPa) and tensile(about 10% higher than that of normal concrete) strengths. Higher shrinkage and slightly lower creep than that of in concrete made with normal strength recycled aggregates were reported as well [41].

2.3.2.4- Effect of interfacial transition zone (ITZ) on strength of RCA concrete

In ordinary fresh concrete, due to the presence of a water film on the aggregates, an interface zone is created between aggregate and cement paste at which the water-cement ratio is twice of that in the cement paste [20]. This issue makes interfacial transition zone becomes the weakest link of the chain by increasing the crack tendency. With increased cement hydration, the interface is filled up with hydrated cement.

In RCA concrete there are two different interfacial zones (ITZ) instead of one in normal concrete: an old ITZ between the original aggregate and adhered mortar and another new ITZ between the recycled aggregate and new cement paste. Figure 2-14 shows a schematic diagram of interfacial transition zones present in concrete made with concrete recycled aggregate [18].

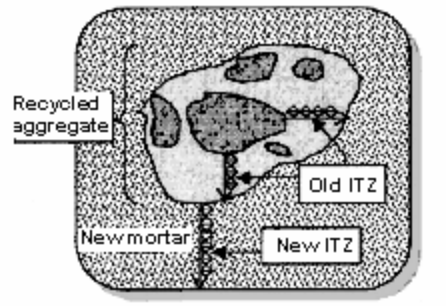

Figure 2-14, The Interfacial Zones (ITZ) in the RCA concrete [18].

The observation of microstructure of ITZ [22], showed a relatively cracked, loose and porous interface (Figure 2-15).

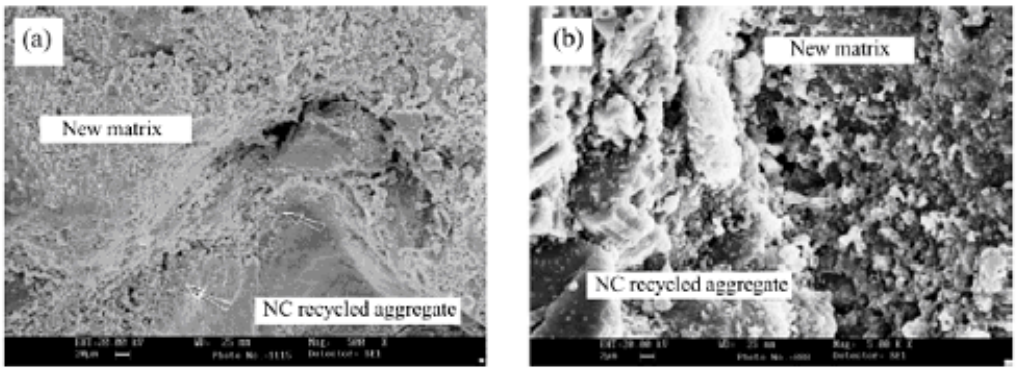

Figure 2-15, Microstructure of concrete prepared with normal concrete RCA [20].

Large amounts of crystallized Ca $(OH)_2$, are responsible for creating the porosity in ITZ, in addition, some whisker-like ettringite crystals and a small granular C-S-H hydrates were seen at the interface of recycled aggregate and new cement paste. This may be due to higher water absorption of adhered porous mortar in the RCA which taking up more water on initial mixing and consequently, loosing the interfacial zone by continuing the hydration [20]. Vickers hardness test was used to measure the micro hardness of the distance from 10-50 micrometers on old and new interfacial transition zones [42].Vickers hardness in ITZ was increased as the water-cement ratio of the concrete was decreased. The compressive and tensile strength of recycled concrete at higher water-cement ratio (0.55) was the same at both interfacial zones and it was not affected by quality of

recycled concrete aggregate. But, at lower water-cement ratio (0.25), the strength of concrete was governed by old ITZ and quality of recycled aggregate played an important role. Figures 2-16 and 2-17 show the relation between Vickers hardness and compressive and tensile strength of recycled concrete [42].

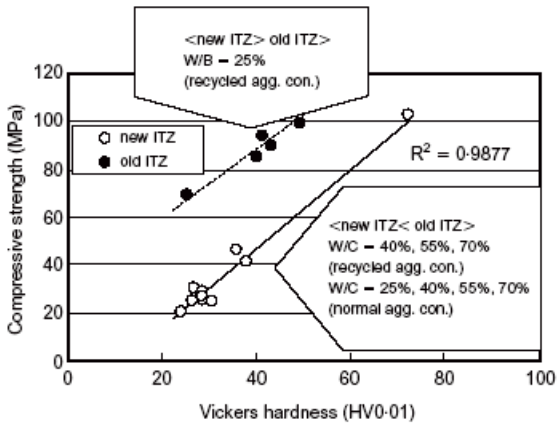

Figure 2-16, Relationship between compressive strength and Vickers hardness [42].

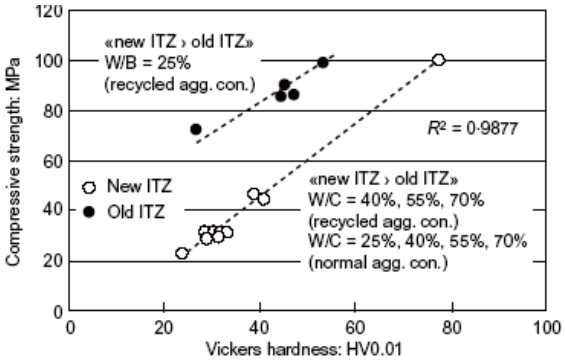

Figure 2-17, Tensile strength and Vickers hardness correlation [42].

2.3.2.5- Effect of curing on the strength of RCA concrete

RCA concrete properties is as sensitive to setting characteristics and initial strength gain (kinetics aspects of cement hydration) as normal concrete .Thus, the correlation between compressive strength and curing time in recycled concrete and normal concrete are similar. Figure 2-18, shows the strength development of RCA and normal concrete with curing time [35].

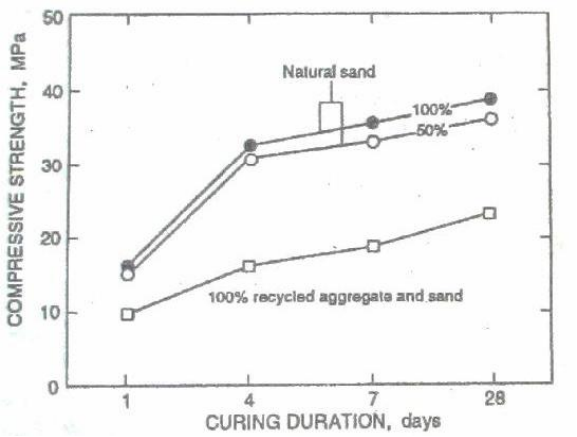

Figure 2-18, Strength development curves of RCA and ordinary concrete [35].

Since the total amount of adhered cement (hydrated and unhydrated) is generally higher in fine than coarse recycled aggregate, the porosity and strength of fine recycled aggregate is more influenced by hydration of adhered cement paste than coarse recycled aggregate. From the other hand, sharp development of compressive strength with curing time at early age is greater for recycled coarse aggregate than for fine ones. The positive effect of appropriate hydration of coarse RCA is due to an improvement in bonding between aggregate and mortar. However, the presence of micro cracks at the interface between aggregate and cement paste, stops the increasing trend of compressive strength at later age, regardless of whether air or water curing is used (Figure 2-19) [43,44].

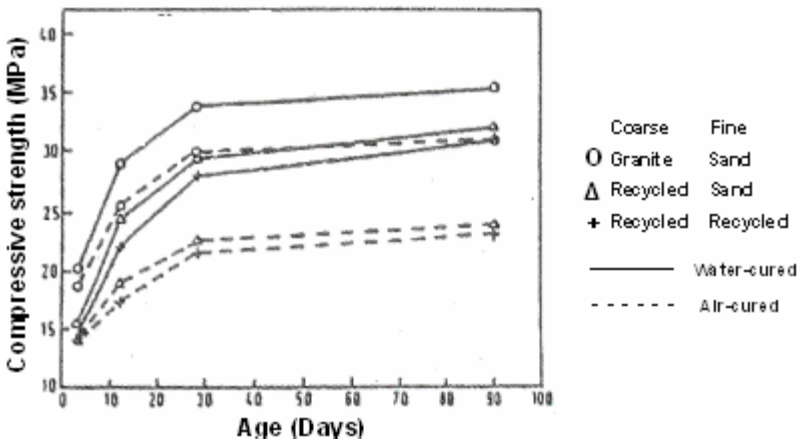

Figure 2-19, Compressive strength of RCA concrete as a function of curing age [44].

2.3.2.6- The effect of mineral admixtures on the strength of RCA concrete

Mineral admixtures or pozzolans react with calcium hydroxide of concrete to form calcium silicate hydrate (C-S-H) which results a cement paste with lower permeability and higher strength. Although the pozzolanic reaction is much slower than the initial cemetitious reaction, using RCA, which may contain unhydrated cement and excess amount of calcium hydroxide, may accelerate the strength development of RCA concrete made with pozzolon at early ages. As a result, the ultimate strength of concrete will be greater than that of RCA concrete made without mineral admixtures.

Some researchers have studied the influence of using fly ash as partial replacement of cement or fine recycled aggregate and all have found a significant improvement of strength and permeability of recycled concrete [12, 31, 32, 33, and 45].

Katz [46], indicated that the RCA surface treatment by impregnation silica fume solution (10 wt%) can result in improving the ITZ between new and old cement paste and the compressive strength of RCA concrete up to 15% at 28 days age. Adding fly ash by 30% weight of cement were compared to using double mixing method and results (Table 2-4) show almost the same improvement in strength recycled concrete [18, 30].

Table 2-4, Test results of various improvement methods [18].

	Type of method		
Properties	Control	DM	FA
Compressive strength (MPa)	31.5	36.2 (17% ↑)	34.0 (8% ↑)
Tensile strength (MPa)	2.3	2.9 (26% ↑)	2.7 (17% ↑)
Vickers hardness (HV0.01)	31	38 (23% ↑)	31 (0%)
Thickness of ITZ (μm)	39	24 (38% ↓)	32 (18% ↓)
Chloride penetration depth (mm)	11.7	8.6 (26% ↓)	9.2 (21% ↓)

2.3.2.7- The effect of ITZ improvement on RCA concrete strength

To improve the characteristics of interfacial transition zone, various researchers have recommended different methods. Nagataki et al. [47], believe that strength improvement of RCA concrete can be achieved by removing the porous adhered mortar through more crushing steps which contribute to reduce the stress concentration at ITZ which has less.

Using a Double Mixing (DM) method is one solution to improve the new ITZ, particularly when the water-cement ratio is higher than 0.5. Figure 2-20, compares the procedure of mixing by using normal and double mixing method [18, 48, and 49].

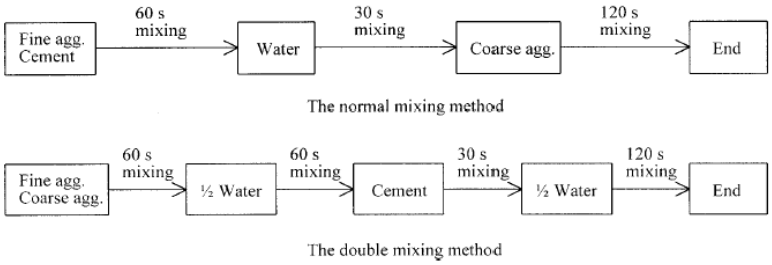

Figure 2-20, Normal and double mixing method [18].

Applying the double mixing method divides the required water to the mixture into two stages through which a thin layer of cement slurry can be coated on the surface of RCA and fill up the old cracks and pores in adhered mortar with a lower water-cement ratio. In this way, a stronger ITZ leads to a greater compressive strength of RCA concrete can be provided [49]. The concept of double mixing method is outlined in Figure 2-21[18].

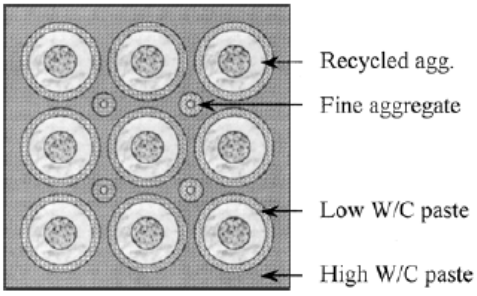

Figure 2-21, Schematic of RCA concrete using double mixing method [18].

Concrete properties were improved when aggregates obtained from high performance concrete (HPC) were used [20]. The microscopic observations shown in Figure 2-22, illustrate the ITZ between the new cement matrix and the HPC recycled aggregate mostly consisted of C-S-H gel and the total volume of large size pores was less than that in concrete made with RCA from normal concrete [20].

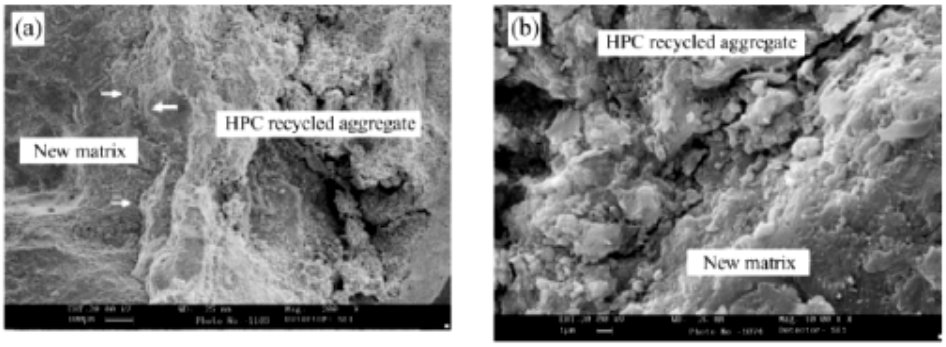

Figure 2-22, Microstructure of concrete prepared with HPC RCA [20].

It can be assumed that HPC recycled aggregates can absorb more water during the initial mixing process and contribute to reduction in water-cement ratio at ITZ. Furthermore, the presence of mineral admixture in HPC can contribute to produce the C-S-H gel by reacting with $Ca(OH)_2$ [20].

2.4- Durability of RCA concrete

Durability is defined as the capability of concrete to resist deterioration from an external environment [8]. The important exposure conditions and deterioration mechanisms in concrete structures may occur as physical attack such as abrasion, external loading, burning and freezing and thawing cycles, or in the form of chemical attack, such as alkali aggregate reaction, sulfate attack and reinforcement corrosion. The durability of RCA concrete can be more endangered by these adverse exposure conditions due to the higher permeability and lower ultimate strength than those of normal concrete.

2.4.1- Freezing and thawing resistance of RCA concrete

Freezing and thawing phenomenon in concrete can be occurred when an osmotic gradient, between low alkaline ice crystals formed in capillary pores and high alkaline unfrozen portions nearby ice, drives more water into the frozen pores. As a result, dilution of the solution adjacent to frozen part causes a further growth of ice leads to create an expansive pressure and deterioration of concrete [50].

Although a lot of search has not covered much work on this subject, RCA must be considered as a more frost susceptible component than natural aggregates due to presence of adhered cement paste, impurities and porous surface. The higher water absorption of RCA may increase the amount of freezable water and, osmotic or hydraulic pressures during the freezing of water in adhered mortar pores. In this case, a cyclic freeze-thaw system could result in early-unwanted expansion and destruction of RCA concrete.

Using an air-entraining admixture during batching can relieve the osmotic, hydraulic and internal stresses caused by water freezing and salt crystals formation in concrete pores. Adding air entrained admixtures to concrete incorporating recycled aggregates showed a very similar positive influence on freeze-thaw resistance compared to ordinary concrete. It is even more effective when a decreased water-cement ratio is being used for improving the concrete performance [51, 52].

Some researchers [50, 53] believe that, pre-saturation of RCA before mixing procedure provides better freezing and thawing performance in fresh and hardened concrete. Among RCA concretes which used aggregates with three different moisture conditions (dry, saturated and semi saturated), concrete made with semi- saturated aggregates (80-90%) was suggested as having the best frost resistible concrete [53].

The effects of water saturation curing methods, representing the real conditions of the environment, on freeze-thaw resistance of recycled concrete were studied. These four conditions are summarized in Table 2-5 [54].

Table 2-5, Treatment of test samples [54].

Type of water saturation	Curing conditions	Preliminary treatment	Treatment before testing
Complete	27 days in water at 20 °C	In water at 20 °C until constant weight	
Initial	60 days in waterproof envelop at 20 °C	No	No
Cyclic	4 cycles: 15 days in air (at 20 °C and RH= 65%), 15 days in water (at 20 °C)	15 days of drying at 40 °C	15 days in water at 20 °C
Hirschwald	27 days in water at 20 °C, then 3 months at 20 °C and RH= 65%	Drying at 55 °C until constant weight	24 h of water absorption by capillary, then 24 h under water at 20 °C

Three types of RCA concrete were studied: (i) concrete made with coarse recycled aggregate and natural sand (RAC1), (ii) concrete made completely with presoaked recycled aggregate (RAC2) and (iii) concrete made entirely with dry recycled aggregate (RAC3). Normal concrete (NAC) was used as a reference. The results showed that, the role of water saturation was significant on frost resistance of recycled concrete. Hirschwwald water saturation as the closest curing method to real exposure condition, defined in Table 2-5, was found efficient for both concretes made with coarse and fine recycled aggregates. RAC2 and RAC3 were not damaged after 300 cycles [54] and, therefore, according to ASTM Standard C 666 [55], they were considered frost resistant.

Air-entrained content in RCA can also have an important role on freezing and thawing resistance. A laboratory experiment used air-entrained and non-air-entrained concretes with w/c = 0.45, as coarse aggregates in new concrete. The relative modulus of

elasticity, which decreased below 60% at 90 freeze-thaw cycles, demonstrated that the frost resistance of non-air-entrained concrete used as aggregate was poor [56].

In real conditions, it is not possible to separate stockpiled air-entrained and non-air entrained recycled aggregates from each other. For that reason, some different blends of them were prepared and their frost resistances were examined. Figure 2-23, shows that the frost resistance has an inverse relation with the amount of non-air entrained recycled aggregates in concrete [56].

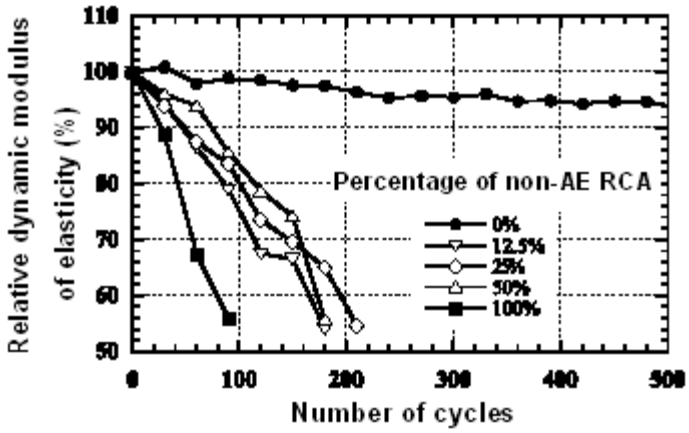

Figure 2-23, Relative dynamic modulus of elasticity vs. number of frost cycles [56].

Another significant aspect of freezing and thawing is salt scaling. In addition to generating pressures through osmosis and crystallization caused by decreasing the freezing point of concrete pore solution, deicing chemicals can increase the risk of decomposition and leaching of cement hydration products by increasing the saturation degree in recycled concrete pores and ITZs [57].

Since, salt concentration changes at different depths from the exposed surface of concrete, the formation of various amount of ice under the concrete surface can produce a hydraulic pressure gradient. As a result, the generation of macro- or micro- cracks in

concrete which has been started with freeze-thaw phenomenon is continued by more susceptible ingression of deicing chemical ions and the scaling of the concrete [8, 57].

Speare and Ben-Othman [51], subjected air-entrained RCA concretes to freezing and thawing cycles in the presence of deicing salts according to ASTM C672 [58] Standard test method. After 50 freeze-thaw cycles, the progress of RCA concrete scaling was monitored visually and quantitavely. The results showed very similar salt scaling resistance for RCA and normal concretes.

2.4.2- Alkali aggregate reaction resistance of RCA concrete

In the presence of reactive aggregate, alkali ions in concrete pore solution (Na^+ and K^+) and high relative humidity, an alkali reaction may occur. An expansive gel in the pores or around the aggregate, as a result of this reaction, causes the internal stresses to develop an excessive expansion which results in cracking of concrete [59].

The deterioration caused by alkali aggregate reaction (AAR) can be prevented by limiting one or more of the essential reaction factors or adding of mineral admixtures such as fly ash which can reduce the permeability of concrete and the alkalis available for the reaction [24, 59].

It appears that there has been only one study of AAR in RCA concrete [60]. When recycled concrete structure, made of the non-reactive new mortar and recycled coarse aggregate, is placed in a humid and aggressive environment, alkali-aggregate reactions should be paid attention. Assuming the original coarse aggregate in recycled aggregate is non-reactive, the old mortar can contain no reactive particles, no longer reactive particles (consumed by previous reactions), reactive particles with ongoing reactions and reactive particles in which no reaction has occurred yet.

To study the effect of old mortar reactivity on new concrete represented above, Gottfredson [60] compared four different types of recycled concrete made with crushed coarse RCA. Table 7 illustrates the description of the four concrete used as coarse RCA.

Table 2-6, Description of the four types of concrete used as RCA [60].

Name	Type	Description
R-0	1	New concrete cast with non-reactive aggregates (dummy)
R-1	3	Old mixed concrete from a demolition site (partly reactive old concrete)
R-2	2	Old concrete from cores taken out of a pavement severely damaged by AAR
R-3	4	New concrete cast with highly reactive sand and non-reactive coarse aggregate

The time-expansion relationships were investigated to know the critical level of expansion (0.5-1%) in which visible cracks were formed on the surface of the concrete cylinders. The results showed that, after one year, the magnitude of the final expansions was about 8% for the new concrete cast with highly reactive sand and non-reactive coarse aggregate and about 2% and a very small level for concretes made with partly reactive and AAR severely damaged recycled aggregates (type 3 and 2) , respectively. Moreover, theses authors [60] also stated that the partial replacement of highly reactive recycled fine aggregate (type 4) up to 20%, the expansion reduced to about 1/25 and it did not demonstrate any expansion lead to crack.

Addition of 35% fly ash to the recycled concrete mix delayed the expansion noticeably when a very reactive recycled aggregate was used. It also depends on the water-cement ratio and the maximum size of the recycled concrete aggregate. The lower level of water-cement ratio (0.45 compared to 0.55) and smaller grain size (16 mm compared to 32mm) made no expansion of cylinders after one year [60].

2.4.3- Sulphate attack resistance of RCA concrete

The products of free calcium hydroxide and calcium aluminate hydrate (C_3A in the cement gel) with sulphates (in soil or sea water) reactions are expansive compounds (gypsum and calcium sulphoaluminate) which cause cracking and deterioration in concrete. To reduce sulphate attack, the use of cement that is low in C_3A and adding mineral admixtures which can react with free calcium hydroxide and reduce the C_3A are recommended [8,24]. Since recycled concrete as aggregate coming from different sources may be contaminated with sulphate, the chemical composition and quality of RCA should be verified before using it in concrete mixture.

Shayan and Xu [34], and Speare and Ben-Othman [51], performed sulphate resistance tests on normal and RCA concrete specimens which were stored for 1 year in 5% and 10% sodium sulphate solutions, respectively .The results did not show significantly values of expansion or length change in RCA concrete than those of in normal concrete specimens.

2.4.4- Reinforcement corrosion of RCA concrete

Concrete protects embedded steel reinforcement from corrosion through its highly alkaline nature. The pH of environment in concrete usually is greater than 12.5, which causes a passive film on the surface of steel rebar. However, this protective film breaks down when the chloride ions present in aggressive environments, such as sea water or de-icing salt, penetrate into the hardened concrete and reach the surface of reinforcing steel.

The penetration time which is the most significant parameter for corrosion initiation of the steel reinforcement and service life of concrete structures depends on the

permeability of concrete as well as concentration and intrusion mechanism of chloride ions into concrete [61, 62, and 63].

2.4.4.1- The role of permeability on reinforcement corrosion of RCA concrete

The high permeability of RCA concrete relative to that of normal concrete can increase the penetration rate of the moisture and aggressive agents such as chloride into concrete. Using porous recycled aggregate with high water absorption can affect not only the size and continuity but also the flow path and fluid driving force of capillary pores in recycled concrete.

Beyond a certain threshold depth, concrete is more durable and the permeability of inner zone of concrete can be lower than the outer region because of wall effect, segregation, bleeding and better compaction [64, 65]. Although no studies have been found on this subject, it is possible that the surface skin of recycled concrete with its higher percentage of drying shrinkage, as explained before, is less resistance to initial penetration of chloride ions than that of normal concrete.

Different defects such as cracks and voids in concrete can contribute to increase the permeability and accelerating the corrosion rate of reinforcing steel by providing direct paths for movement of moisture and oxygen. The development of a connected crack network caused by drying shrinkage (due to higher water absorption) , structural loadings (due to less strength) and chemical attacks such as corrosion of reinforcing steel, sulphate attack, carbonation and alkali aggregate reactions (depends on mix proportions and aggregate quality) still needs to be investigated for recycled aggregate.

Microscopic observation of RCA concrete can be used for understanding of reaction mechanisms, diagnosis of damage processes and microstructural properties such

as size and distribution of pores and cracks [59]. However, it should be integrated with results from the other techniques, such as chemical analysis techniques to confirm the achieved results. For instance, applying different corrosion measurement techniques accompanying with measuring the chloride diffusivity through the cover depth and microscopic observation, can provide accurate results for an adequate corrosion research.

2.4.4.2- Chloride diffusion mechanism in RCA concrete

The mechanism of reinforcement corrosion in recycled concrete is similar to the one in normal concrete. Introducing chloride ions into concrete from external sources can be divided into initiation and propagation sates.

The initiation stage or breaking down the passive layer depends on the time taken for chloride ions to diffuse into the concrete cover in a sufficient amount. This time period is dependent on chloride diffusion rate (Dcl^-), the chloride threshold value (Cl_{TV}) and the thickness of cover depth.

In second stage or propagation, increasing the amount of corrosion products results in expansion of steel surface and exceeding the tensile stresses in concrete. The propagation stage is determined by the rate of corrosion which is a function of moisture content and the rate of oxygen diffusivity (D_{O2}), gradients in chloride ion concentration (Ccl^-), resistivity of concrete (ρ) and environmental factors such as relative humidity (RH) and temperature. Consequently, deterioration of physical barrier for reinforced concrete can be occurred in the forms of scaling and spalling [66, 67].

The effect of time for corrosion initiation and corrosion rate on the service life of the structure is shown schematically in Figure 2-24 [67].

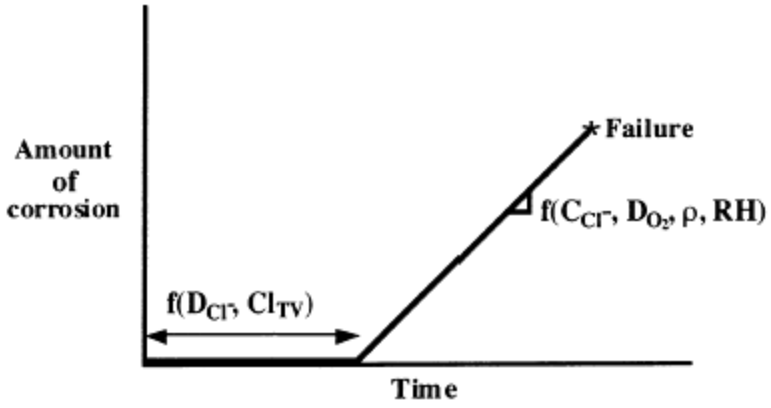

Figure 2-24, Stages of steel reinforcement corrosion as a function of service life [67].

As a definition [61], the content of chloride ion level at which steel reinforcement corrosion begins in concrete is called chloride threshold. As most chloride present in concrete is soluble in acid (nitric acid), this amount can be considered as total chloride content of concrete. Water-soluble chlorides are explained as unbound chloride and they are the only available chlorides that can participate in corrosion reactions. The chloride threshold is about 0.2% to 0.4% by mass of cement for acid soluble and 0.15% to 0.3% as water- soluble content [61]. The amount of chloride threshold in RCA concrete has not been determined yet but it can predict that it could be affected by different sources such as admixtures, RCA, cement, mixing water or the environmental parameters mentioned above.

Measuring the apparent chloride diffusion coefficient (D_a), a chloride transport parameter calculated form acid-soluble chloride profile data without considering the effect of chloride binding, can provide an indication of chloride diffusion rate [68, 69 and 70] . For measuring the chloride diffusion rate into concrete two major methods, steady state and non-steady state, can be considered to use.

According to definition, the “steady state” chloride diffusion coefficient is determined by a rapid chloride test method. In this method, the chloride content passing through a sliced concrete exposed to a constant direct current voltage (60V) is determined versus time. As a result, this test method provides a rapid indication of concrete resistance to penetration of chloride ions [71].

In non-steady state diffusion coefficient measurement, the diffusion of chloride ions is determined based on the transportation of ions by absorption mechanism of concrete. The results obtained from this method seem to be more realistic. In this method, concrete specimens are exposed to a constant chloride concentration solution at a specified time and the chloride profile can be performed over time [72].

2.4.4.3- Experimental results of steel corrosion behaviour in RCA concrete

Shayan and Xu [34] considered two methods mentioned above to evaluate the penetration of chloride into reinforced RCA concrete as a corrosion protection criterion. They [34] concluded that the concrete made with RCA shows good resistance against chloride penetration and corrosion of steel reinforcement particularly when silica fume is used as a supplementary cemntitious material.

Determining the value of resistivity of concrete against the passage of electric charge may not be representative of concrete performance and corrosion of reinforcing steel in real conditions due to the limitations which are involved in this method [68, 69, 70, and 72,]. Moreover, corrosion involves in electrochemical reactions and the effect of the electrode surface reactions such as metal dissolution, evolution of gases, migration of produced ions and ions leaching due to their high ionic mobility are ignored during resistivity and ponding tests [68].

Friedl et al. [73], assumed that chloride contaminated recycled aggregate may be located adjacent to steel reinforcement accidentally and causes the initiation of corrosion on the surface of reinforcing steel. For this purpose, they prepared concrete prisms with embedded steel rebar (anode) and platinized titanium electrodes (cathode) in which a single chloride contaminated (in 3% NaCl) RCA of 15 to 20 mm diameter was connected to the anode.

The macrocell current between the two electrodes was measured continuously with a 10 Ohm shunt-resistor and a voltmeter while the bottom of concrete prisms was exposed to water. Using this method could not provide any correlation between the measured current and the environment of recycled concrete. However, they observed that the chloride ions could diffuse from recycled concrete aggregate into concrete and cause the severe pitting corrosion of steel rebar [73].

From the electrochemical aspects behind the corrosion theory, the presence of microcells at electro-conductive reinforcing steel accompanying with the concrete pore solution as electrolyte in concrete can provide an adequate cell for progressing corrosion of concrete specimens exposed to deicing salt. Therefore, measurement of macrocell corrosion between two different rebars in concrete which has a non-homogenous composite material can not provide an appropriate technique to assess the microcell corrosion of reinforcing steel.

Tittareli and Moriconi [74] exposed pre-cracked reinforced bare steel and galvanized steel plate RCA concrete prisms to weekly wet-dry cycles (2days dry and 5days wet) in a 10% NaCl solution. The probability and the behaviour of corrosion in both steel plates were evaluated by calomel electrode (SCE) and galvanodynamic

technique using an external graphite bar as counter electrode. After 7 wet-dry cycles the concrete prisms were split and the mass loss of steel plates was calculated.

They found that, immediately after exposing the concrete prisms into the salt solution, both types of steel plates represented the high probability and low polarization resistance of corrosion while after few weeks' wet-dry cycles those values were leveled off to the values showing less corrosion risk. Weight loss test was also was in good agreement with the electrochemical measurements. Finally they concluded that, using galvanized steel and addition of fly ash can improve the corrosion resistance of reinforcing steel embedded in RCA concrete even if the concrete has cracked and exposed in an aggressive environment.

2.5- Research Significance

Recycling of demolished concrete and its utilization as aggregate in new concrete is increasingly being considered for production of sustainable concrete construction. Although much is known about physical and mechanical properties of RCA concrete, some physical properties and durability aspects of concrete made with old RCA, obtained from building and bridge structures, is still not well understood.

The experimental research presented herein attempts to study the physical and mechanical properties of very well hydrated RCA (about 50 years old) and new RCA. Also, the effects of RCA on the durability aspects of concrete such as corrosion of reinforcing steel and salt scaling resistance, which were not found in literature review, were comprehensively compared with that of concrete made with natural aggregate.

Chapter 3

Experimental Procedure

3.1- Aggregates background information

Due to the negative effects, reported in the literature [7, 11, and 12], of using RCA with small size on the workability and strength of recycled concrete, coarse recycled aggregate and natural sand as fine aggregate were considered for the fresh concrete mixture design. To achieve a multilateral study on the most effective characteristics of RCA such as contamination, hydration age and physical properties of recycled aggregates on reinforced concrete durability, three types of coarse aggregate were selected for the experimental work as follows.

1) The Natural Aggregates (NA), containing good quality gravels with an appropriate strength and porosity commonly used in the Kitchener area, were used as control materials to produce the normal concrete.

2) The New Clean Recycled Concrete Aggregates (NC-RCA) were obtained from crushing the concrete returned to the Dufferin concrete division ready mix yard located in Kitchener. This type of aggregate is currently being used as back-fill or road sub-base materials in pavements. It would be significant to extend its use to higher strength structural applications.

3) The Old Contaminated Recycled Concrete Aggregates (OC-RCA) were obtained from a demolished reinforced bridge, the Townline Road Bridge, over Highway 401 in Ontario. The concrete material of this bridge, built in 1959, was considered as a highly de-icing salt contaminated after on-site and laboratory investigations performed by Ministry of Transportation of Ontario (MTO). Corrosion of reinforcing steel, caused by penetration of chloride ions present in deicing salt which had been used on the bridge

deck in winter times, was responsible for deterioration of this bridge. Figure 3-1 shows a view of this bridge just prior to its demolition in 2004.

Figure 3-1, Deteriorated Townline Road bridge over highway 401 before demolition.

3.2- Production of recycled aggregates

A crushing machine was used for producing of the New Clean Recycled Concrete Aggregates (NC-RCA). The hardened left over concrete batches were loaded into the crushing machine hopper and jaw crushed. Then, the different sizes of aggregates (larger and smaller than 20 mm diameter) were separated and larger sizes went through secondary crushing with an impact crusher. Figure 3-2 shows the general perspective of the crushing machine used for producing the NC-RCA.

Figure 3-2, Crushing machine was used for manufacturing NC-RCA.

Figure 3-3 illustrates the stock-pile of crushed concrete chunks obtained from the reinforced concrete bridge which was demolished by Capital Paving Inc.

Figure 3-3, Stock-pile of demolished concrete from the bridge.

It was necessary to crush the concrete pieces into smaller sizes to be used as (OC-RCA) aggregates in new concrete. For this purpose, the amount of demolished concrete required for the mixture design was crushed into fist-size by sledge hemmer. The further crushing was conducted using laboratory crushing machine to produce the aggregate with sizes smaller than 20 mm diameter. This machine consists of a top feeding hopper and a fixed jaw crusher at the bottom. The size of aggregates could be changed by adjusting the spacing of jaws using a knob provided on the side of the crusher (Figure 3-4).

Figure 3-4, The laboratory crushing machine used for producing the OC-RCA.

3.3- Grading of aggregates

The fresh concrete mixture for the reinforced concrete prisms was designed based on Ministry of Transportation of Ontario (MTO) requirements. Thus, the nominal maximum size of 16 mm diameter of coarse aggregate used for concrete prisms should confirm the grading requirements as outlined in ASTM C 33, Table 3-1 [75], and MTO laboratory testing manual LS-602, Table 3-2 [76]. According to the CSA standard A23.1 [77], the maximum aggregate size of reinforced concrete should not exceed one-half of the specified cover depth for concrete exposed to chlorides. Since the cover depth of concrete prisms was to be 45 mm, the coarse aggregate nominal maximum size of 16 mm of diameter easily complied with this requirement.

Table 3-1, Grading requirements for coarse aggregates, ASTM C33 [75].

Nominal size (sieves with square openings)	Amounts finer than each laboratory sieve (square openings), mass percent				
	25.0 mm (1in.)	19mm (3/4 in.)	12.5 mm (1/2in.)	9.5 mm (3/8in.)	4.75 mm (No.4)
19.0 to 9.5 mm (3/4 to 3/8 in.)	100	90 to100	20 to 25	0 to15	0 to 5

Table 3-2, Gradation requirements (MTO LS-602) - Coarse aggregate for structural concrete, sidewalks, curb & gutter [76].

Nominal Maximum Size	19.0 mm	16.0 mm	13.2 mm	9.5 mm	6.7 mm
MTO Sieve Designation mm	Percent Passing				
26.5	100	-	-	-	-
19.0	85-100	100	100	-	-
16.0	65-90	96-100	-	-	-
13.2	-	67-86	90-100	100	100
9.5	20-55	29-52	40-70	85-100	-
6.7	-	-	-	-	75-100
4.75	0-10	0-10	0-15	10-30	40-80
2.36	-	-	-	0-10	0-20

Table 3-3, Gradation (MTO LS-602) requirements for fine aggregates [76].

MTO Sieve Designation	Percent Passing
9.5 mm	100
4.75 mm	95 - 100
2.36 mm	80 - 100
1.18 mm	50 - 85
600 μm	25 - 60
300 μm	10 - 30
150 μm	0 - 10
75 μm	0 - 3 Natural Sand 0 - 6 Manufactured Sand

Gradation of aggregates was achieved by using superimposed square opening wire-mesh sieves shown in Figure 3-5.

Figure 3-5, Superimposed sieves used for grading the aggregates.

By measuring the weights of aggregates retained in each sieve after shaking, the percentage of weight passing through or retained in each sieve was determined.

According to the obtained weight values, the combined aggregate grading of coarse and fine aggregates together was determined after sieving, Table 3-4. Aggregates of 4.75 mm diameter were intentionally missed in gradation size for each type of

aggregate to minimize the water demand of fresh concrete mix due to high water absorption of recycled coarse aggregates with small size.

Table 3-4, Combined gradation of aggregates.

Sieve Designation	Percent retained
19mm	0
16 mm	5.82
11.2 mm	32.05
8 mm	20.35
4.75 mm	-
2.36 mm	12.36
1.18 mm	12.06
600 μm	8.03
300 μm	4.63
150 μm	2.65
75 μm	1.11

Coarse aggregate (RCA)

Fine aggregate (natural sand)

The particle-size distribution curve was plotted according to the weight percent of passing aggregates through the sieves with the designated opening sizes in Figure 3-6.

The presence of a near-horizontal shift indicates that 4.75 mm aggregate size has been missed. However, relatively uniform shape of the curve demonstrates a suitable gradation resulting in a workable mixture with adequate proportion of RCA.

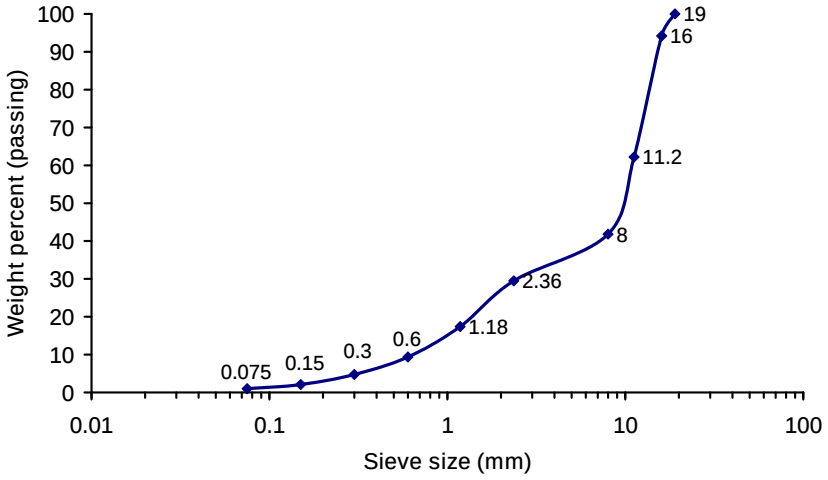

Figure 3-6, Aggregate grading distribution curve.

3.4- Physical properties of aggregates

According to the MTO design requirements standard [78], coarse aggregate should meet the physical property requirements for concrete pavement and/or structures in Table 3-5. This Standard indicates that "when coarse aggregate contains more than 15% passing the 4.75 mm sieve, the material finer than 4.75 mm shall also meet the physical requirements of fine aggregates". Since coarse aggregate considered for the fresh concrete mixture did not contain any 4.75 mm sieve size particles, this requirement did not apply.

Table 3-5, Physical requirements of coarse aggregates (MTO mix design) [78].

MTO or CSA Laboratory Test	MTO or CSA Laboratory Test Number	Acceptance Requirements	
		Pavement	Structures, Sidewalk, Curb and Gutter, and Concrete Base
Material Finer than 75.μm Sieve, by Washing, % maximum - for gravel - for crushed rock	LS-601	 1.0 2.0	 1.0 2.0
Absorption, % maximum	LS-604 or CSA A23.2-12A	2.0	2.0
Unconfined Freeze-Thaw Loss, % maximum (Note 1)	LS-614 or CSA A23.2-24A	6	6
Flat and Elongated Particles, % maximum	LS-608	20	20
Petrographic Number, Concrete, maximum	LS-609	125	140
Micro-Deval Abrasion Loss, % maximum	LS-618 or CSA A23.2-29A	14	17
Accelerated Mortar Bar Expansion, % maximum at 14 days (Notes 2 and 3)	LS-620 or CSA A23.2-25A	0.150 (Note 4)	0.150 (Note 4)
Potential Alkali-Carbonate Reactivity of Quarried Carbonate Rock (Note 5)	CSA A23.2-26A	Chemical Composition Must Plot in the Non-Expansive Field of Fig. 1 of Test Method	
Concrete Prism Expansion Test, % maximum at one year (Notes 2 and 6)	CSA A23.2-14A	0.040	0.040
Alternative Requirement to Unconfined Freeze-Thaw Loss (LS-614)			
Magnesium Sulphate Soundness, 5 Cycles, % maximum loss (Note 1)	LS-606	12	12

Due to the specific characteristics of recycled concrete as aggregates (RCA), some of the physical properties require more attention for investigation. Therefore, the physical characteristics mentioned in Table 3-5, namely chloride and adhered cement content,

density, water absorption, abrasion and salt scaling resistance of original as well as recycled coarse aggregates, were evaluated.

3.4.1- Adhered cement content evaluation

The determination of adhered cement on recycled aggregates was made by using the ASTM C 33 (the standard specification for concrete aggregates) test method for the estimation of an acid-insoluble substance in any type of cement [75].

500 grams of NC-RCA and OC-RCA with gradations of 10% of 16 mm, 55% of 11.2 mm, and 35% of 8 mm sizes were used for this test. Aggregates were thoroughly washed and dried at 110° C over night. After air cooling for 1 to 3 hours, the aggregates were weighed and digested in 20 % nitric acid. The solution was heated gently on a hot plate while the aggregates were stirred by the flattened end of a glass rod. This process was continued for a few minutes until adhered cement paste started to dissolve.

Thereafter, the mixture was covered and heated to near boiling temperature for 2-3 hours and the residue of adhered mortar and aggregates were separated. The solution of adhered paste was filtered through a medium-textured paper in a new beaker and the residue on the filter and the undissolved aggregates were washed and dried in the oven at 110° C over night and weighed again.

The difference between the dried mass before dissolving and the mass of residue particles after second drying gives the amount of adhered cement paste in the RCA.

3.4.2- Determination of density and absorption of recycled aggregates

The bulk relative density, apparent relative density, and the water absorption of coarse aggregates were evaluated by using CSA A23.2-12A and ASTM C 127 standard test methods [79, 80]. All three types of aggregates were tested. According to the standard

test requirements, the nominal size of 8.00 mm was obtained by passing three kilograms of the coarse aggregate through a 9.5 mm sieve and retaining on the 4.75 mm sieve.

All aggregates were washed and dried to a constant mass (mass A) at a temperature of 110 $\pm 5^{\circ}$ C for 24 hours and cooled in air at room temperature for 4 hours. Then, the aggregates were immersed in tap water at room temperature for another 24 hours. After removing the aggregates from the water, they were rolled in absorbent cloth until the surface of aggregates would have no visible moisture film. In fact, in the saturated surface dry (SSD) condition, all of the pores in aggregates were filled with water while the surface of aggregate was dry. The saturated surface-dry aggregates were weighed (mass B) and immediately placed in a wire basket while it was suspended in a bucket filled with water and weighed again. The total mass of saturated aggregate in water (mass C) was determined after the deduction of the weight of basket. The bulk density, in dry and in saturated surface-dry basis conditions, apparent density and water absorption of coarse aggregates were determined as indicated below.

$$\text{Bulk density} = \frac{A}{B-C} \tag{3-1}$$

$$\text{Bulk density (saturated surface-dry) basis} = \frac{B}{B-C} \tag{3-2}$$

$$\text{Apparent density} = \frac{A}{A-C} \tag{3-3}$$

$$\text{Absorption, \%} = \frac{B-A}{A}\times 100 \tag{3-4}$$

3.4.3- Chloride content evaluation of OC-RCA

One kilogram of OC-RCA was selected randomly from different sizes (16, 11.2 and 8mm maximum diameter) of aggregates and hand ground by mortar and pestle. Five different powder samples were passed through 250 μm sieve and were weighed (10 gram for each

sample) to the nearest tenth of a gram. The acid-soluble chloride test based on ASTM C114 and C1152 standard test methods was performed to measure the total chloride content of the concrete powder specimens [81, 82].

Powders were dissolved in 120 milliliters of dilute nitric acid (1:10 concentration acid dilution with distilled water by volume).The samples were mixed with magnet stirrer. As soon as the dissolution apparently finished, the slurries were boiled for 5 minutes while the beakers were covered by watch-glasses. Then, the slurries were filtered through Whatman No. 4 filter paper into 400 mL beakers. The beakers and filter papers were washed at least 6 times with hot distilled water and the volume of solution was increased to 250 ml by distilled water.

Three solution samples of volume of 50 ml were made for each titration test and they were titrated against 0.08 eq/lit $AgNO_3$ using a Radiometer TIM800 semi-automatic titrator. The weight percent of chloride in concrete was calculated as follows.

$$\text{The value from titration test } (\frac{Mol}{lit}) \times 0.250\,(lit) = \text{X (Moles of chloride ions)} \quad (3\text{-}5)$$

$$\text{X} \times 35.4 = \text{Y (grams of chloride in solution)} \quad (3\text{-}6)$$

$$\frac{Y}{10(grams)} \times 100 = \text{Z (weight percent of chloride in concrete)} \quad (3\text{-}7)$$

3.4.4- Abrasion resistance assessment of aggregates (Micro-Deval test)

CSA A23.2-29A and AASHTO TP 58-02 standard test methods [25, 26] were used for evaluating the resistance of coarse aggregate to degradation by abrasion using the Micro-Deval apparatus shown in Figure 3-7 [27]. The standard test method uses 1500 ± 5 g of each type of aggregate with the nominal size of 8.00 mm (defined above) and the following procedure.

Figure 3-7, Micro-Deval instrument used for aggregate abrasion resistance test [27].

The aggregates were washed and dried in the oven at a temperature of 110 ± 5°C to a constant mass. They were weighed every two hours until they did not they did not lose more than 0.1% of their moisture in a 2 hour period. The final constant mass was determined (mass A).Thereafter, aggregates were placed into the abrasion jar and were saturated in tap water (temperature 20 °C ± 5°C) for 2 hours. Then, 5kg of 9.5 mm diameter steel balls were added and the jar was placed on the machine. The jar was rotated at 100 r/min ± 5 r/min for 95 ± 1 minutes and the aggregates were poured over two superimposed sieves with square openings of 4.75 mm and 1.18 mm afterwards.

The retained materials were washed with water until all materials smaller than 1.18 mm passed the sieve. Then, all steel balls were removed from the aggregates by a magnetic pick up. Materials smaller than 1.18 mm were discarded. All the retained aggregates on the 4.75 mm and 1.18 mm sieves were combined and oven dried at 110 ± 5°C for an equal or longer period than that previously found adequate for producing the dried constant mass condition. The oven-dry aggregates were weighed to the nearest 0.01 g again (mass B) and the aggregate abrasion loss was expressed as a

percent by mass of the original dried aggregates before the abrasion resistance test (Equation 3-8).

$$\text{Percent loss due to abrasion} = \frac{A-B}{A}\times 100 \quad (3\text{-}8)$$

3.5- Fresh concrete mixture design

Type 10 ordinary Portland cement (OPC) concrete and a water-cement ratio of 0.43 was used for casting concrete prisms made with three different types of aggregates. Table 3-6, gives the structural concrete mixture proportion used for three different types of concrete.

Table 3-6, Mixture proportions for generating 1 m^3 of structural concrete [83].

Component	Amount
Type 10 Portland, kg	355
Sand,kg	770
Stone,kg	1070
Water,l	153
Air entrainment	40 ml/100 kg cemntitious
Water reducer	250 ml/100 kg cemntitious

Since the surface moisture contents of different aggregates become part of the mixing water in concrete, the water requirements were individually determined.The surface moisture was calculated as described in Appendix A.

3.6- Design and casting of reinforced concrete prisms

Reinforced concrete prisms made with dimensions of $200\times100\times100$ mm were cast with a centrally placed 10 M carbon steel rebar giving a cover depth of 45 mm. Four prisms of normal concrete and five prisms of NC-RCA and OC-RCA concretes were cast. The two ends of the 320 mm long rebars were epoxy coated for the length of 100 mm to provide a 120 mm exposed length of reinforcing steel in concrete. Figures 3-8 and 3-9 show the

schematic diagram and a photograph of the formwork with the rebars in place designed for casting, respectively.

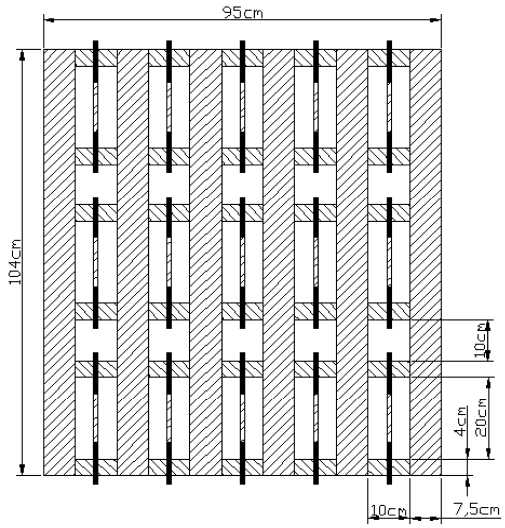

Figure 3-8, The schematic diagram of mould for casting the concrete prisms.

Figure 3-9, Moulds with rebars in place.

Also, standard concrete cylinders (five from each type of concrete) with 100 × 200 mm dimensions were cast to be used for investigation of concrete properties.

After casting, the concrete prisms were wet cured under burlap and plastic for two days, and then allowed to mature in the laboratory for ten weeks. Since the concrete prisms were to be immersed in saturated salt solution for corrosion measurement tests, their vertical four faces were sealed by epoxy to allow chloride diffusion into the concrete from top and bottom faces in contact with saturated salt solution.

3.7- Physical and mechanical properties of hardened concrete

The following properties of the different concretes were measured using the hardened concrete cylinders: the compressive strength; density; water absorption and air voids.

3.7.1- Compressive strength

The compressive strength tests were made according to ASTM C39 standard test method [84] on three of the standard cylindrical specimens of the three different types of concrete cured for 28 days.

3.7.2- Density, absorption and voids in hardened concrete

CSA A23.2-11C and ASTM C 642 test methods were used for determining the density, water absorption, and air void content of the concretes [85, 86].

Eleven months after casting, concrete cylinders were dried at $110 \pm 5^{\circ}$ C for 24 hours periods (72 hours) until the loss in mass reached less than 0.5 % of the lowest value obtained. The cylinders were allowed to cool in air to room temperature and the values of mass were determined (mass A).

Afterward, specimens were fully immersed in water between 21-23 $^{\circ}$ C for 48 hours, surface dried with a dry cloth, and weighed to give mass B.

The concrete cylinders were placed in a container, submerged in tap water and boiled for 6 hours. Then, they were allowed to cool for 16 hours to room temperature. Again, the surface moisture film was removed by a dry cloth and the mass of specimen was determined (mass C).

Finally, the immersed apparent mass (D) of cylinders was determined by placing them in a wire basket and weighing the specimens suspending in a bucket of water

covering the top surface of cylinders. The values of absorption, density and void percentage of concretes were calculated by using below equations.

Absorption after immersion, %= $\frac{B-A}{A}\times 100$ (3-9)

Absorption after immersion and boiling, % = $\frac{C-A}{A}\times 100$ (3-10)

Bulk density, dry = $\frac{A}{C-D}\times 100$ (3-11)

Bulk density after immersion = $\frac{B}{C-D}$ (3-12)

Bulk density after immersion and boiling = $\frac{C}{C-D}$ (3-13)

Apparent density = $\frac{A}{A-D}$ (3-14)

Volume of permeable pore space (voids), %= $\frac{C-A}{C-D}\times 100$ (3-15)

3.8- Exposure conditions of prisms for reinforcement corrosion studies

One of the acceleration techniques for increasing the driving force of chloride diffusion into concrete is applying wetting and dying cycles. Ten weeks after casting, five concrete prisms of each type of concrete were subjected to wet-dry cycles. For the first two weeks, the specimens were fully immersed horizontally in saturated salt (NaCl) solution with the level of the solution kept at 2-3 cm above the top surface of specimens all time.

Also, the prisms were inverted at each exposure time to eliminate the effect of any bleeding which may have occurred during the casting on ingress of chlorides. Due to the low chloride ion mobility in highly concentrated salt solution [87], an air compressor was provided for each container to accelerate the diffusivity of chloride into concrete prisms. The operational time period of each air compressor was set for half an hour in every four hours by using an adjustable timer. In Figure 3-10, the container and related equipment established for wetting cycle of concrete prisms are demonstrated.

Figure 3-10, The container and prisms for corrosion experiments.

Ninety days after exposing the specimens in saturated salt solution, they were dried at an approximately constant temperature (36°C) and low relative humidity (18%) in a sealed chamber for the second two week period the dry cycle. This was accomplished by placing the prisms in a glove box with a heater and a de-humidifier. The relative humidity and temperature were detected by a digital Thermometer/ Hygrometer during the dry-cycle. The glove box and contents are shown Figure 3-11.

Figure 3-11, A perspective of the chamber used for drying the concrete prisms.

3.9- The electrochemical corrosion measurement techniques

The measurements were performed at the end of each wet- or dry-cycle. The following measurement techniques were used for studying the corrosion behaviour of the steel reinforcement embedded in concrete prisms:

1) half cell (corrosion) potential, E_{corr}, using a silver-silver chloride reference electrode;
2) corrosion rate measurements, using the Linear Polarization Resistance (LPR) technique;
3) localized corrosion susceptibility, using cyclic polarization technique;
4) concrete electrical resistance, using Galvanostatic Pulse and Electrochemical Impedance Spectroscopy (EIS) techniques.

Under natural corrosion conditions, the value of the current for oxidation (the anodic dissolution rate) and reduction (cathodic reduction of oxygen rate) at the corroding surface is equal and there is no net corrosion current at the equilibrium condition. Thus, the direct measurement of corrosion rate, which is correlated to both anodic and cathodic reactions, is not possible [88].

Using LPR and cyclic polarization techniques, a potential is applied between working electrode (steel rebar) and reference electrode to shift the corrosion potential of steel away from equilibrium state. As a result, a net current is created and the corrosion rate can be calculated by measuring the current flow between the steel rebar and the counter electrode as described below.

3.9.1- Design of corrosion cell for electrochemical measurements of steel

Monitoring of reinforced steel corrosion in a concrete prism is different from the common electrochemical measurement techniques which are used for cells that contain

liquid solutions in a laboratory. The single steel rebar plays the role of electric conductor between the micro-anodes and cathodes at the surface of rebar while the concrete pore solution is the electrolyte in concrete.

In order to measure the current resulting from applied potential between the rebar and reference electrode, an appropriate electrode was designed. A wet sponge was used to make contact between the reference and counter electrodes and the surface of the concrete specimen. A stainless steel plate, as a counter electrode, was placed on the sponge surface to supply the current flowing to the working electrode (steel rebar) during the test. A saturated calomel electrode (SCE), as a reference electrode, was placed in the centre of a piece of wood in contact with the sponge.

The whole cell was connected to a multi-purpose potentiostat/galvanostat from Princeton Applied Research (PAR) model Parstat 2263-2. The obtained data were displayed on the computer screen connected to Parstat. Figures 3-12 and 3-13 show a schematic diagram and a photograph of the electrode assembly and the equipment for concrete corrosion measurement tests.

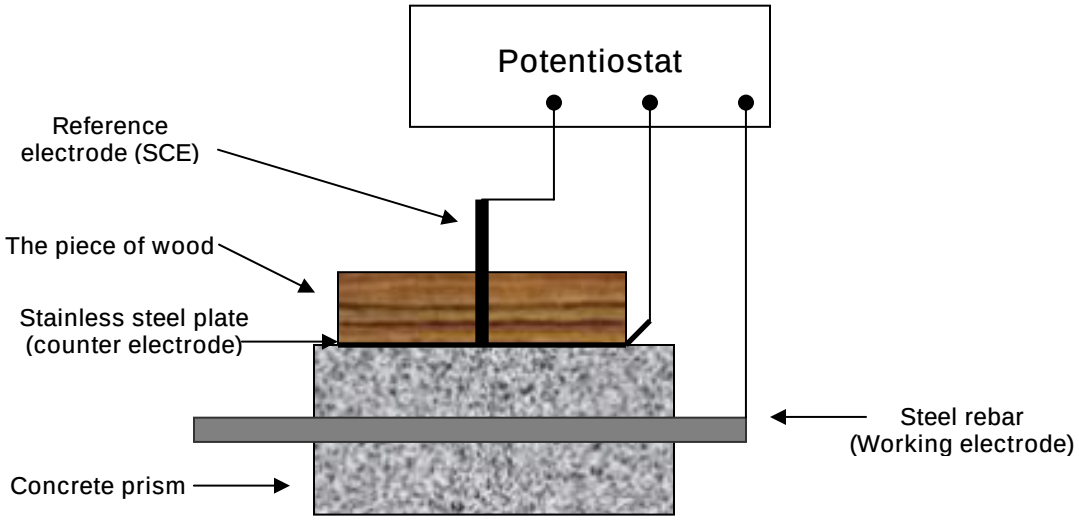

Figure 3-12, Schematic diagram of electrode set for corrosion measurements.

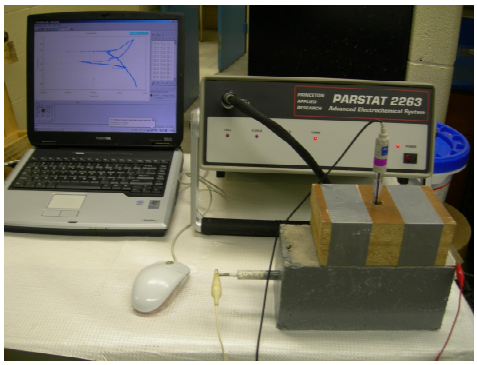

Figure 3-13, The equipments used for corrosion measurements.

3.9.2- Half-cell potential measurement technique

The half-cell potential or corrosion potential gives the corrosion probability at the different regions of reinforcing steel surface. Since all voltage measuring devices measure a potential energy difference, the corrosion potential (E_{corr}) is measured against a known reference electrode such as SCE or silver-silver chloride reference electrodes. The Galvapulse instrument is a portable unit designed to measure the corrosion potential, corrosion current density and concrete resistance in the field. The electrochemical potential of steel rebar in concrete prisms was measured versus silver-silver chloride reference electrode embedded in the hand held electrode system of Galvapulse. Although the electrochemical reactions in concrete can lead to the development of regions on the surface of reinforcing steel with different electrochemical potentials, the measured potentials were uniform for all concrete prisms due to the small exposed length (120 mm) of steel rebars. In order to ensure a good contact with the reference electrode, the concrete surface was pre-wetted by tap water.

3.9.3- Linear polarization resistance (LPR) technique by potentiosatat

The linear polarization resistance technique (LPR) makes use of the linear relationship between applied potential and corrosion current at very low values of potential (in a range

of ± 20 mV about the open circuit potential) as illustrated in Figure 3-14 [90]. As a result, the polarization resistance of steel (R_p) can be determined [89, 90 and 91].

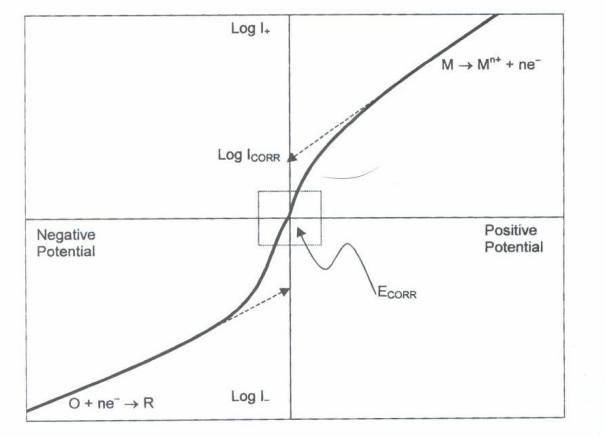

Figure 3-14, A schematic polarization resistance plot [90].

To calculate the corrosion current density of reinforcing steel in concrete prisms, the distinction between the steady state responses of anodic and cathodic current (ΔI) from the polarization resistance plot was determined when the ± 20 mV polarization the open circuit potentials were applied for 180 seconds (Figure 3-15).

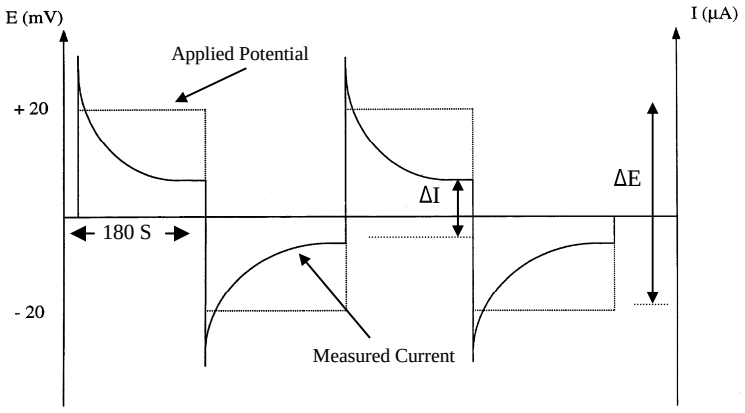

Figure 3-15, The polarization resistance plot obtained after 180 sec.

The corrosion current, I_{corr}, is determined using the Stearn-Geary equation [61, 91].

Where R_p is termed the polarization resistance

$$\frac{\Delta E}{\Delta I} = R_p = \frac{B}{(I_{corr})} \tag{3-16}$$

$$B = \frac{\beta_A \beta_C}{2.3(\beta_A + \beta_C)} \tag{3-17}$$

Where β_A and β_C are the slopes of the linear regions of the plots of log (i) versus E.

According to the literature [92, 93], the value of constant B is 0.026 Volt per decade of current for reinforcing steel in concrete and, therefore, I_{corr} was determined based on the followed equation (3-18).

$$I_{corr} = \frac{0.026}{R_p} \tag{3-18}$$

Finally, the corrosion current density (A/m^2) was obtained when the exposed area of steel rebar to chloride ions was considered as one–third of the rebar circumference. Corrosion of steel in concrete due to chlorides is never uniform over the whole exposed area of steel. However, the actual corroding area cannot be determined without destroying the specimen. Therefore, one third of the exposed area was chosen arbitrarily for calculations of the corrosion current density.

3.9.4- Galvanostatic pulse technique

Figure 3-16 shows a schematic diagram of the Galvapulse monitoring equipment was used in this work is represented [96]. Using this instrument, a galvanostatic pulse (25 µA) was applied from a central counter electrode to polarize the steel rebar for 60 seconds. A guard ring located concentrically around the central counter was responsible to confine

the pulse signal in a well-defined region of the steel (70 mm length). The resulting change of the reinforcing steel potential was recorded as a function of time by an Ag/AgCl reference electrode centrally placed in the electrode. The R_p and, as a result, the corrosion current of steel rebar ($\mu A/cm^2$) as well as the resistance of concrete prisms ($k\Omega$) were determined from this technique [92, 94, and 95].

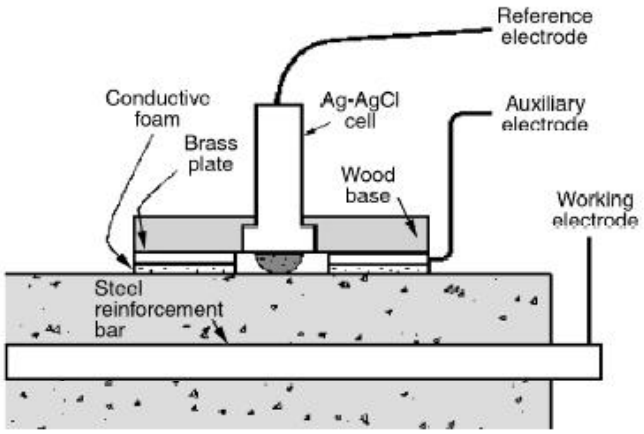

Figure 3-16, Schematic diagram of the Galvapulse monitoring equipment [96].

3.9.5- Cyclic potentiodynamic polarization technique

The potentiostat and electrode set equipment explained in previous sections were used for this technique. The potential cycling in a positive (anodic) direction was started from 50 mV more negative than the corrosion potential to 500 mV vs. SCE and then reduced in a negative (cathodic) direction to -900 mV at a scan rate of 1mV/sec. The results are graphed as a plot of the applied potential versus the logarithm of the measured current.

3.10- Concrete resistance evaluation of concrete prisms

The resistance of concrete prisms was evaluated by using galvanostatic pulse and electrochemical impedance spectroscopy (EIS) techniques. Both techniques used the Parstat instrument. In the galvanostatic pulse technique, a constant anodic current pulse

(25 μA) was applied for 10 seconds on the reinforcing steel. As a result, the ratio of constant current pulse and ΔE (the distinction between the initial and the next response potential represented in potential-elapsed time curve) caused by a potential ohmic drop ($I.R_{Ohm}$) was expressed the resistance of concrete prisms (Figure 3-17) .

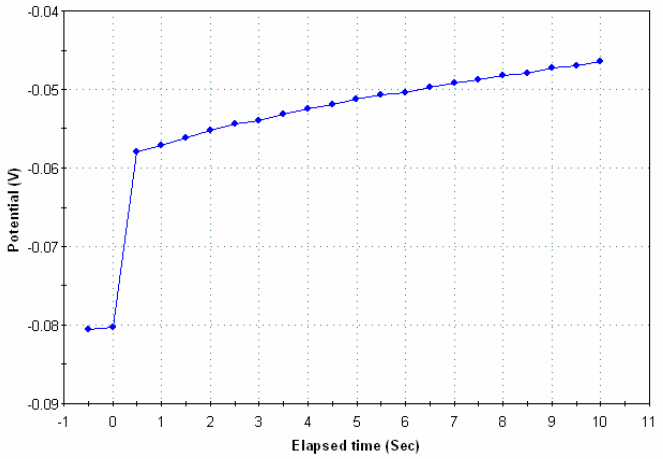

Figure 3-17, Galvanostatic pulse method used for concrete resistance measurements.

Electrochemical impedance spectroscopy (EIS) technique applies an AC voltage sinusoidal wave along the reinforcing steel surface. The response can be modeled as an analogue circuit. The model circuit can be assumed to include the Helmholz double layer (as a capacitor) in parallel with R_p (as a resistor) and in series with the concrete resistance (another resistor and/or capacitor). The current response to the AC voltage signal is a sinusoidal wave with the same frequency but different phase and amplitude [97].

If the frequency of the AC voltage is applied from 1 MHz to 0.1 mHz and the data plotted as the imaginary versus the real impedances, two arcs with high and extended frequency ranges appear in the Nyquist plot. The small high frequency and the large extended frequency arcs are representative of concrete (or pore solution) resistance and polarization resistance of reinforcing steel, respectively. Figure 3-18 shows a typical Nyquist curve for concrete or pore solution [98].

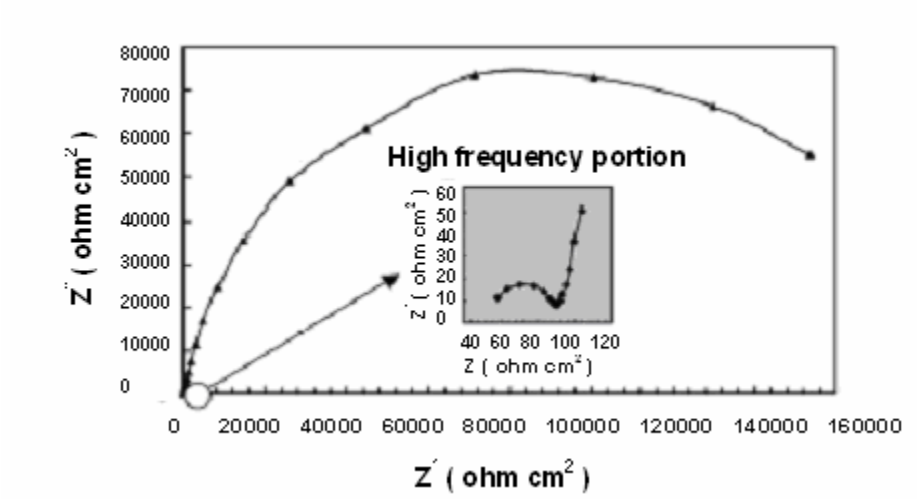

Figure 3-18, A typical Nyquist plot of steel in concrete [98].

By applying an AC high frequency voltage in the range from 2MHz to 0.1 Hz, the concrete resistance can be determined from data such as that shown in Figure 3-19.

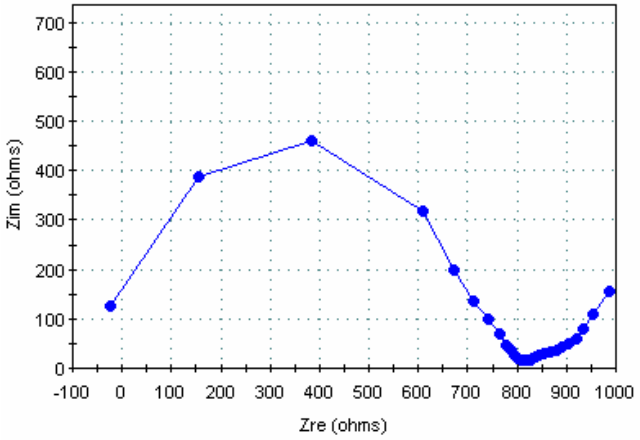

Figure 3-19, The Nyquist plot obtained for measurement of concrete resistance.

3.11- Chloride analysis of concrete prisms

The time needed by chloride ions to penetrate the concrete cover and reach the surface of the rebar depends on the mechanism of intrusion of the chloride ions into concrete. Since the concrete prisms were fully saturated in water prior to exposure to salt solution, the mechanism of chloride penetration into concrete cover would be diffusion due to the driving force caused by the differential concentration gradient [68]. On the other hand,

the chloride ions might penetrate into dry concrete by absorption and the force of the capillary pores due to the wet-dry cycle applied to the concrete prisms. Therefore, to assess the chloride intrusion time, chloride analysis was performed qualitively and quantitatively on concrete prisms.

Silver nitrate solution was used as an indicator to qualitatively measure the penetration depth of chloride ions into concrete [99]. For this purpose, one concrete prism from each type of concrete were broken after 165 and 365 days exposure to saturated salt solution, and 0.1 N silver nitrate solution was dropped onto the fracture surface of prisms. In the first moments that silver nitrate solution in contact with concrete surface, some white spots due to the silver chloride precipitates were observed in areas where chloride had penetrated. After a while, the white colour turned into a pinkish colour and the boundary between the chloride penetrated and free chloride areas was evident.

A measurement of the coloured area with respect to the concrete surface provided the penetration depth of chloride into concrete prisms. According to the literature [99], the chloride ion concentration, at the colour change boundary necessary for silver nitrate to precipitate, was about 0.15% by weight of cement and it may significantly vary with the properties of concrete. Therefore, this technique was not very accurate quantitatively.

For a quantitative measure, the chloride content penetrated into concrete was evaluated by acid-soluble chloride test ASTM C1152 and C114 standard test methods explained in previous sections [81, 82]. The measurement of chloride concentration in different levels of cover depth can allow evaluation of the chloride diffusion coefficient in concrete specimens. A profile grinder allowed concrete powder to be collected at depth

increments of 1.00 mm of concrete prisms. A schematic diagram of the profile grinder used for making powder samples is illustrated in Figure 3-20 [100].

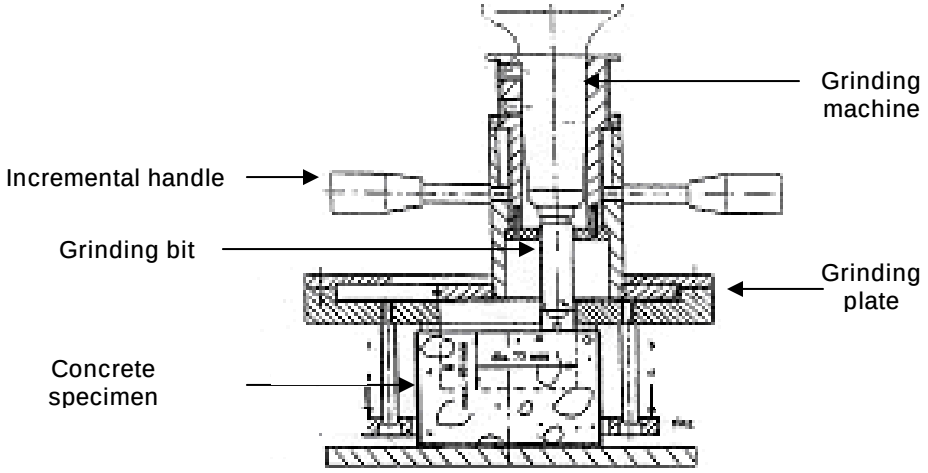

Figure 3-20, Schematic diagram of profile grinder [100].

After more than one year of the wet-dry cycles, one specimen of each concrete was placed centrally between the grinding holder and the bench which was designed for grinding out of dust on specimens of 100 mm thickness. Powders were collected at 5 mm increments to a dept of 30 mm depth with a grinding area of 4180 mm^2.

After each 5 mm grinding sequence, the dust on the side of the cavity was released and collected with a brush, poured into a plastic bag and transferred to the laboratory for titration test. Six different powder samples obtained from 5, 10, 15, 20, 25, and 30 mm depth of each specimen were selected for titration test. The powder was weighed (1.5 gram for each sample) and prepared for acid-soluble chloride test.

The chloride content of the solutions was measured by a chloride ion selective electrode and compared with standard solutions of known chloride content. The results were then converted to percentage by weight of concrete.

3.12- Microscopic observations

Optical and Scanning Electron microscopes were used for observation of different concrete microstructures.

For the optical microscopic observation, at approximately 60 days after casting, one cylindrical standard specimen was randomly selected from each concrete type. Two samples were cut from each cylinder at the depth of 50 and 100 mm of the top of the cylinders. After cutting, one face of the samples was ground with a fine emery paper to obtain a plane surface. Then, samples were placed in the moulding cups and vacuum impregnated to allow the epoxy to be drawn into the microstructure by capillary suction. The importance of utilizing epoxy impregnation technique is strengthening the microstructure and, thereby, preventing the pulling out of cement grains leading to voids [103].

The epoxy was cured at room temperature and made ready for grinding. Abrasive papers of 120, 240, 400,600, 800, 1200 and 2500 (ASTM standard numbers for silicon carbide papers) were used for grinding purpose. Between each stage, specimens were cleaned by immersing in isopropyl alcohol in an ultrasonic bath. Polishing laps, at a low speed were performed with two grades of diamond polishing grit paste; 1 and 0.25 μm.

Also, two series of 120 and 420 day old samples were prepared in the same way for investigation of microstructures by SEM. All mounted samples were carbon-coated after preparation and chloride diffusion of contaminated recycled aggregate into the surrounding cement paste was studied on the 120 and 420 day old samples by EDS technique. For calibration, four cement paste cylinders with water-cement ratio equal to 0.5 and with different chloride contents (0.05, 0.1, 0.5, and 1%) were cast and allowed to

rotate for 24 hours to prevent bleeding and to homogenize the chloride content.

Two samples from each type of cement were cut and prepared for the EDS analysis. The chloride content of the different spots of the cement paste samples was detected by EDS and the average of the values were obtained. As a result, a calibration plot was obtained in which an extrapolated line showed the correlation between the chloride content of concrete samples and the values obtained by EDS.

3.13- Salt scaling resistance test

De-icer salt scaling resistance of concrete slabs to freezing and thawing cycles was measured in accordance with ASTM C 672 [58] and MTO LS-412 [101]. The ASTM C 672 test method can be used to evaluate the effect of mixture proportioning, surface treatment, curing or other variables on resistance to scaling [58].

The slabs were cast with the same mixture proportions as for the first casting. The calculation of the fresh concrete mix proportions can be found in Appendix A. The dimensions of the slabs were 266 mm× 266 mm× 76 mm (Figure 3- 21) to meet the minimum required surface area (0.045 m^2) and depth (75 mm) of concrete specimens specified in standard test methods. In order to overcome the weaknesses of adhered mortar including high porosity and cracks and improve the new interfacial transition zone, a two-stage mixing approach (TSMA), as described in Chapter two), was performed.

The slab surface was levelled off with several passes of a wood strike-off board and was finished with a flat trowel. After the concrete stopped bleeding, the surface was finished with a medium-stiff broom. A 216 mm× 216 mm× 76 mm plastic dike was placed on the top of the slab surface immediately after the final finishing as a ponding

wall. The dike was surrounded by mortar which bonded very well to the concrete slab's surface and provided support to the dike. The interior edges and corners of the plastic dike were sealed with epoxy glue which was resistant to chloride penetration. After finishing, the specimens were covered with wet burlap and plastic sheets and were cured for 24 hours in the moulds.

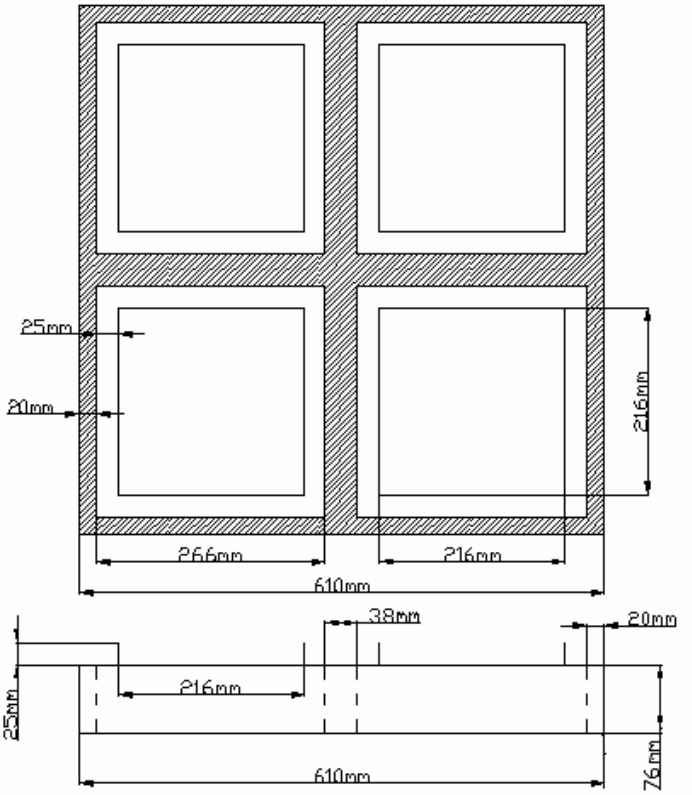

Figure 3-21, The mould dimensions of the concrete slabs.

Thereafter, the specimens were removed from the moulds and kept in a moist room for 14 days at $23 \pm 2\ ^{\circ}$C and 100% relative humidity. The specimens were then taken out from the moist room and stored in room temperature for another 14 days. Figure 3-22 shows the concrete slab for salt scaling resistance test.

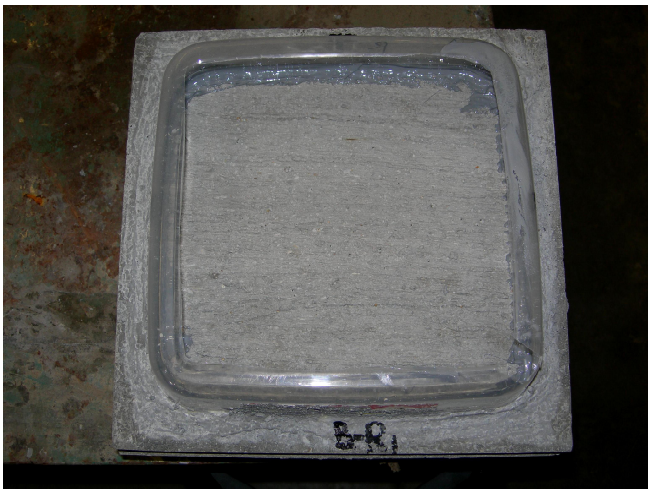

Figure 3-22, Concrete slab for salt scaling resistance test.

The surface of the concrete slabs was covered to a depth of 6 mm with solution of 4% anhydrous calcium chloride and water. The specimens were placed in a freezing and thawing chamber and subjected to 55 freeze-thaw cycles. Each cycle takes 24 hours in which the specimens were exposed to 17 hours at $-18 \pm 3\ ^{\circ}$C and 7 hours at $23 \pm 3\ ^{\circ}$C and 45% to 55% relative humidity. At the end of each series of five cycles, the salt solution was flushed off thoroughly and renewed. The severity of the surface scaling was evaluated by visual observation after each 5 cycles.

The visual rating is very subjective, particularly when the surface is not deteriorated very severely [102]. Therefore, the scaling resistance was also characterized by cumulative mass loss (kg/m^2) method (MTO LS-412) [101] which provides a better quantitative assessment of the surface deterioration than the visual rating of the ASTM C 672. After each five cycles, the scaled-off particles were collected, dried and weighed and, after 55 cycles, the total mass loss of the debris were calculated and divided by the total exposed area.

Chapter 4

Results and Discussion

4.1- Abbreviations used for results and discussion

The results obtained from experimental work are described with accompanying discussion. The abbreviations, NA, NC-RCA and OC-RCA are used for natural aggregate, new clean and old contaminated recycled aggregate while O, R and C with different indices have been displayed in the graphs are representative of concrete made with NA , NC-RCA and OC-RCA.

4.2- Physical properties of coarse aggregates

The results of standard test methods [25, 26, 75, 79, 80, 81, 82, and 84] performed on the three types of coarse aggregates for determining the physical properties are given in Table 4-1. The related calculations are included in Appendix B.

Table 4-1, The physical properties of coarse aggregates.

Concrete types / Test results	Natural aggregate (NA)	New clean recycled aggregate (NC-RCA)	Old contaminated recycled aggregate (OC-RCA)
Water absorption,%	1.42	11.55	5.23
Bulk density (kg/m^3)	2.66	2.28	2.05
Bulk density (SSD) (kg/m^3)	2.69	2.40	2.28
Apparent density (kg/m^3)	2.76	2.58	2.68
Micro-Deval abrasion loss ,%	11.04	34.28	10.59
Adhered cement loss,%	-	37.62	62.61
Chloride content,% of concrete (Ave.)	-	-	0.023

The adhered cement loss after dissolving in nitric acid for old contaminated RCA (62.61%) was greater than that of new clean recycled aggregate (37.62%). Although the

amount of adhered mortar in RCA counts as a determinant parameter for properties of RCA, this can not be the basis of high quality of RCA alone. The water absorption and abrasion resistance of RCA can provide alternative measures of quality.

Comparing coarse aggregate water absorption values, which do not include water adhering to the outside surface of the aggregates, indicates that despite the lower adhered mortar, the NC-RCA was more than twice as permeable as OC-RCA. On the other hand, in the saturated surface dry condition (SSD), the bulk density of OC-RCA was the lowest (2.28 kg/m^3).This shows that the surface of OC-RCA held less water than the other two types of aggregate. Because the NC-RCA is less mature concrete, it may have extra water which would result in a higher porous texture in NC-RCA adhered mortar than those of in OC-RCA.

In addition, the results obtained from Micro-Deval abrasion test showed that the abrasion loss of OC-RCA (10.59%) was about the same as that of natural aggregate (11.04%) but almost three times lower than that of NC-RCA (34.28%). All of these results demonstrate the presence of a dense adhered mortar in OC-RCA with high strength and low porosity.

The average of the OC-RCA concrete chloride content was about 0.023 ± 0.009 % by weight percent of concrete. According to ACI committee 222 [61], the acid-soluble threshold of chloride which may cause the corrosion of reinforcing steel is in the range of 0.025% to 0.0375% chloride by weight of concrete. Therefore, the application of the OC-RCA in new concrete will be acceptable if the diffusion rate of the chloride from old mortar into the adjacent new cement paste in OC-RCA concrete over a certain time remains at a reasonable value.

4.3- Compressive strength test

The measurement of aggregate strength is difficult but it can be obtained by the regular compressive strength test performed on concrete cylinders by implying that "the compressive strength of concrete cannot significantly exceed that of the major part of the aggregate contained therein" [24]. Accordingly, the compressive strength test was performed on the 28 days standard cylindrical specimens. The values obtained for three types of concretes are given in Table 4-2.

Table 4-2, The compressive strength of concrete cylinders after 28 days air curing.

Concrete types / Test results	Concrete made with NA	Concrete made with NC-RCA	Concrete made with OC-RCA
Compressive strength MPa, first measurement	43.5	29.3	51.0
Compressive strength MPa, second measurement	50.3	30.6	49.7
Compressive strength MPa, third measurement	51.0	33.1	49.7
Compressive strength (Ave.) MPa	48.3	31.0	50.1

The results showed that the compressive strength of OC-RCA concrete was comparable to normal concrete while the strength of concrete made with NC-RCA was significantly lower. The fracture surfaces of concrete cylinders were visually examined and are shown in Figure 4-1. It was observed that the fracture passed through the original aggregates in OC-RCA concrete while it passed around the aggregates in normal and NC-RCA concretes. It is likely that the presence of a very well hydrated and a relatively large surface area of adhered mortar in the crushed OC-RCA provided better adhesion between

old and new cement paste than that of is formed in the other two concretes. A layer of fine particles was observed on the fracture surface of NC-RCA which suggests that the adhered mortar in NC-RCA did not possess enough strength and could be fragile under compressive loads.

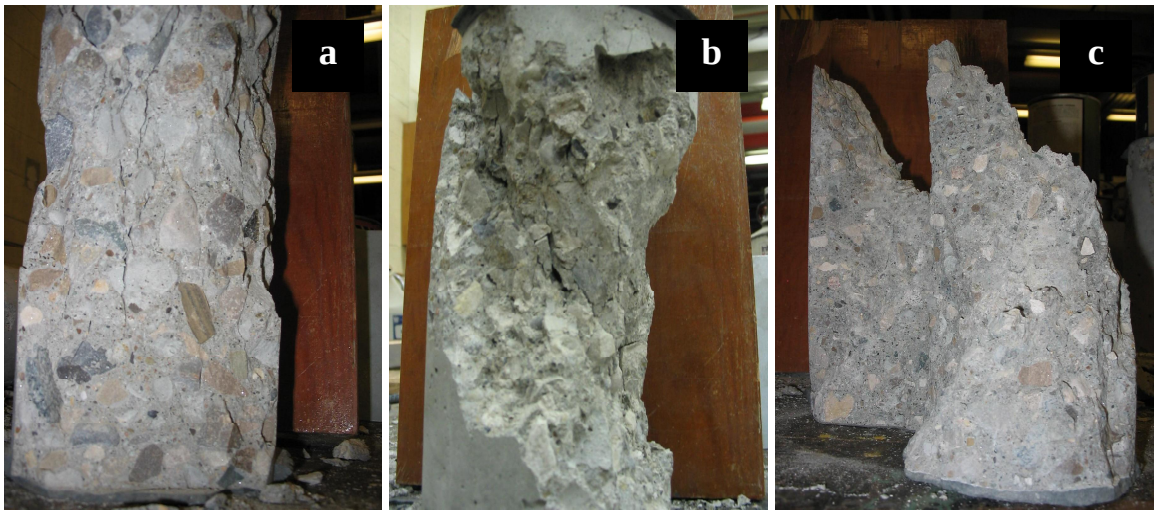

Figure 4-1, the fracture surface of concrete cylinders made with a) natural aggregate, b) NC-RCA and c) OC-RCA after compressive strength test.

4.4- Physical properties of concrete

Due to the influence of porous adhered mortar in RCA on concrete permeability, the evaluation of water absorption and volume of permeable pore space (voids) of the concrete was an essential step to study the durability of RCA concrete. Since these two parameters depend on the mix proportions and the properties of aggregates [8, 19], for a given water-cement ratio (0.43), the water absorption of RCA must be taken into consideration.

Table 4-3 shows the results of ASTM C642-97 Standard test method [88] performed for assessment of density, absorption, and void content in the hardened concretes. The water absorption after immersion and the volume of permeable pore space

(voids) of concrete have received more attention than concrete densities in different conditions which were needed to be measured according to the test procedure. The related calculations are described in detail in Appendix B.

Table 4-3, The properties of different concretes using ASTM C642-97standard test.

Concrete types / Test results	Concrete made with natural aggregate	Concrete made with new clean recycled aggregate	Concrete made with old contaminated recycled aggregate
Absorption after immersion ,%	4.40	9.48	5.11
Absorption after immersion and boiling , %	4.55	10.01	5.32
Bulk density, dry (Kg/ m^3)	2.33	2.04	2.20
Bulk density after immersion (Kg/ m^3)	2.44	2.24	2.31
Bulk density after immersion and boiling (Kg/ m^3)	2.44	2.25	2.32
Apparent density (Kg/ m^3)	2.62	2.57	2.49
Volume of permeable pore space,%	10.62	20.47	11.71

The results showed that, while the water absorption of OC-RCA concrete was slightly greater than that of normal concrete, the value for NC-RCA concrete was more than twice that of the normal concrete. The variation in water absorption of the different aggregates (1.42, 11.55 and 5.23% for NA, NC-RCA and OC-RCA, respectively), described above in Table 4-1, studied with respect to the water absorption of concretes. It shows that, the natural aggregates in normal concrete did not absorb a large amount of water during the mixing and most of the concrete water absorption percentage (about 3%)

must be attributed to the presence of defects and pore spaces (such as capillary pores, air voids and ITZ) in mortar after hardening of concrete.

As far as the water absorption of RCA concretes is concerned, the results indicate that, although RCA had higher water absorption capacity than natural aggregate, the quality of bonding between old and new mortar in RCA concretes controls the water absorption. Concrete made with old and very well hydrated RCA had almost the same water absorption (5.11%) as the aggregate itself (5.23%). Assuming a high quality of original aggregates and 3% of water absorption of new mortar observed in ordinary concrete, the results indicate that this amount was not absorbed in adhered mortar of OC-RCA concrete. Since the volume of voids in OC-RCA concrete (11.71%) was slightly higher than that of concrete made with natural aggregate (10.62%) for the comparable range of strength (48.4 and 50.1MPa for normal and OC-RCA concrete, respectively) , the presence of a very high-quality bond between the old adhered and new mortar can be predicted. In fact, most of the defects in OC-RCA (such as ITZ cracks and voids adjacent to old RCA) which could absorb water might have sealed with the new mortar.

In contrast, NC-RCA concrete showed higher water absorption (almost twice) than those of normal and OC-RCA concrete. Comparing the water absorption of NC-RCA (11.55%) and of concrete made with those aggregates (9.48%) suggests that, the increase in water absorption of NC-RCA concrete is mostly due to the presence of a weak bond between aggregate and new mortar with cracks or other defects. The high volume of permeable pore spaces (20.47%) and the low strength (31.0 MPa) of NC-RCA concrete can be a sign of microstructural defects in adhered mortar, and the microscopic observation was essential to confirm this hypothesis.

4.5- Microscopic observations

Due to its availability and the requirement for less time and less preparation of samples, optical microscopy in reflection mode was a more capable technique than SEM which requires pre-drying and carbon coating of samples. Nevertheless, since there was need to obtain information on the chemical composition of phases and to get a higher resolution, SEM technique was used 120 days after casting the concrete specimens as well.

4.5.1- Optical microscopy observations

Figures 4-2, 4-3 and 4-4 show the microstructure of concretes made with the different aggregates. The normal concrete (Figure 4-2) showed the presence of a relatively good bond between the mortar and aggregate with a small gap along the interfacial transition zone and some disconnected air voids which are distributed randomly in the mortar. Generally, the mortar and aggregates were not cracked.

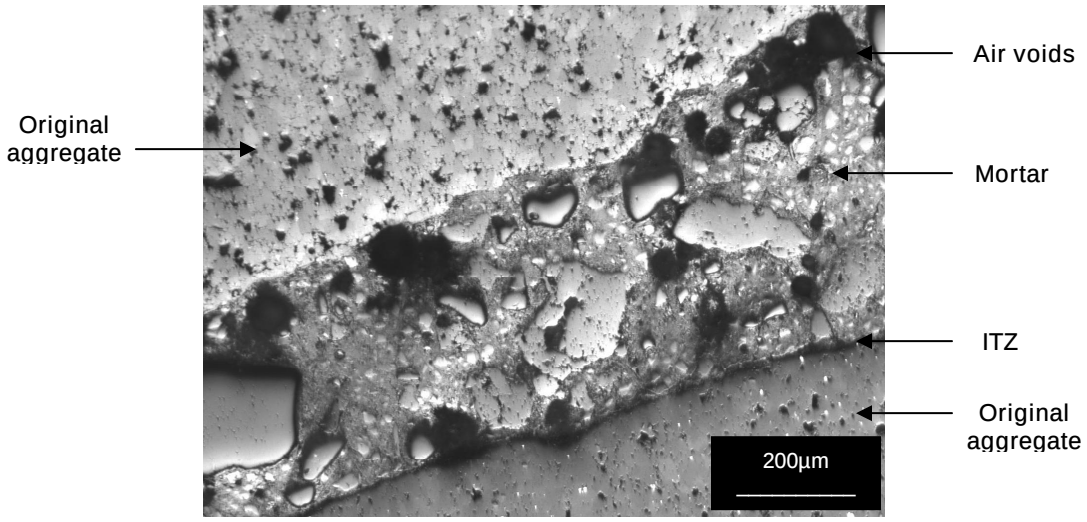

Figure 4-2, The optical micrograph of normal concrete.

The microstructure of NC-RCA concrete, shown in Figure 4-3, consists of cracked old adhered mortar (with a light appearance), the ITZ gap and the new mortar. The density of

cracks in old adhered mortar was high and it might be due to the load applied on the low strength NC-RCA during the crushing.

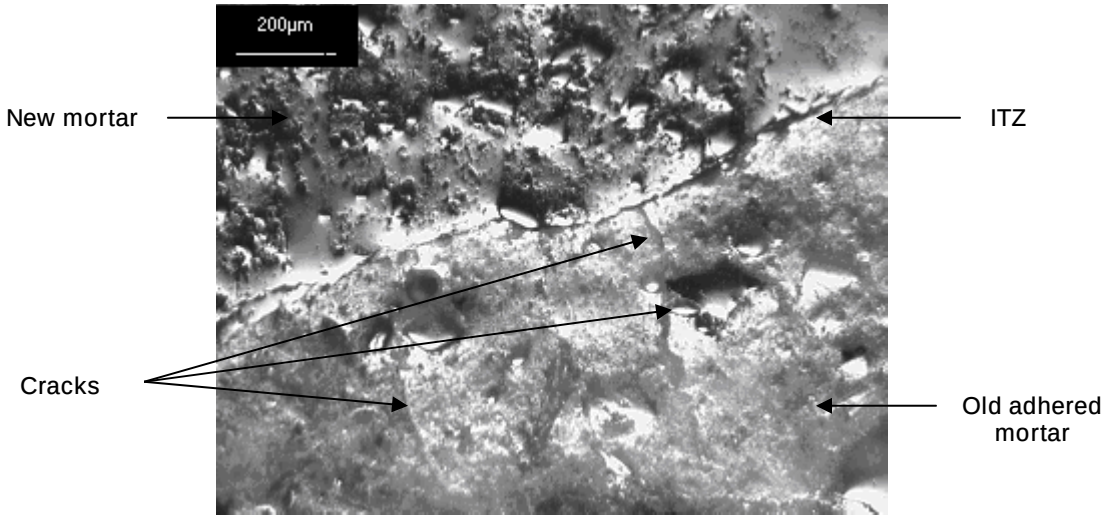

Figure 4-3, The optical micrograph of NC- RCA concrete.

In contrast to NC-RCA concrete, the old adhered mortar of OC-RCA was not highly cracked and high-quality bond between the original aggregate and old adhered mortar, and between the old and new mortars at the ITZs, was observed (Figure 4-4).

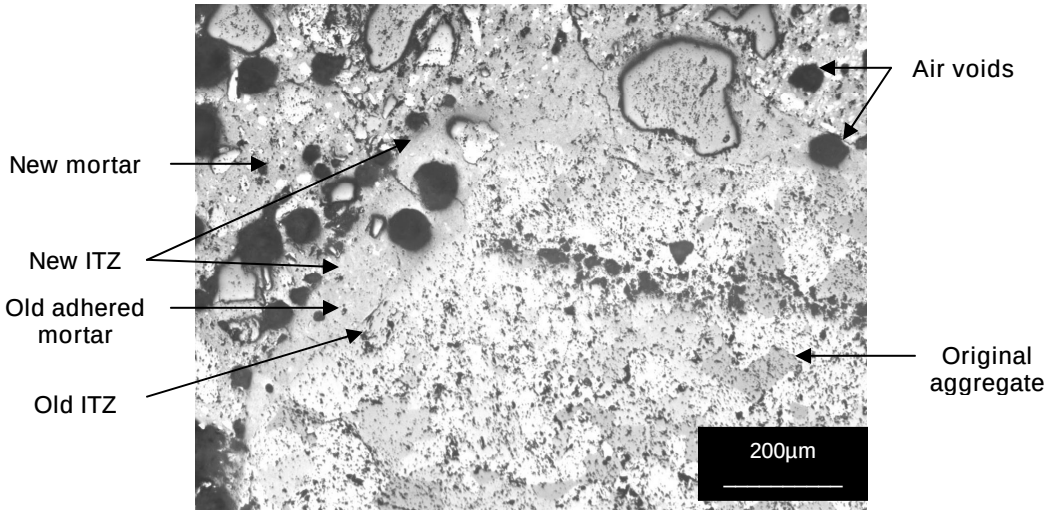

Figure 4-4, The optical micrograph of OC-RCA concrete.

According to the optical observations, the stronger adhered mortar in RCA results in lower cracks and better bonding between the hardened mortar and the RCA.

4.5.2- Scanning Electron Microscopy (SEM) observations

The SEM image of the normal concrete microstructure confirmed the results obtained by optical microscope since no cracks were observed in the mortar (Figure 4-5).

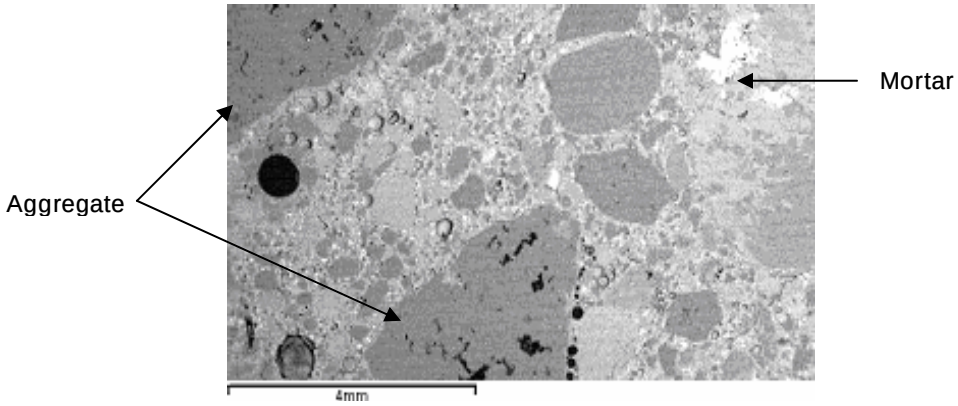

Figure 4-5, SEM image of normal concrete.

The condition of old mortar around the original aggregate in NC-RCA concrete can be observed in Figures 4-6 and 4-7.

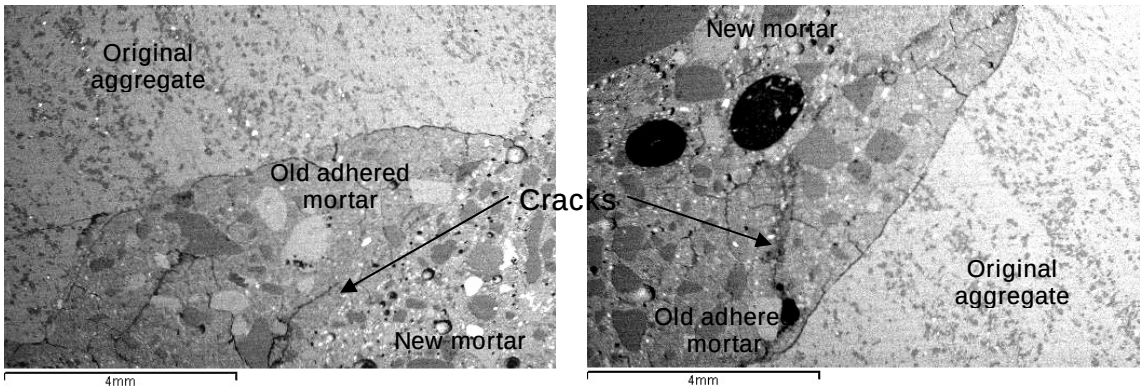

Figure 4-6, The cracked old mortar around original aggregate in NC-RCA concrete.

In addition to the presence of cracks in the old adhered mortar, a longitude opening space was observed on the boundary of original aggregate and old mortar, and between the old and new mortar.

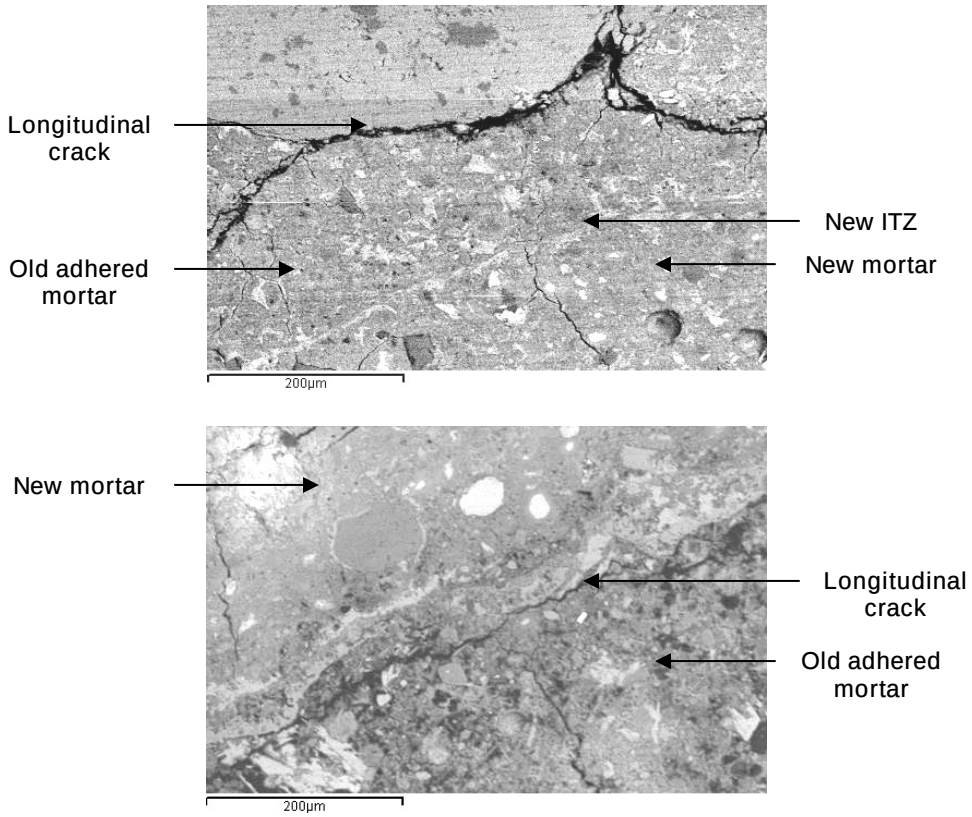

Figure 4-7, longitudinal cracks around the original aggregate and between the old and new mortar in NC-RCA concrete.

A general view of OC-RCA concrete in Figure 4-8 indicates not only that the density of cracks in old adhered mortar was much lower than NC-RCA concrete but also that the bond between constituents in OC-RCA appeared to be significantly better.

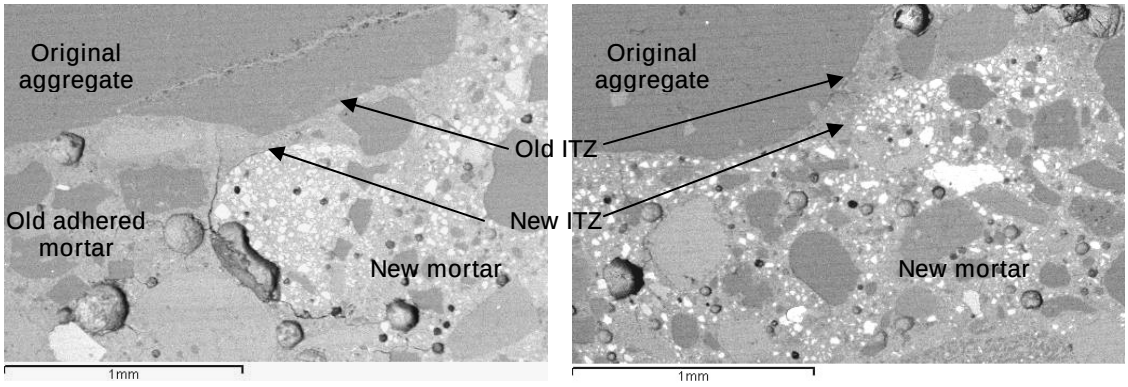

Figure 4-8, The microstructure of OC-RCA concrete.

Although a few cracks initiating from the original aggregate and propagating through the old adhered mortar were observed, it seems that a high quality bonding between the very well hardened old mortar and the new mortar is sufficient to make an appropriate physical and impermeable barrier against the movement of various fluids through OC-RCA concrete. The higher magnified image of the OC-RCA concrete microstructure can be observed in Figure 4-9.

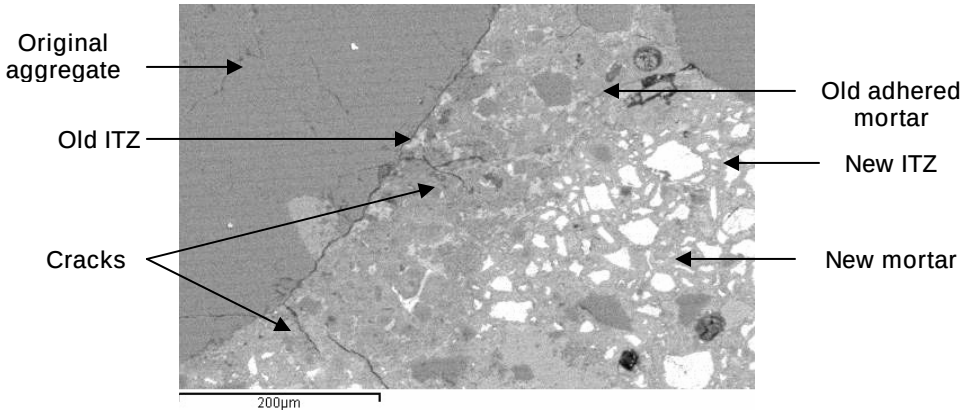

Figure 4-9, OC-RCA microstructure.

In order to study the effect of two-stage mixing approach (TSMA) on the microstructure of adhered mortar, 120 day old samples, taken from the second concrete mixture, were observed under SEM microscopy.

The images (Figures 4-10, 4-11, and 4-12) illustrated that the cracks in old adhered mortar and the new and old interfacial transition zones were healed by the cement slurry in all three concretes. This indicates that applying this mixing method can be used as an efficient technique to provide an improved microstructure leads to a greater compressive strength of RCA concrete.

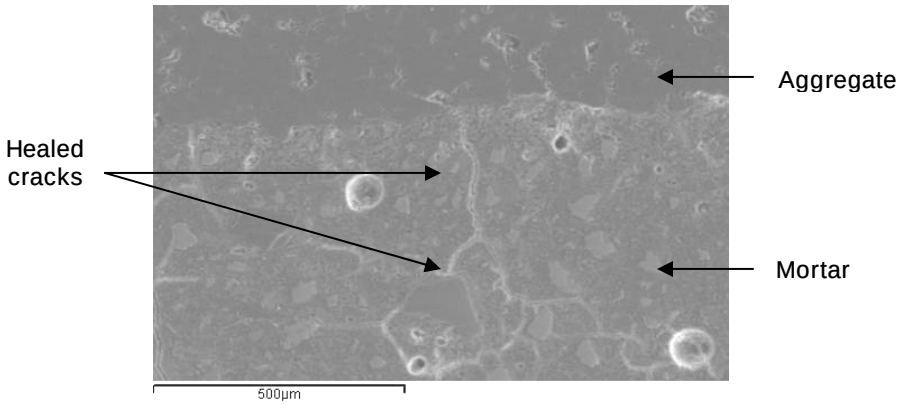

Figure 4-10, The microstructure of 120 day old normal concrete samples.

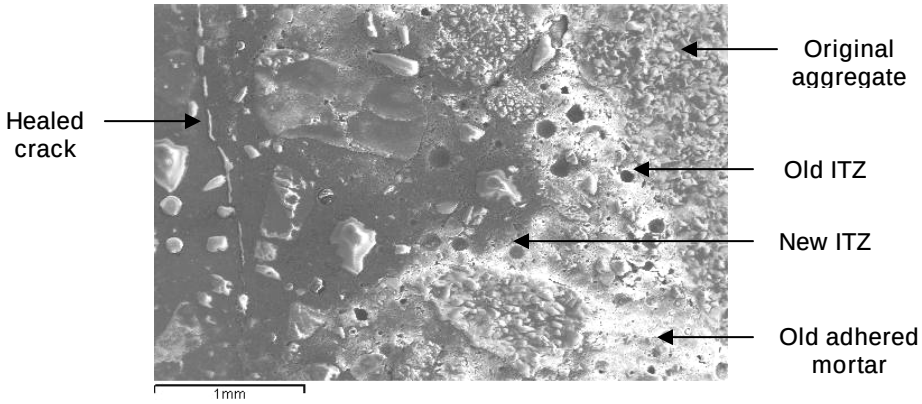

Figure 4-11, The microstructure of 120 day old NC-RCA concrete samples.

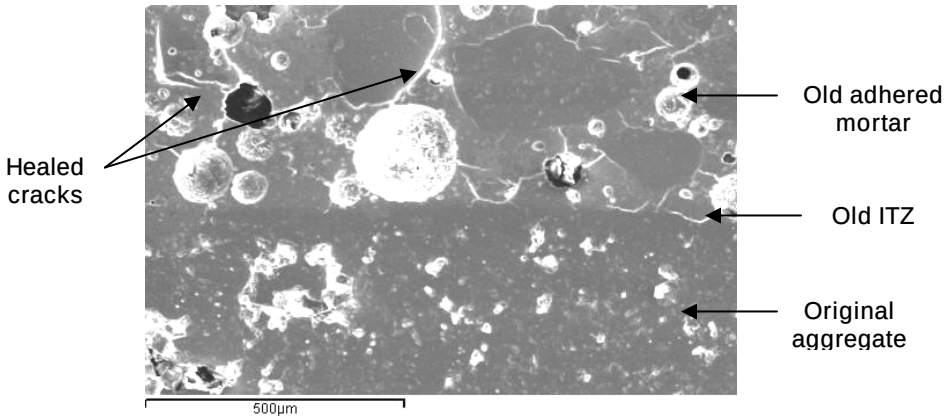

Figure 4-12, The microstructure of 120 day old OC-RCA concrete samples.

4.5.2.1- The chloride analysis of OC-RCA concrete by EDS

To investigate the rate of the chloride diffusion from OC-RCA into the surrounding cement paste, 120 and 420 day old samples were studied by EDS. Figures 4-13 and 4-14

show the re-calibrated percentages of the chloride by weight of concrete on the different distances from the original aggregate.

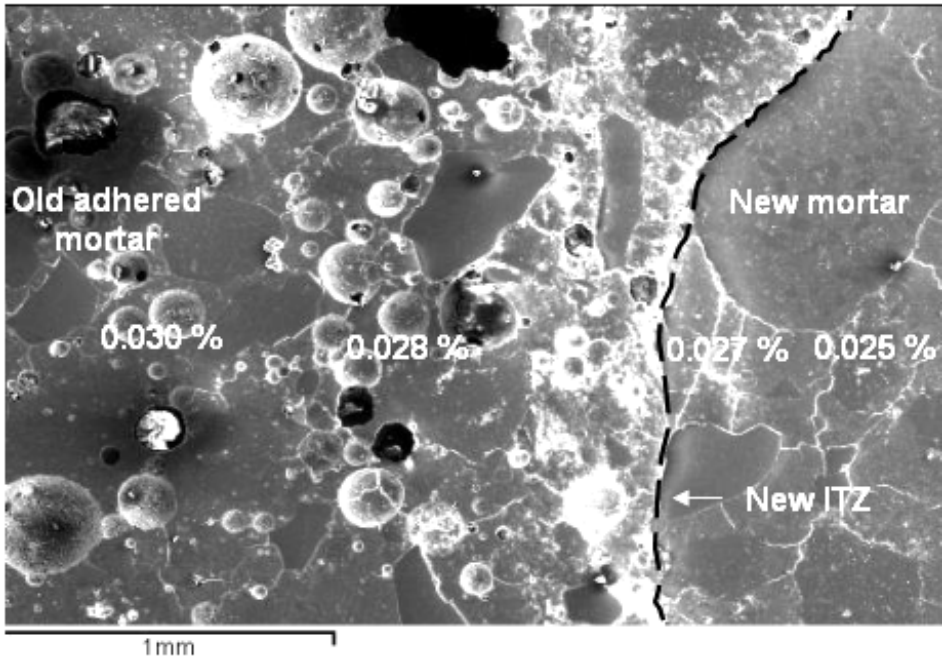

Figure 4-13, Distribution of chloride in 120 day old OC-RCA concrete.

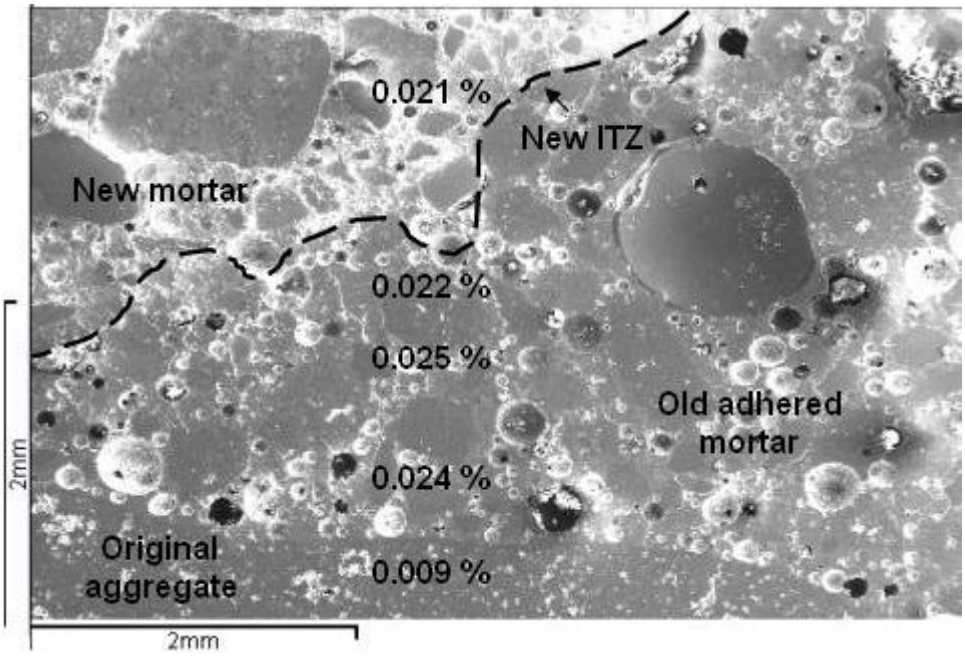

Figure 4-14, Distribution of chloride in 420 day old OC-RCA concrete.

Comparing the distribution of chloride in OC-RCA concrete at different ages indicates that the diffusion rate of chloride is relatively fast and, therefore, is not influenced by the age of the concrete. Although Figure 4-13 indicates that the greater the distance from the old mortar, the lower the chloride concentrate in the new mortar, the values are too close to be definitive.

4.6- Corrosion measurement of reinforcing steel

4.6.1- Corrosion probability of reinforcing steel

The half cell potential was measured between the steel rebar in the concrete prisms and a silver-silver chloride reference electrode embedded in the hand held electrode set of the Galvapulse instrument. Although this technique does not provide the information on the corrosion rate, the corrosion probability of reinforcing steel can be evaluated provided that the effect of variables such as ambient temperature, moisture content, cover depth quality and conductivity of concrete will be considered on the obtained results [104, 105]. Among these factors, the laboratory ambient temperature and the cover depth of different concretes were almost constant but the moisture content and concrete resistance would change due to the wet-dry cycles on the concrete prisms. With respect to this, a "sinusoidal" variation of corrosion potentials was observed for all reinforced concretes over the one year period of measurement.

The more negative values at the high points of sinusoidal curves represented the corrosion potentials measured after wet cycles while the more positive values at the low points corresponded to the steel corrosion potentials measured after dry cycles. Figure 4-15, shows the variations of the steel rebar corrosion potential over the one year for three types of concrete.

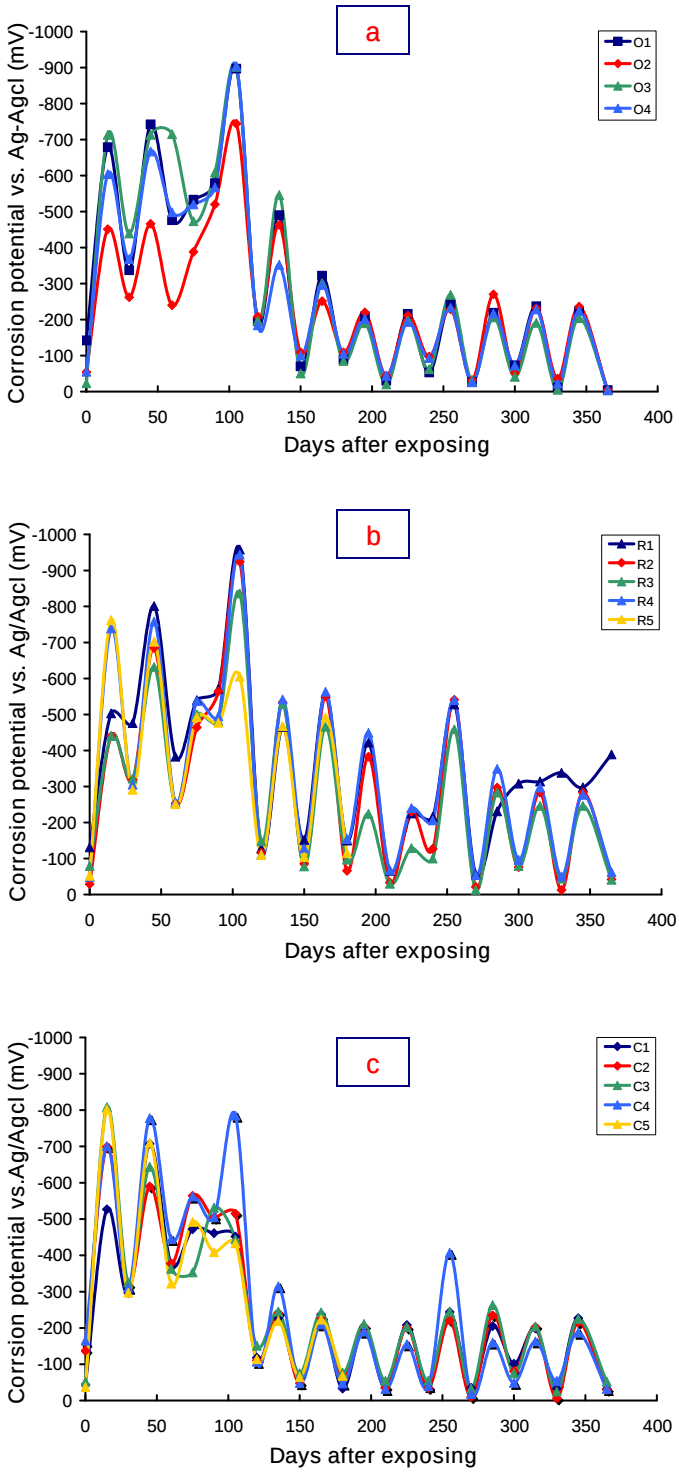

Figure 4-15, The corrosion potential of reinforcing steel in a) NA concrete b) NC-RCA concrete and c) OC-RCA concrete vs. Ag-AgCl for 1 year of wet-dry cycles.

The corrosion potential values were in good agreement with the ones obtained by means of Parstat instrument which used saturated calomel reference electrode. The results indicated that the corrosion potentials reached very negative values after the exposing of concrete prisms in saturated salt solution without a significant increase of corrosion current density, which will be described later.

After almost 3 months, the corrosion potentials shifted to more positive values and remained almost at the same levels for the remainder of the year. Although the trend of corrosion potential behaviour over the time was the same for all concretes, more fluctuations were seen for the concrete made with NC-RCA than those of normal and OC-RCA concrete. It might be due to the greater porosity of this concrete compared to other types of concretes, and consequently greater access of the steel to oxygen and moisture.

Since the concrete prisms had remained at room temperature for 45 days after casting and were then exposed to chloride-free water, the capillary absorption of pores would have been high enough to fully saturate the concrete with water at the beginning of the exposure. Therefore, in wet concrete, the potential of rebar could shift to the more negative values (up to -1000 mV vs. Ag/Agcl) [106].

During drying cycles, the reinforcing steel potentials increased to more positive values. Since the relative humidity of concrete in dry and wet cycles could be varied, the corrosion potential of steel showed the sinusoidal bahaviour during the measurement.
Among all the concrete prisms, R_1, presented in Figure 4-15 (b), did not continue to follow the normal sinusoidal trend of graphs. Instead, it showed a constant active corrosion potential (about -300 mV vs. Ag/AgCl) after 285 days. Thus, the probability of

steel corrosion in this prism seemed to be higher than that of the other prisms and the steel rebar in this prism was inspected visually.

4.6.2- Corrosion current density results measured by Parstat

Figures 4-16, 4-17 and 4-18, illustrate the corrosion current density values of rebar in concretes measured over the one year in wet-dry, wet and dry cycles, respectively, assuming the corrosion rate is uniform over one-third of the exposed area of rebar.

The LPR data have lower overall values and lower and more consistent fluctuations between the wet and dry cycle measurements. This was particularly true for the steel in NA and OC-RCA concrete prisms which showed a very good agreement with each other (0.15 to 0.2 $\mu A/cm^2$ and 0.3 to 0.8 $\mu A/cm^2$ in wet and dry conditions, respectively).

The steel in NC-RCA, on the other hand, exhibited high corrosion rates and greater and more variable fluctuations than the other two sets of specimens. Deviations from the regular "sinusoidal" trend of the curves and the i_{corr} values started to increase approximately from 0.18 $\mu A/cm^2$ at 270 days and ended up to 1.7 $\mu A/cm^2$ at 365 days. Note that, the values of i_{corr} were average values based on the overall polarized steel surface, and it was not representative of corrosion current density values caused by localized attack [108]. A typical curve obtained by Parstat used for current density measurement is shown in Appendix C.

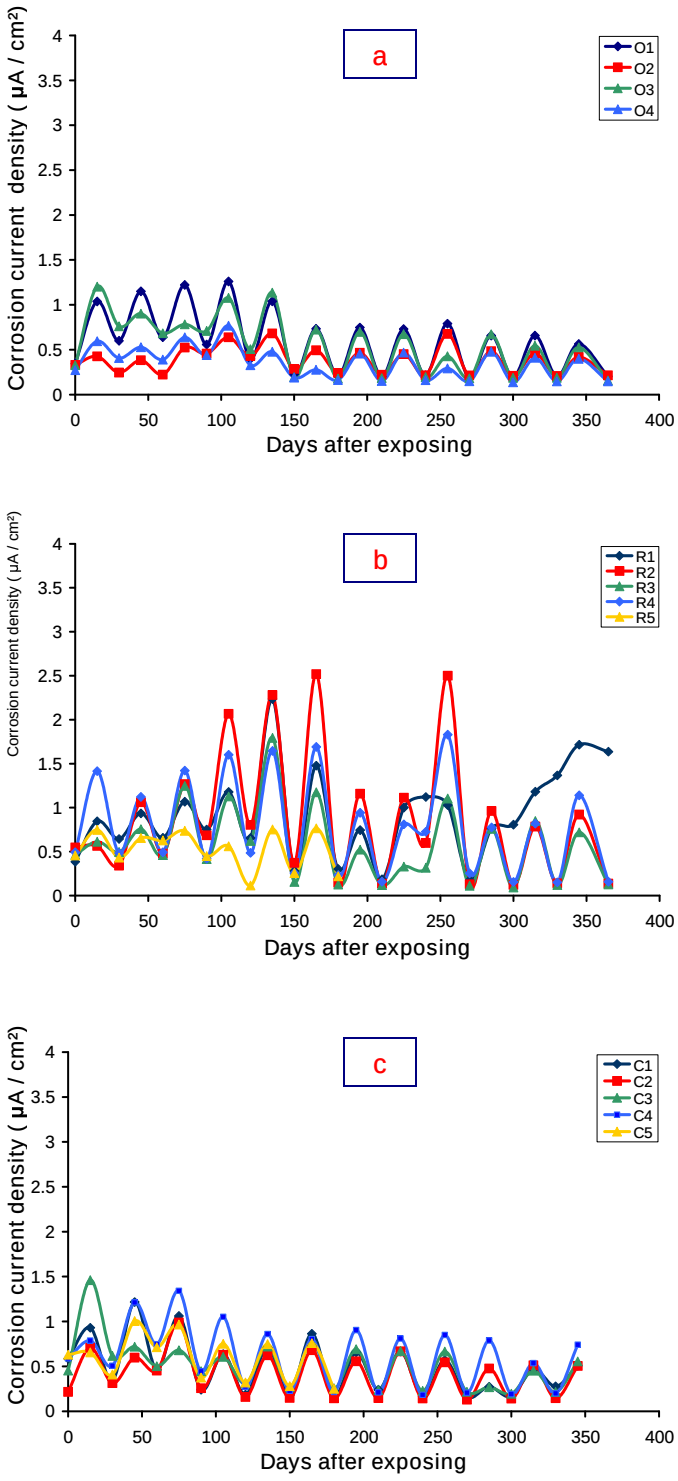

Figure 4-16, Corrosion current density of steel measured by Parstat over 1 year wet-dry cycles for a) NA concrete b) NC-RCA concrete and c) OC-RCA concrete.

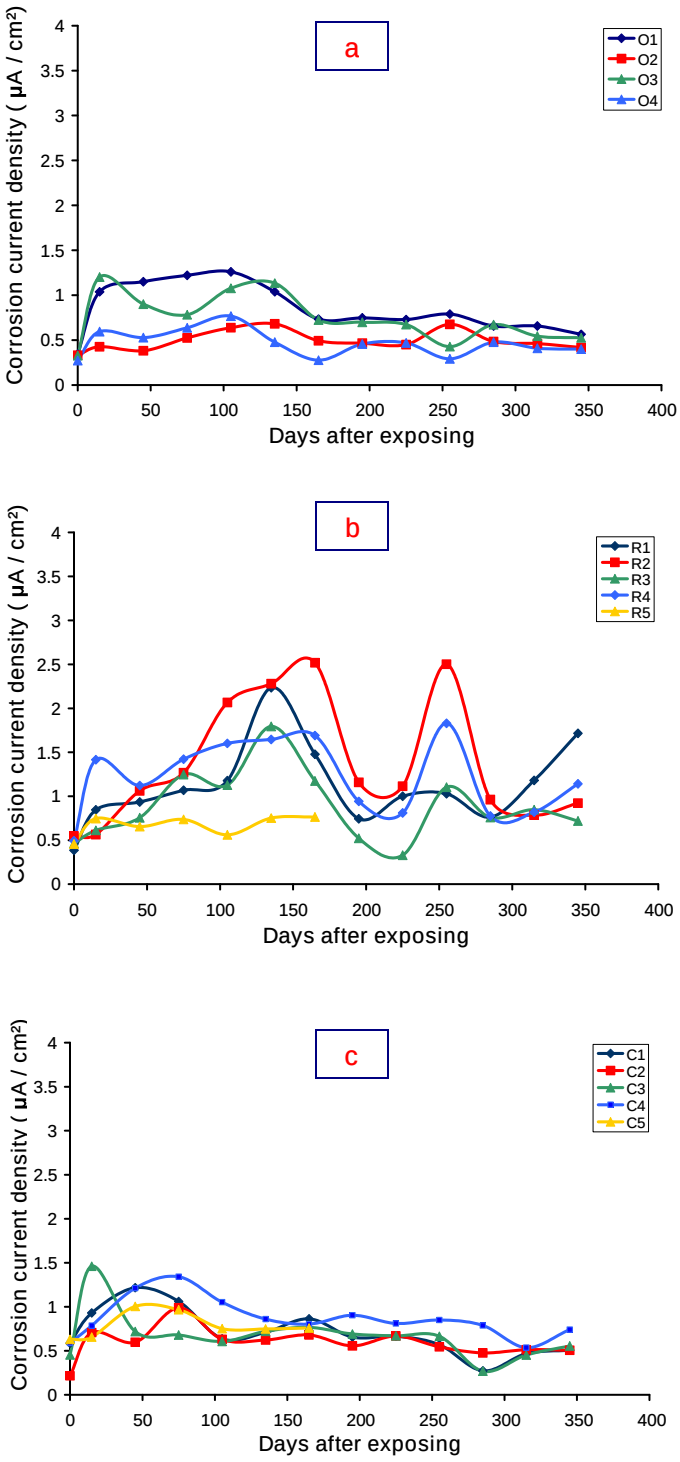

Figure 4-17, Corrosion current density of steel measured by Parstat over 1 year wet cycles for a) NA concrete b) NC-RCA concrete and c) OC-RCA concrete.

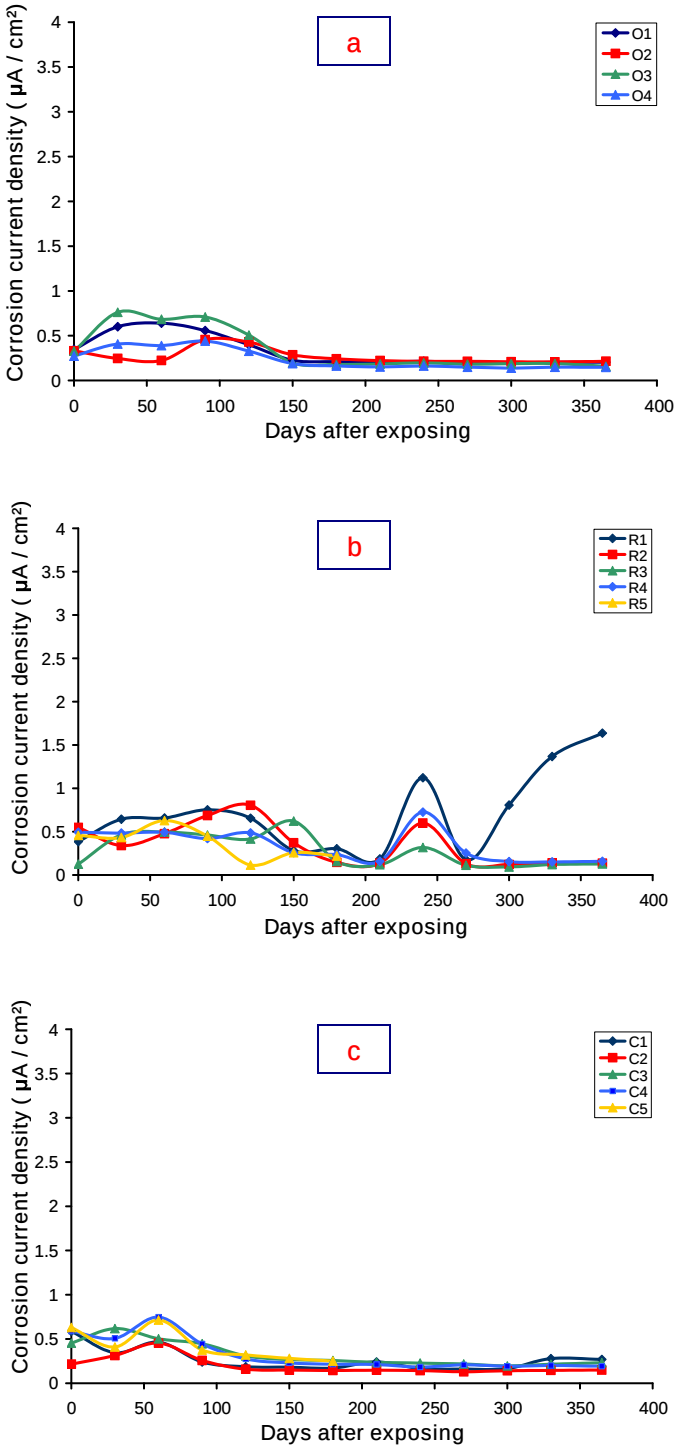

Figure 4-18, Corrosion current density of steel measured by Parstat over 1 year dry cycles for a) NA concrete b) NC-RCA concrete and c) OC-RCA concrete.

4.6.3- Corrosion current density results measured by Galvapulse

Generally, the corrosion current density (i_{corr}) results obtained from the galvanostatic pulse technique using the Galvapulse instrument (Figures 4-19, 4-20 and 4-21) were greater (almost 2 to 4 times) and exhibited more fluctuations than those obtained from the potentiostatic LPR using the Parstat equipment, particularly at the beginning of the exposure time.

The visual chloride penetration test performed after 165 days exposing on the NC-RCA and OC-RCA concrete prisms indicated that the chloride ions had not reached the surface of the passive steel rebar while the measured corrosion current density values of the steel rebar were still high . This suggests that the basic idea of using a guard ring in the Galvapulse to minimize and confine the electrical pulse in a defined region of the reinforcing steel [92, 94,106], could not be accomplished in the case of passive steel rebar.

The effective parameters on the over-estimating of I_{corr} have not been very well understood, but some variables such as “the effect of wetting conditions, surface morphology and presence of resistive layers in concrete” [107] can influence the corrosion current density values.

The “sinusoidal” behaviour of the corrosion current density was seen for all types of concretes and exposure conditions particularly for concrete prisms after wet-cycles.

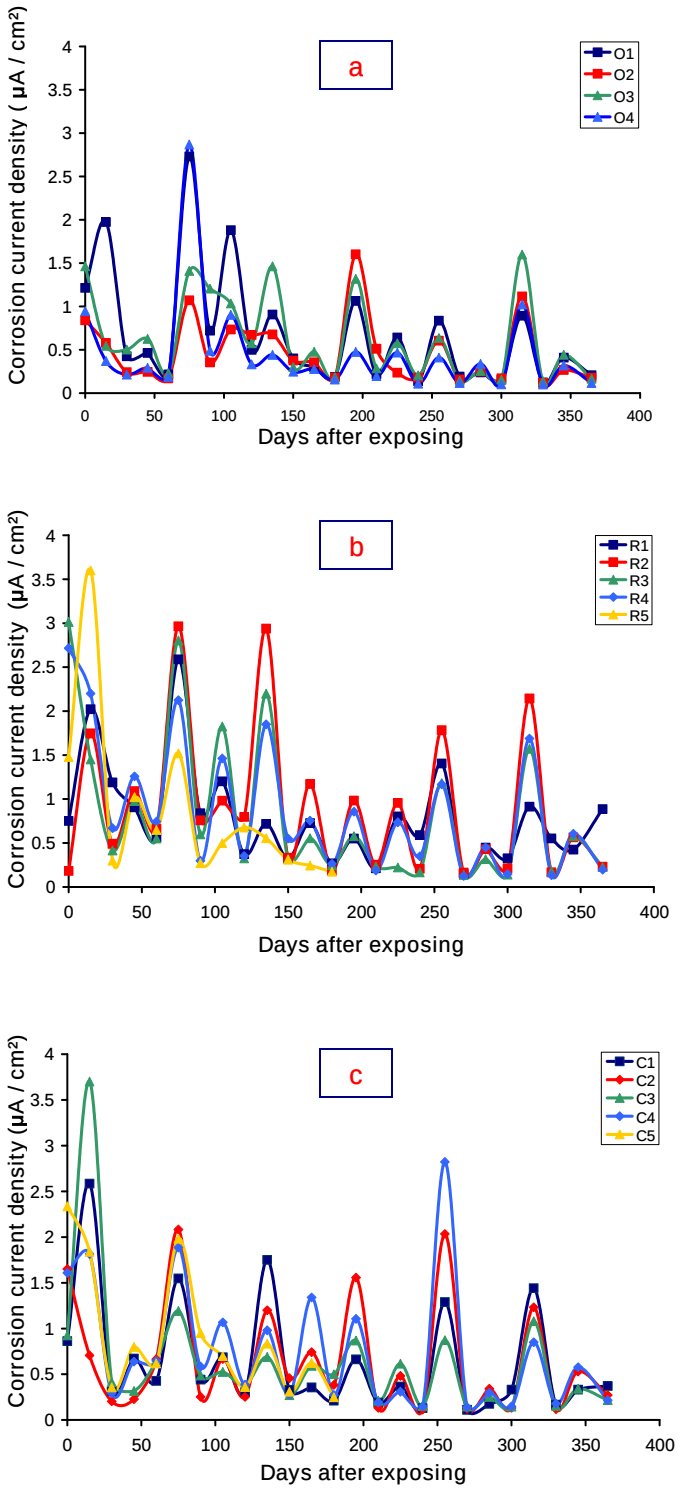

Figure 4-19 , Corrosion current density of steel measured by Galvapulse over 1 year wet-dry cycles for a) NA concrete b) NC-RCA concrete and c) OC-RCA concrete.

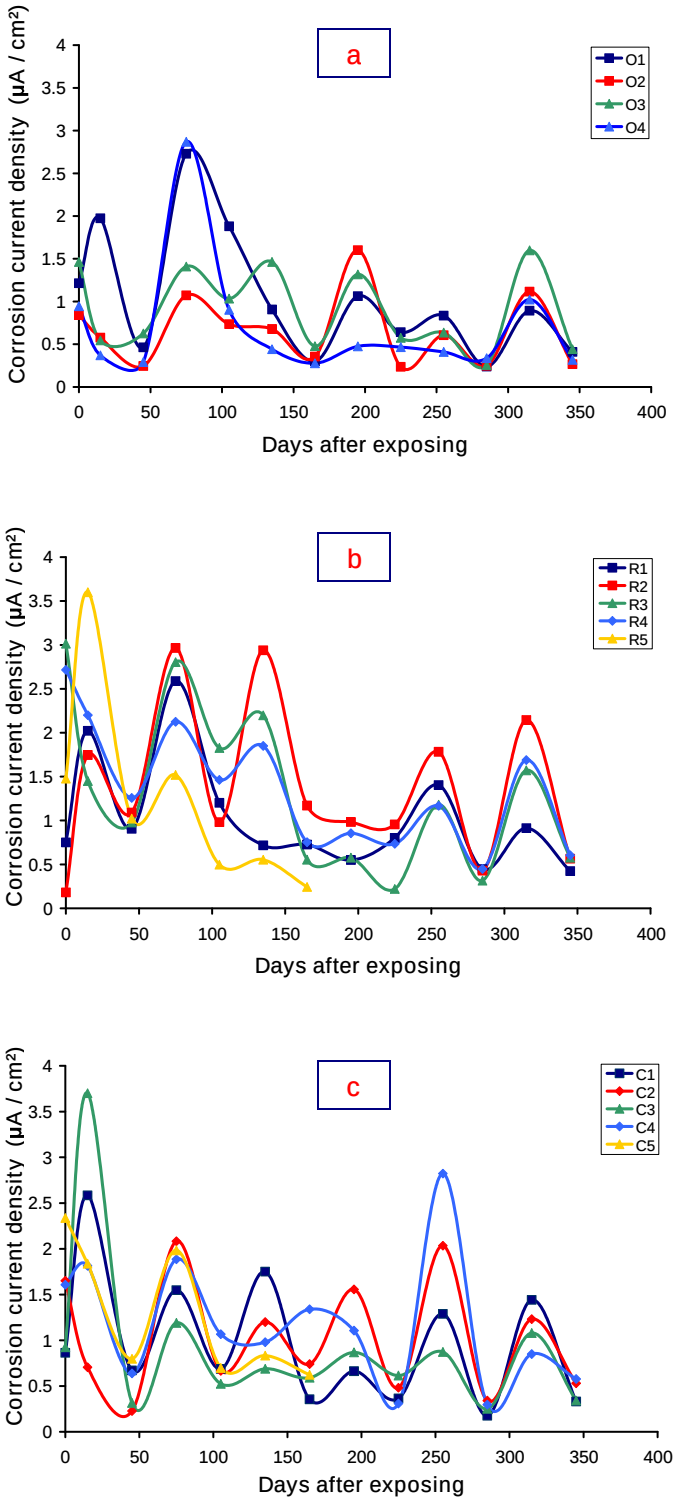

Figure 4-20, Corrosion current density of steel measured by Galvapulse over 1 year wet cycles for a) NA concrete b) NC-RCA concrete and c) OC-RCA concrete.

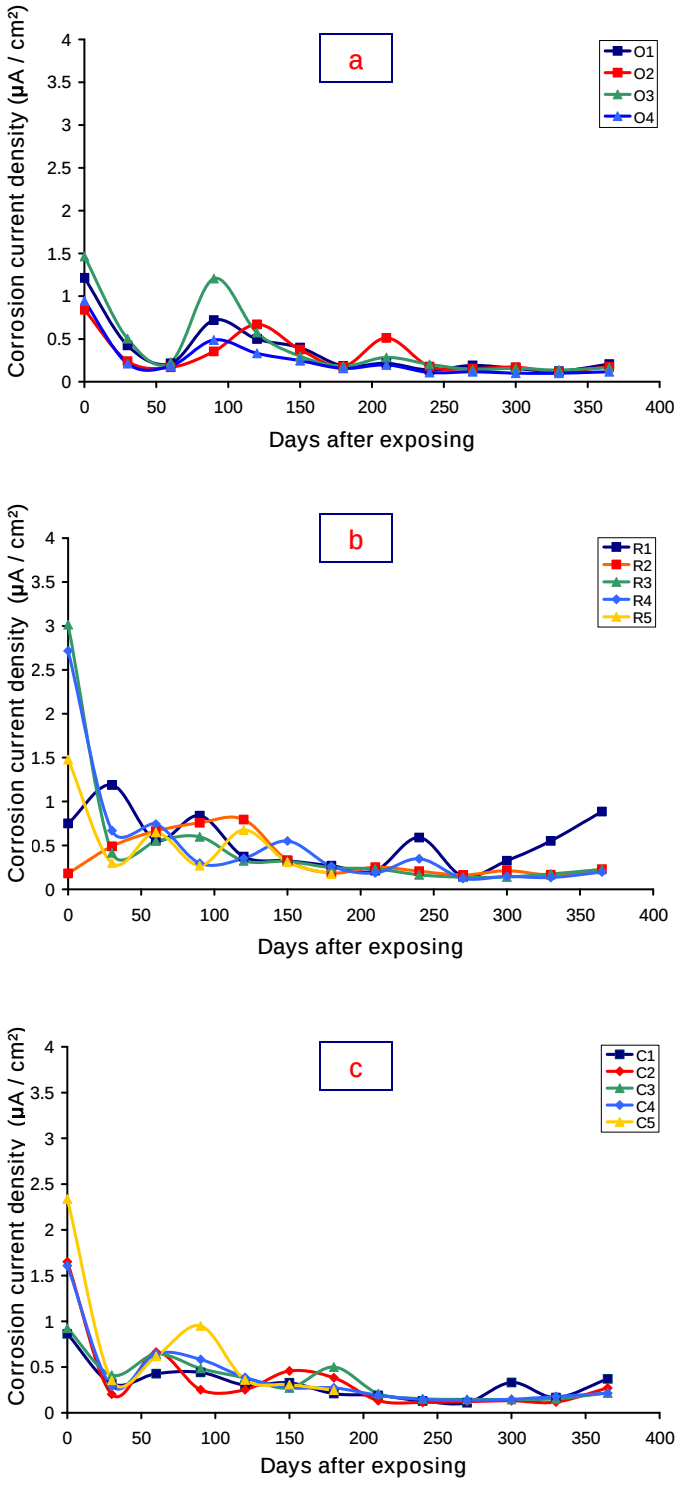

Figure 4-21 , Corrosion current density of steel measured by Galvapulse over 1 year dry cycles for a) NA concrete b) NC-RCA concrete and c) OC-RCA concrete.

4.6.4- Cyclic polarization results

Cyclic polarization was performed on the selected prisms (namely O_1, R_1 and C_1) to determine the localized corrosion susceptibility of reinforcing steel in three different types of concrete. This test was performed (i) before beginning of the prism immersion in saturated salt solution and (ii) every 45 days after one of the NC-RCA concrete prisms (R_1) showed a continued increase in corrosion rate. The cyclic polarization curves are illustrated in the Appendix C. Pitting potentials were not observed through the overall view of the plots for all types of concrete including the R_1 concrete prisms which showed the highest value of corrosion current density among the concrete prisms. It may be because the potential was not increased to a sufficient positive value or the corroded area was relatively small. Figure 4-22, 4-23 and 4-24 show the cyclic polarization curves obtained at 380 days after exposing the O_1, R_1 and C_1 concrete prisms, respectively.

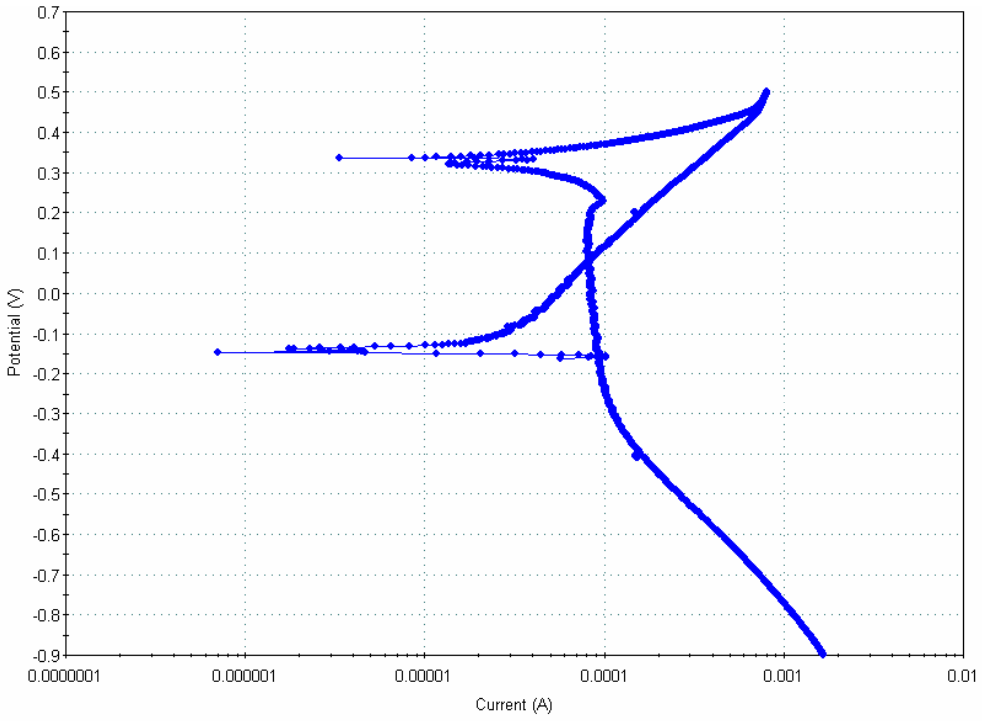

Figure 4-22, Cyclic polarization curve for steel in O_1 prism after 380 days exposure.

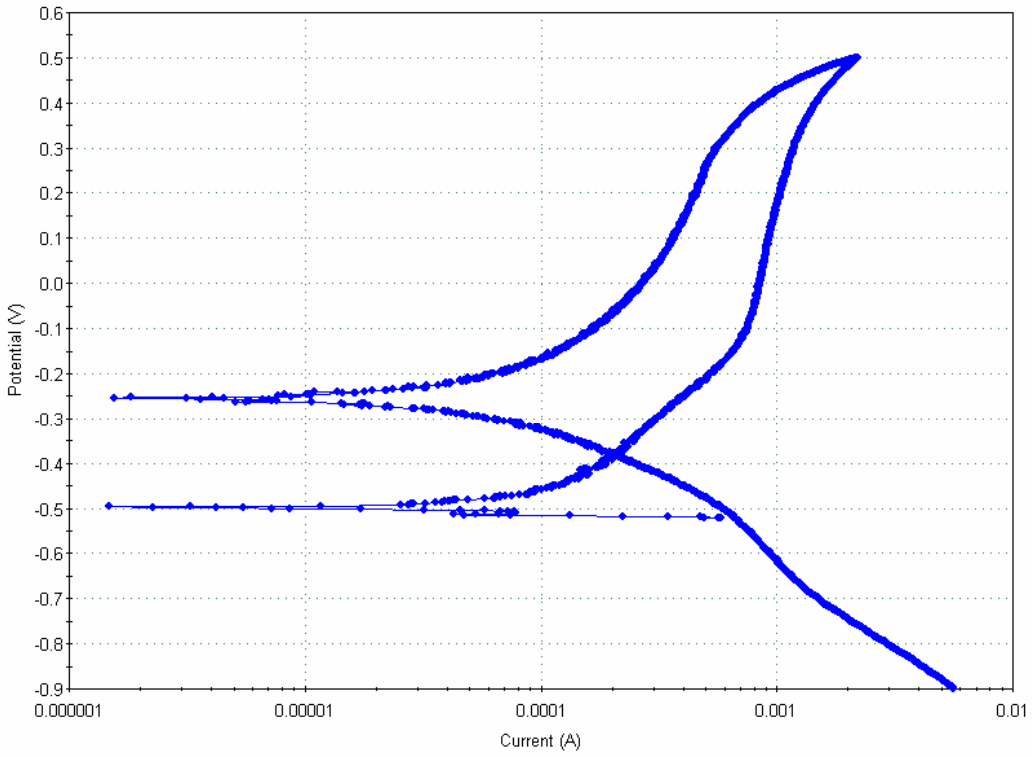

Figure 4-23, Cyclic polarization curve for steel in R_1 prism after 380 days exposure.

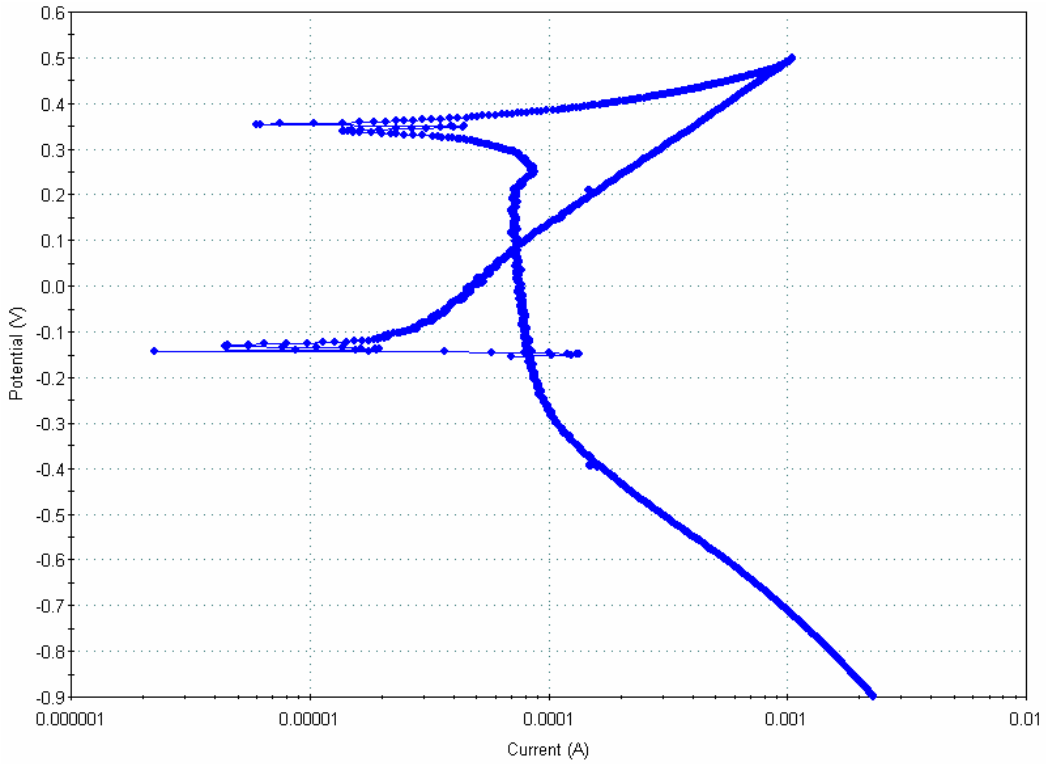

Figure 4-24, Cyclic polarization curve for steel in C_1 prism after 380 days exposure.

Generally, on decreasing the potential from + 500 mV vs. SCE, all the curves shifted to lower currents indicative of passive behaviour, however, the size of the hysteresis loop, decreased over time. The corrected values of corrosion current density ($\mu A/cm^2$) obtained by extrapolating the anodic branch, were 2.1, 10.6 and 1.6 $\mu A/cm^2$ for O_1, R_1 and C_1 concrete prisms, respectively. These values are based on an exposed area of steel rebar to chloride ions was considered as one–third of the rebar circumference.

The appearance of the curves for O_1 and C_1 was very similar at all measurement times, and the sharp downward shift of the reversed branch after the second open circuit potential (about 0.35V) indicates the probability of oxygen limitation at 8×10^{-5} A for these two concrete prisms. No such oxygen limitation was observed in any of the R_1 cyclic polarization curves which confirms the high permeability of this prism.

4.7- Concrete electrical resistance results

Figure 4-25, compares the electrical resistance of concrete prisms measured by different techniques. GP, EIS and GS in the legends represent for Galvapulse, EIS and Galvanostatic pulse techniques.

The galavnostatic pulse measurement of concrete resistance by means of Galvapulse was started from the beginning of the exposure of the concrete prisms in saturated salt solutions and was continued every two weeks on wet and dry conditions of concrete. It was obviously found that, by increasing the concrete electrical resistance, the corrosion current density of reinforcing steel decreased. The results were almost in good agreement with the corrosion current density measurements until 150 days after exposing the concrete prisms. The relatively sharp increase in concrete electrical resistance values after that time, suggested the use of other techniques to evaluate these results. For this

purpose, the galvanostatic pulse technique (GPT), applying the same current (25μA) and time (60 seconds) as the Galvapulse, and the EIS technique, both by means of Parstat instrument, were used after 225 days. The results illustrated the same "sinusoidal" trend that was observed for corrosion current density and corrosion potential for all types of measurement techniques, but the GPT and EIS techniques exhibited much lower "amplitudes".

Although the values of concrete resistances measured by EIS and gavanostatic pulse technique (GPT) using the Parstat were similar, they were almost 3 to 5 times lower than those of measured by the Galvapulse. This difference was the least for NC-RCA concrete prisms which showed higher corrosion rate and permeability than those of the other sets of concrete prism. Among the three different types of concrete, NC-RCA concrete showed the lowest and almost a constant range of resistance (average less than 1KOhm) over time from which R_1 prism remained at the lowest concrete resistance values all the times. The low electrical resistivity of NC-RCA concrete is consistent with the high negative values of corrosion potential and higher current density of steel in this type of concrete.

The presence of the corrosion products on the surface of the reinforcing steel at the end of the measurements (after 365 days) in R_1 concrete prism, shown in Figure 4-29, specifies that, the accuracy of the values measured by Galvapulse is more dependent on the permeability of the concrete and consequently the active behaviour of reinforcing steel. In contrast, the Parstat can be used as an accurate instrument for electrochemical measurements (using potentiostatic LPR technique) and the concrete electrical resistance regardless the condition of the concrete.

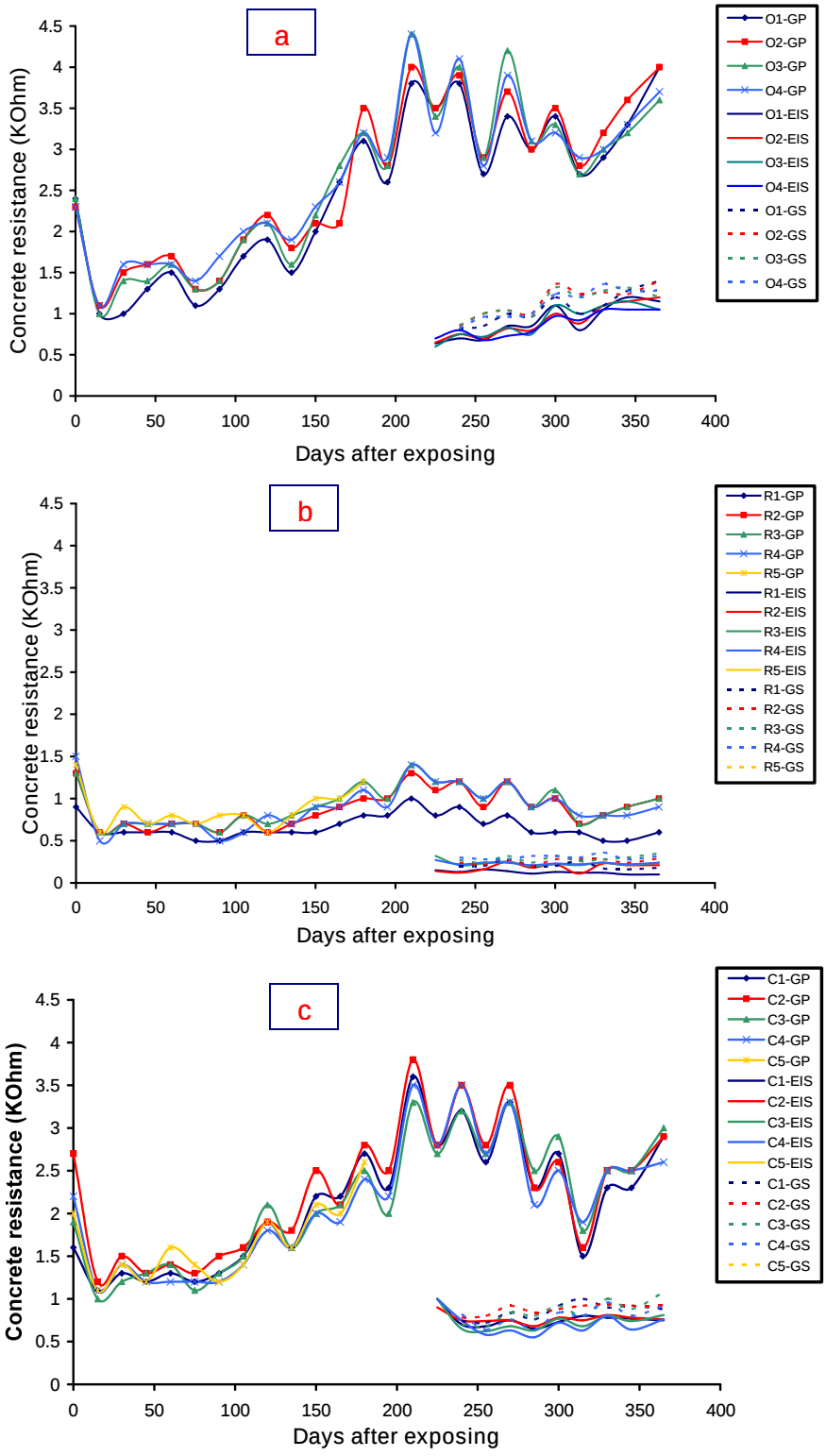

Figure 4-25, The resistance of a) NA concrete b) NC-RCA concrete and c) OC-RCA concrete measured by GalvaPulse, GPT and EIS (in Parstat) over 1 year.

4.8- Chloride penetration analyses

For applying the silver nitrate solution indicator method, R_5 (from the NC-RCA concretes) and C_5 (from the OC-RCA concretes) were selected randomly and were broken after 165 days exposure to saturated salt solution. The 0.1 N silver nitrate solution on the fractured surface of broken prisms indicated a maximum of about 35 and 20 mm depth of chloride penetration into NC-RCA and OC-RCA concrete, respectively, as illustrated in Figures 4-26 and 4-27.

Figure 4-26, The depth of penetrated chloride in NC-RCA concrete after 165 days.

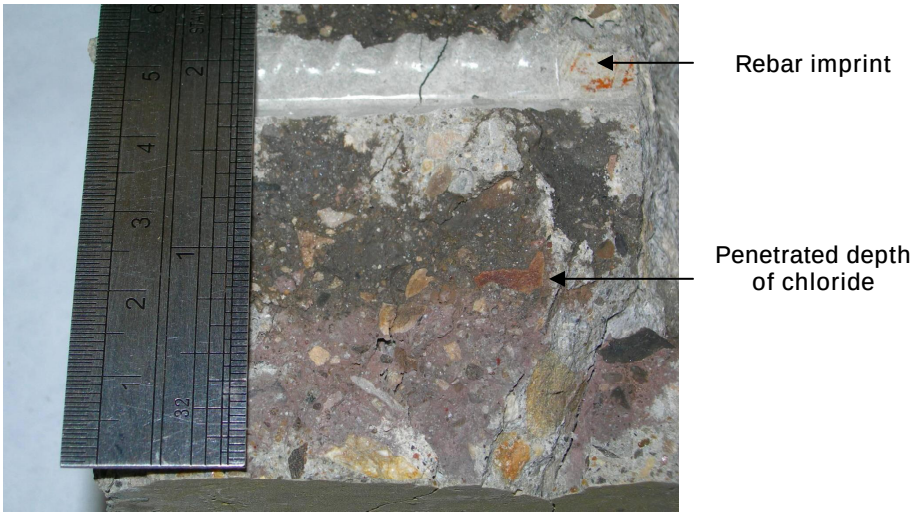

Figure 4-27, The depth of penetrated chloride in OC-RCA concrete after 165 days.

Concrete profile grinding was performed on one sample from each set of concrete prisms (O_1, R_1 and C_1) at 380 days after the exposure time to determine the chloride content (by weight percent of concrete) penetrated into concrete at different depths.

Since the grinder was not able to pulverize the concrete at depths greater than 30 mm, the surface layer of the concrete adjacent to the rebar after cutting the prisms was also ground by a cylindrical-radius end carbide burr and analyzed to give the chloride content at the surface of the rebar. Figure 4-28, shows the trend of the chloride diffusion into the depth of concrete prisms.

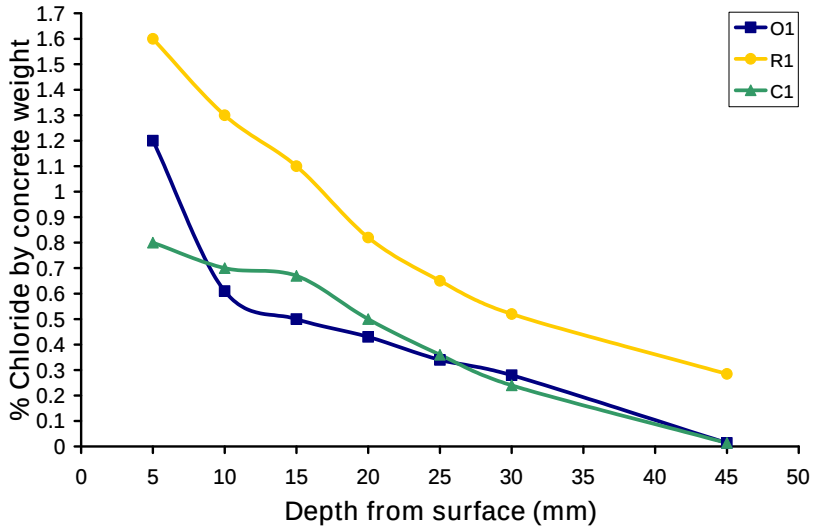

Figure 4-28, chloride content of prisms at different depths, 380 days after exposure.

The values of the apparent chloride diffusion coefficient, using linear curve fitting and Fick's 2nd law [109], were 15.6, 16.5 and 14.1$\times 10^{-11}$ m^2/s for O_1, R_1 and C1 concrete prisms, respectively. The chloride content continuously decreased from the surface of the concrete toward the surface of the rebar in O_1 and C_1 concrete prisms. While, the chloride content at the surface of rebar (45 mm from the surface of the concrete) for these two concretes were almost the same, 0.014% by weight of concrete, this value in the R_1

concrete prism was 0.285% by weight of concrete. The high value of the chloride at the rebar-concrete interface and the downward sharp slope of the chloride diffusion curve in R_1 concrete prism indicate that the NC-RCA concrete was more permeable than NA and OC-RCA concretes. To confirm this issue, the ground concrete prisms were cut and the steel rebars were removed. While the bottom part of the reinforcing steel surface in the R_1 concrete prism, with respect to the cast surface, was corroded (Figure 4-29), no corrosion products were found at the surface of the rebar in NA and OC-RCA concrete prisms.

Figures 4-29, Steel rebar condition in R_1 concrete prism, 380 days after exposure.

The values of the corrosion current density measured by LPR, using Galvapulse and Parstat, and cyclic polarization, using Parstat, techniques were re-calculated with respect to the actual corroded area (about 0.1384 cm^2) of the reinforcing steel in this prism. The values measured by Parstat (222.54 and 1445.08 $\mu A/cm^2$ for potentiostat LPR and cyclic polarization techniques, respectively) and Galvapulse (137.28 $\mu A/cm^2$) were higher, about 136 and 155 times in order of magnitude, respectively, than the average values of

i_{corr} referred to the overall polarized steel surface with respect to the last time of measurements.

Figures 4-30, 4-31 and 4-32, illustrate the surface condition of the O_1, R_1 and C_1 concrete prisms after using the silver nitrate solution as indicator at 380 days after exposure time.

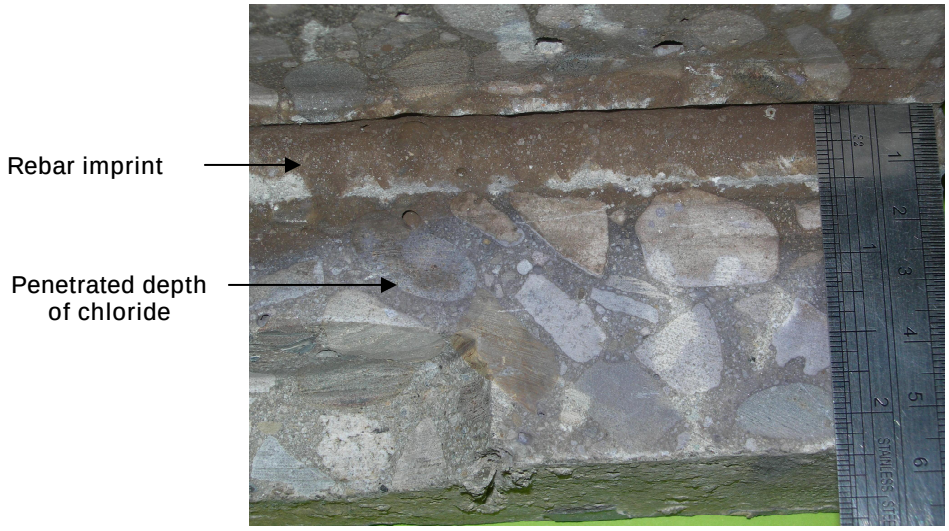

Figure 4-30, The depth of penetrated chloride in NA concrete after 380 days.

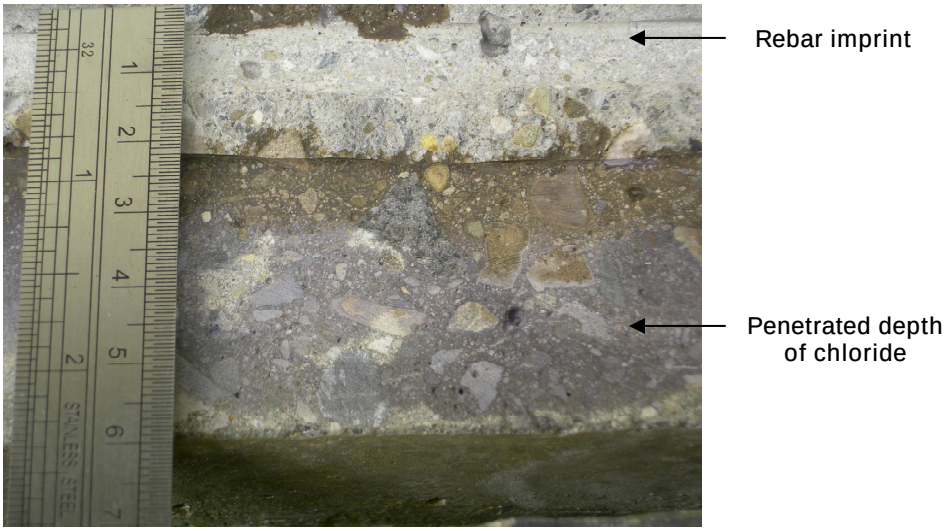

Figure 4-31, The depth of penetrated chloride in NC-RCA concrete after 380 days.

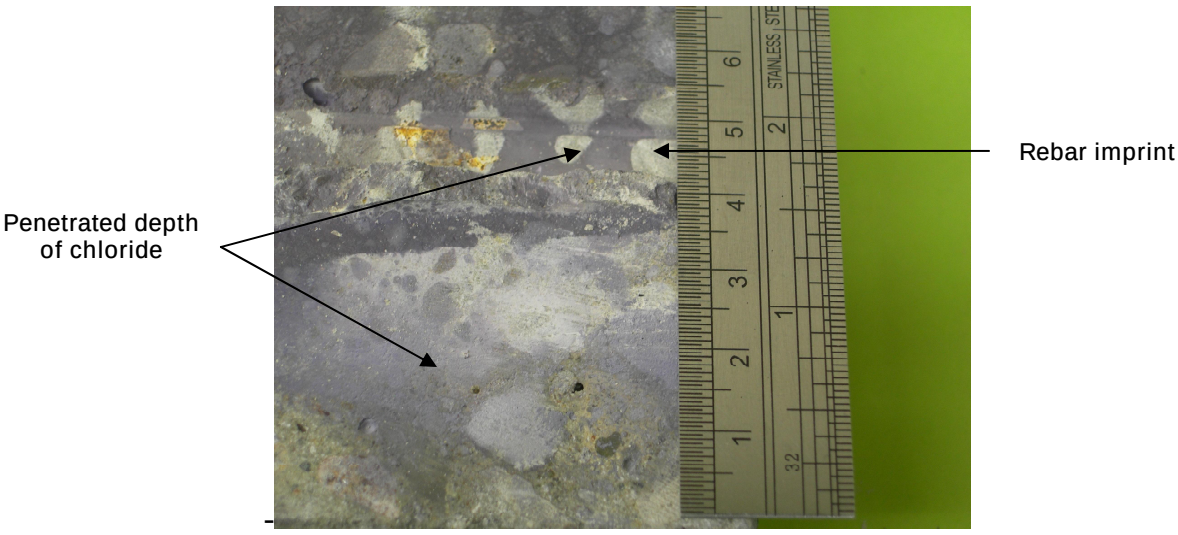

Figure 4-32, The depth of penetrated chloride in OC-RCA concrete after 380 days.

A measurement of the coloured area with respect to the concrete surface showed that the depth of penetrated chloride in O_1 and C_1 concrete prisms was about 40 mm and 25 mm, respectively, while chloride reached to the surface of the steel rebar in R_1 concrete prism after passing through 45 mm concrete cover.

Since the chloride content at the interface with the removed rebar in O_1 and C_1 concrete prisms was about 0.014% by weight of concrete and the surface of the rebars in these two concrete were in a good condition, it can conclude that, the permeability of the OC-RCA concrete was significantly low (and better than the normal concrete) to resist the penetration of chloride and to protect the reinforcing steel from corrosion despite the initial chloride concentration of the aggregate which was 0.023% by weight of concrete.

4.9- Salt scaling test results

Concrete slabs were subjected to 55 freeze-thaw cycles in a chamber in which the air temperature was detected by a temperature sensor and the temperatures of four dummy concrete slabs (the same size as the real concrete slabs used for the salt scaling test) were detected by thermocouple wires embedded in slabs.

The relative humidity of chamber was also checked regularly using a digital Thermometer/ Hygrometer. The variation in temperatures detected by data acquisition system during every 5 cycles of freezing and thawing in Figure 4-33, showed almost a 2 hour concrete temperature phase delay relative to the air temperature in chamber.

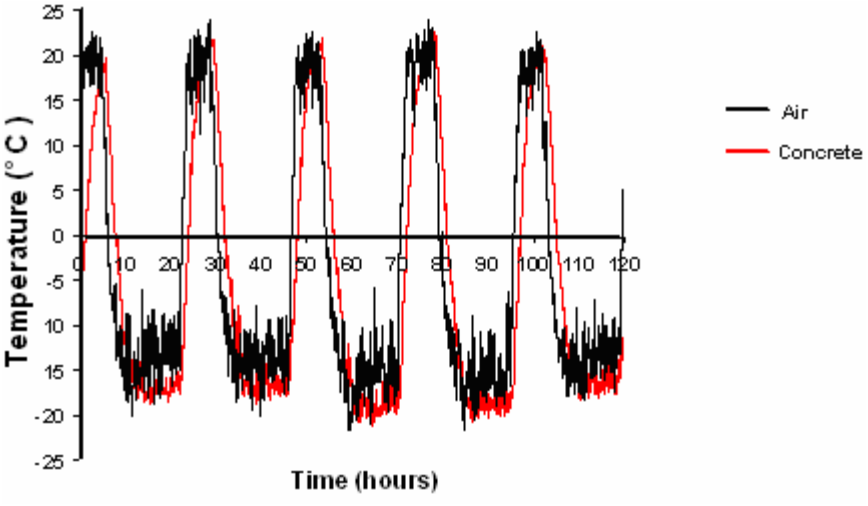

Figure 4-33, The variation of concrete and air temperature during every 5 cycles.

The mass of scaled-off debris was measured after every 5 freezing and thawing cycles and, after applying 55 cycles of freezing and thawing , the scaled concrete slabs were rated visually, according to the ASTM C 672 Standard test method [58], and quantitatively, with respect to MTO LS-412 [101].

In Table 4-4, the categorized visual rating ranges used for the surface scaling of concrete slabs are described. Also, in Figures 4-34, 4-35 and 4-36, the perspectives of the scaled concrete slabs after 55 freezing and thawing cycles are shown. O_1, R_1 and C_1 are representative of NA, NC-RCA and OC-RCA concretes, respectively.

Table 4-4, Visual rating of scaled surfaces, ASTM Standard C 672 [102].

Rating	Condition of surface
0	No scaling
1	Very slight scaling (3mm depth ,max, no coarse aggregate visible)
2	Slight to moderate scaling
3	Moderate scaling (some coarse aggregate visible)
4	Moderate to sever scaling
5	Severe scaling (coarse aggregate visible over entire surface

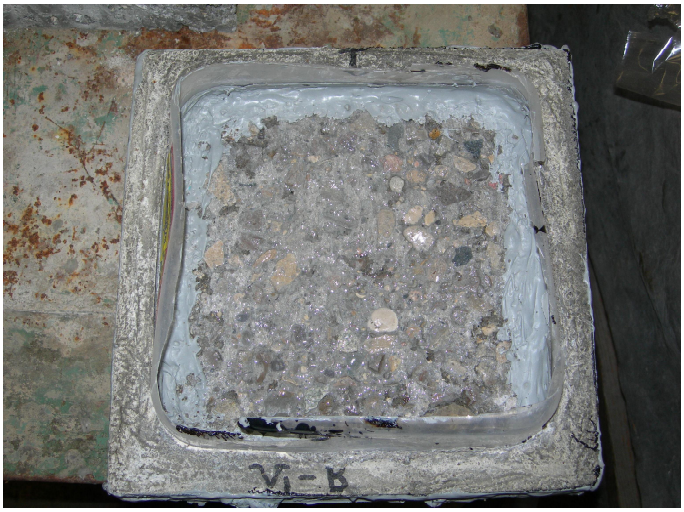

Figure 4-34, O_1 Concrete slab used for salt scaling test after 55 freeze-thaw cycles.

Figure 4-35, R_1 Concrete slab used for salt scaling test after 55 freeze-thaw cycles.

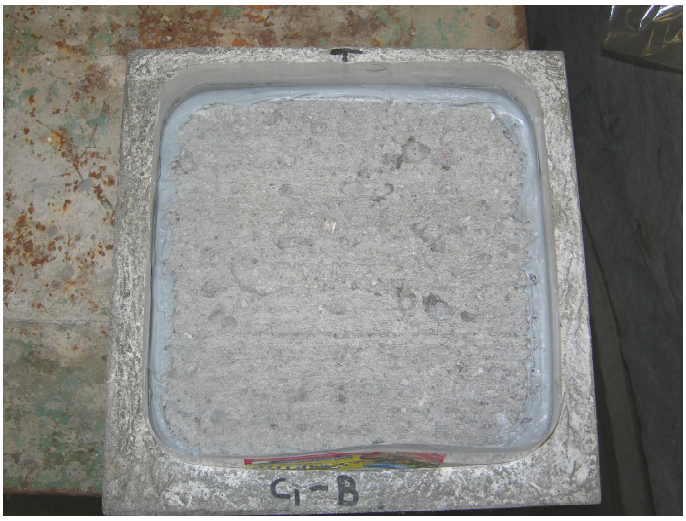

Figure 4-36, C_1 concrete slab used for salt scaling test after 55 freeze-thaw cycles.

Generally, the visual inspection indicated that, while the OC-RCA concrete demonstrated a good scaling resistance performance, the normal and NC-RCA concretes could not resist the 55 freeze-thaw cycles. The surfaces of normal concretes were severely scaled such that most of the aggregates were exposed. Among the NC-RCA concretes, R_1 showed the worst surface resistance performance compared to two other slabs in which the surface scaling was rated between moderate and severe.

According to the MTO Standard [101], concrete is generally resistant to scaling if the cumulative mass of particles does not exceed 0.8 kg/m^2 after at least 50 cycles. This is equal to a loss of 37 grams of scaled mass over the exposed area (0.046 m^2) of the current slabs.

In Table 4-5, the cumulative mass of scaled particles (kg/m^2) and the visual rating damage of concrete slabs went through the salt scaling resistance test are summarized.

Table 4-5, The results of salt scaling resistance test after 55 freeze-thaw cycles.

Concrete types	O_1	O_2	O_3	R_1	R_2	R_3	C_1	C_2	C_3
Weight loss, kg/m^2	2.09	1.43	1.36	4.34	1.72	1.63	0.56	0.42	0.42
Visual rating damage	5	4	4	5	3	3	1	1	1

The variation of cumulative scaled masses for different concretes with the number of freeze-thaw cycles, illustrated in Figure 4-36, indicated an appropriate linear relationship for normal concretes during the first few cycles while the increasing trend of mass loss was quite linear for NC-RCA concretes over the entire 55 cycles. The mass of scaled OC-RCA concretes remained below the acceptance limit 37 grams per exposed area of concrete slab during the test and is, therefore, considered acceptable by both ASTM and MTO Standards.

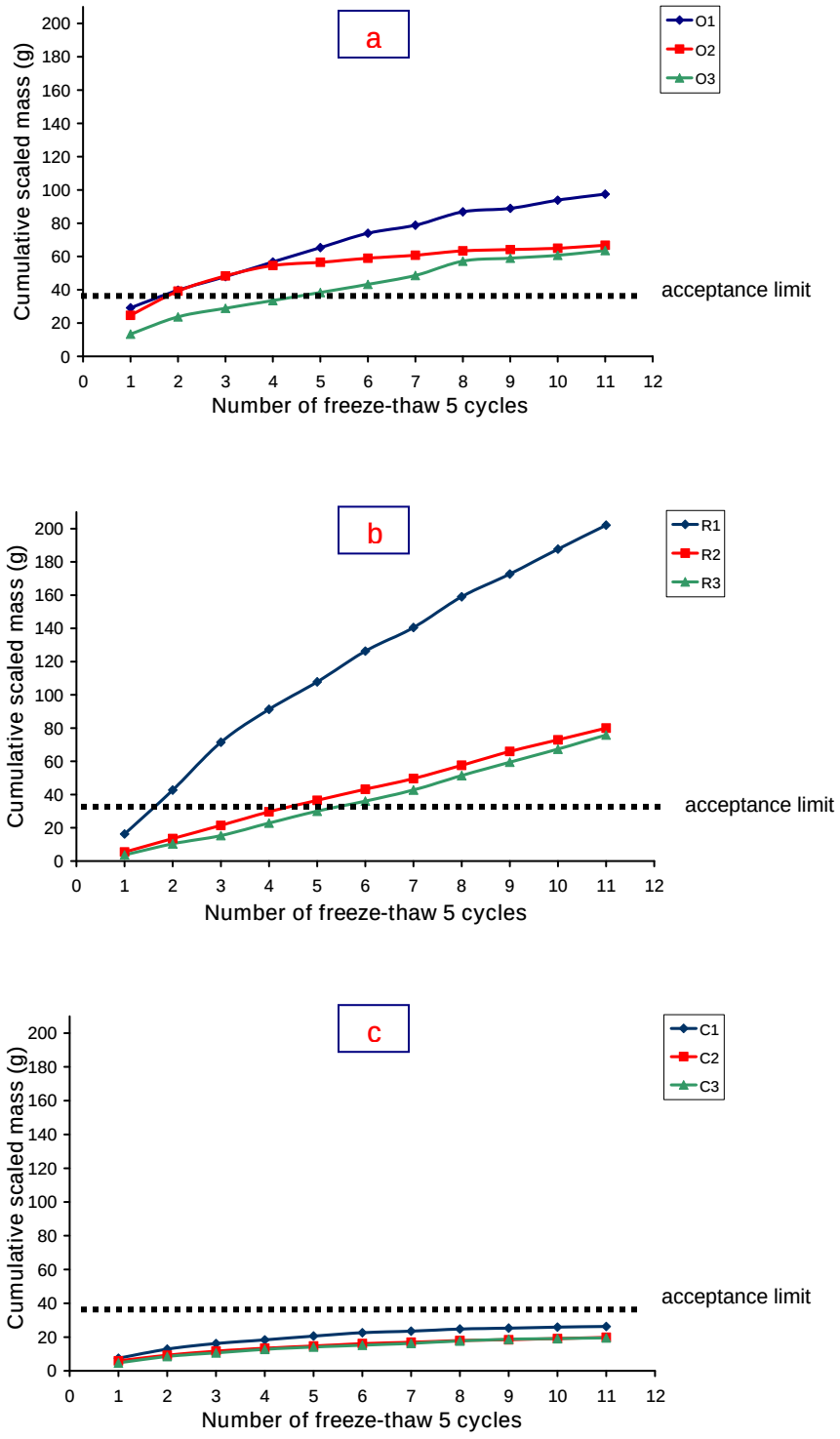

Figure 4-36, Cumulative scaled mass during 55 freeze-thaw cycles for a) NA concrete b) NC-RCA concrete and c) OC-RCA concrete.

Chapter 5

Conclusions and Recommendations

On the basis of the results obtained by a performing a comparative study on physical and mechanical properties such as water and chloride permeability, age, and strength of different aggregates and their influence on reinforced concrete durability, the conclusions and recommendations are expressed as follows.

1. The durability of the RCA concrete is very dependent on the age of the RCA aggregate. Using a very well hardened old recycled concrete as coarse aggregate with 16 mm nominal maximum size accompanying natural sand in structural concrete can be efficient if the properties such as water absorption, chloride permeability, salt scaling and reinforcing steel corrosion resistance of RCA concrete meet the required acceptance limit obtained by the same concrete made with natural aggregate.
2. The strength and the quality of the OC-RCA were competitive enough with those of natural aggregates to be used as an aggregate in structural applications.
3. The microscopy observation indicates that, the presence of a very well hydrated porous adhered mortar in OC-RCA provided better adhesion between old and new cement paste than that of is formed in the NC-RCA and normal concretes.
4. The average of chloride acid-soluble content in OC-RCA was about 0.023 ± 0.009 % by weight of concrete. The diffusion rate of chloride from the old adhered mortar to the new cement paste in 420 day old OC-RCA concrete was such that the chloride content was approximately constant after a few months. The chloride permeability test showed an acceptable range of chloride

penetration during the one year accelerated wet and dry cycle test and did not indicate any effect of the corrosion at the surface of reinforcing steel. It is concluded that, this type of aggregate is safe to use in structural applications.

5. Since the penetration depth of chloride in OC-RCA concrete was less than that of normal concrete, which was very close to the surface of rebar, corrosion measurements and visual inspection of reinforcing steel are recommended to be continued to obtain the exact amount of chloride threshold in these concrete prisms.
6. The OC-RCA concrete exhibited an acceptable scaling resistance performance, while the normal and NC-RCA concretes were failed according to ASTM and MTO Standards.
7. The presence of corrosion products at the surface of the steel rebar in NC-RCA concrete indicated that the permeability of this concrete is not adequate enough to resist the chloride ingress from the external sources such as de-icing salt in reinforced concrete structures. However, NC-RCA, obtained from Dufferin concrete division ready mix yard located in Kitchener, may still be used as road sub-base materials in pavements.
8. Although the amount of adhered mortar in OC-RCA was greater than that of NC-RCA, the water absorption of NC-RCA was more than twice as much as the OC-RCA. This is attributed to the greater porosity and the larger size of pores in the NC-RCA adhered mortar, which was only a few months old and probably had a high water-cement ratio in comparison to OC-RCA that contains a dense and a high strength adhered mortar.

9. The water absorption of NC-RCA concrete was almost as twice as those of normal and OC-RCA concrete. The optical and SEM microscopy observations indicates that weak bonding between aggregate and new mortar and the presence of defects such as cracks in NC-RCA adhered mortar was responsible for low strength and high water absorption of this concrete.
10. A good agreement among the results of concrete electrical resistance, half cell potential and the corrosion current density of the reinforcing steel in normal, NC-RCA and OC-RCA indicates that applying the two of every four weeks wet and dry cycles is an efficient technique for accelerating of the chloride diffusion into reinforced prisms exposed to a saturated de-icing salt solution. The measured values obtained after the dry cycles were more consistent than those of obtained after the wet cycles.
11. The cyclic polarization technique may be used as a complementary technique to LPR for confirmation of corrosion current density and oxygen limitation in concrete specimens. It seems that the accuracy of the values measured by the Galvapulse is more dependent to the parameters that can influence the concrete electrical resistance, such as permeability and moisture content of the concrete, than that of the Parstat device.
12. Reducing the susceptibility to cracking of the interfacial transition zone and healing the cracks in the old adhered mortar by a two-stage mixing approach (TSMA) was an efficient method that showed acceptable results for all types of concretes.

13. The properties such as contamination, permeability and strength of RCA as well as the durability aspects of the RCA concrete should be evaluated before the possible use of these aggregates in structural concrete.
14. To improve the quality of RCA made from the waste/leftover concrete, the ready-mixed plant can minimize the amount of water added to the waste concrete. Adding retarder to the remaining fresh concrete mixture after placing the concrete seems to be efficient for this purpose. Also, it would be beneficial for the waste concrete to be vibrated and consolidated after its discharging from the truck and stored in an indoor environment in the form of concrete slabs or blocks for the further use as aggregate.
15. It is recommended that the air void distribution of the slabs be determined when the equipment becomes available in order to identify the reason for the poor performance of the normal concrete.

References

1. Kuroda, Y., Hashida, H., **A closed-loop concrete system on a construction site**, Proceeding of international symposium on sustainable development of cement, concrete and concrete structures, Toronto, Canada (2005) 371-388
2. Lauritzen, E.K. **Recycling concrete-an overview of challenges and opportunities**, Recycling concrete and other materials for sustainable development, ACI text, SP-219-1, Farmington Hills, Michigan (2004) 1-10
3. Naik, T., R., Moriconi, G., **Environmental-friendly durable concrete made with recycled material for sustainable concrete construction,** Proceeding of international symposium on sustainable development of cement, concrete and concrete structures, Toronto, Canada, (2005) 277-291
4. Kasai, Y., **Recent trends in recycling of concrete waste and use of recycled aggregate concrete**, Recycling concrete and other materials for sustainable development, ACI text, SP-219-2, Farmington Hills, Michigan (2004) 11-34
5. Dosho,Y., **Application of recycled aggregate concrete for structural concrete: a recycling system for concrete waste,** Proceeding of international symposium on sustainable development of cement, concrete and concrete structures, Toronto, Canada, (2005) 459-478
6. Masood, A., Ahmad, T., Arif, M., Mahdi, F. **Waste management strategies for concrete**, ACI Journal, Environment Engineering Policy (2002) 3:15-18
7. Buyle-Bodin, F., Hadjieva-Zaharieva, R., **Influence of industrially produced recycled aggregates on flow properties of concrete**, Materials and Structures, Vol. 35,September- October (2002) 504-509
8. Kosmatka.S.H, Kerkhoff, B., Panarese.W.C, **Design and control of concrete mixtures**, Seventh Canadian edition, Cement Association of Canada (2002) 100-104
9. CSA Standard A23.1, **Concrete Materials and Methods of Concrete Construction/Methods of Test and Standard Practices for Concrete**, 2004
10. Mamlouk,M.S., Zaniewski, J.P., **Materials for civil and construction engineers**, Second edition, Pearson Prentice Hall, New Jersey, 2006
11. Topcu, I.B., Sengel, S., **Properties of concretes produced with waste concrete aggregate**, Cement and concrete research 34 (2004) 1307-1312
12. Ghosh, S., **Recycled aggregate concrete exposed to high temperature**, Proceeding of the international symposium, Dundee, Scotland, UK, September 9-11 (2003) 399-408
13. Hansen, T.D., Narud, H. **Strength of recycled concrete made from crushed concrete coarse aggregate**, Concrete international, Vol.5, No 1,January (1983) 79-83
14. Topcu, I.B., **Physical and mechanical properties of concretes produced with waste concrete**, Cement and concrete research, Vol. 27,No.12 (1997) 1817-1823
15. Topcu, I.B., **Using waste concrete as aggregate**, Cement and concrete research Vol. 25, No. 7 (1995) 1385-1995
16. ACI committee 555-01 Report, **Removal and reuse of hardened concrete**, march (2001) 555R 1-26
17. Gomez-Soberon, J.M.V., **Porosity of recycled concrete with substitution of recycled concrete aggregate**, Cement and Concrete research 32 (2002) 1301-1311

18. Ryu.J.S. **Improvement on strength and impermeability of recycled concrete made from crushed concrete coarse aggregate**, Journal of Materials Science Letters 21 (2002) 1565-1567
19. Padmini, A.K., Ramamurthy, K., Mathews,M.S., **Relative moisture movement through recycled aggregate concrete**, Magazine of concrete research V54 , No.5 (2002) 377-384
20. Poon, C.S., Shi, Z.H., Lam, L. **Effect of Microstructure of ITZ on compressive strength of concrete prepared with recycled aggregate**, Construction and Building Materials (2004) 461-468
21. Mukai, T., Kikuchi, M., and Koizumi, H., **Fundamental study on bond properties between recycled aggregate concrete and steel bars**, Cement Association of Japan (1978).
22. Lin, Y.H. et al, **An assessment of optimal mixture for concrete made with recycled concrete aggregates**, Cement and concrete research 34 (2004) 1373-1380
23. Limbachia,M.C., **Coarse recycled aggregates for use in new concrete**, Proceedings of the institution of civil engineers, Engineering sustainability 157, Issue ES2 , June (2004) 99-106
24. Neville, A.M. **Properties of Concrete**, Third Edition, Longman Scientific and Technical, London, 1990
25. CSA A23.2-29A, **Method of test for the resistance of coarse aggregate to degradation by abrasion in the Micro-Deval apparatus** , 2004
26. AASHTO TP 58-02, **Standard test method for the resistance of coarse aggregate to degradation by abrasion in the Micro-Deval apparatus** (2003)
27. Gilson company Inc., Operation and maintenance manual of MD-2000 Micro-Deval Apparatus, Copyright 2003, Revision 6
28. Personal communication with C.M. Hansson, July 2006
29. Zaharieva, R., Buyle-Bodin, F., Skoczyls, F., Wirquin, E. **Assessment of the surface permeation properties of recycled aggregate concrete**, Cement and Concrete Composites 25 (2003) 223-232
30. Levy, M.S., Helene, P., **Durability of recycled aggregates concrete, safe way to sustainable development**, Cement and Concrete Research 34 (2004) 1975-1980
31. Corinaldesi, V., Moriconi, G., **Durability of recycled-aggregate concrete incorporating high volume of fly ash**, Proceeding of the 9th international conference on " Durability of building materials an components", Brisbane, Queensland, Australia, March 17-20 (2002) paper 71.
32. Sagoe- Crentsil, K.K., Brown,T., Taylor, A.H. **Performance of concrete made with commercially produced coarse recycled concrete aggregate**, Cement and Concrete Research 31 (2001) 707-712
33. Hansen, C.,T, **Recycled concrete aggregate and fly ash produce concrete without Portland cement**, Cement and Concrete Research Vol. 20(1990) 355-356
34. Shayan, A., Xu, A., **Performance and properties of structural concrete made with recycled concrete aggregate**, ACI Materials Journal, September-October (2003) 371-380

35. Sagoe-Crentsil, K.K. et all**, Engineering properties and performance of concrete made with recycled construction aggregates**, Proceeding of national symposium on the use of recycled materials in engineering construction, Sydney, Australia, (1996) 132-135
36. Hansen, C.,T, Narud,H., **Strength of recycled concrete made from crushed concrete coarse aggregate**, The second RILEM State of the art report on recycled aggregates and recycled aggregate concrete, Materials and structure, Vol. 1, No.111, May –June (1986) 201-246
37. Merilet, J.D., Pimenta, P., **Mechanical and physico-chemical properties of concrete produced with coarse and fine recycled concrete aggregates**, Proceeding of third international RILEM symposium on demolition and reuse of concrete and masonry, Odense, Denmark, October 24-27 (1993) 343-353
38. Tavakoli, M., Soroushian, P. **Strength of recycled aggregate concrete made using field-demolished concrete as aggregate**, ACI Materials Journal, March-April (1996) 182-190
39. Shokry, R.M., Abourizk, S., **The properties of recycled concrete**, Concrete international, July (1997) 56-60
40. Katz, A., **Properties of concrete made with recycled aggregate from partially hardened concrete**, Cement and concrete research 33 (2003) 703-711
41. Ajdukiewicz, A., Kliszczewicz, A., **Influence of recycled aggregates on mechanical properties of HS/HPS**, Cement and Concrete Composites 24 (2002) 269-279
42. Ryu, J.S., **An experimental study on the effect of recycled aggregate on concrete properties,** Magazine of Concrete Research 54,No.1 (2002) 7-12
43. Montgomery, D.G., Strugiss, D. **Properties of concrete incorporating recycled concrete aggregate**, Proceeding of national symposium on the use of recycled materials in engineering construction, Sydney, Australia, (1996) 153-156
44. Ravindrarajah, R.S. **Effects of using recycled concrete s aggregate on the engineering properties of concrete**, Proceeding of national symposium on the use of recycled materials in engineering construction, Sydney, Australia, (1996) 147-152
45. Wainwright, P.J., Trevorrow, A., Yu.Y., Wang, Y., **Modifying the performance of concrete made with coarse and fine recycled concrete aggregates,** proceeding of third international RILEM symposium on demolition and reuse of concrete and masonry, Odense, Denmark, October 24-27 (1993) 319-330
46. Katz, A., **Treatments for the improvement of recycled aggregate**, Journal of materials in civil engineering, Vol.16, No.6 (2004) 597- 603
47. Nagataki, S., Gokce, A., Saeki, T., Hisada, M. **Assessment of recycling process induced damage sensitivity of recycled concrete aggregate**, Cement and concrete research 24(2004) 965-971
48. Asce, M.N.O., Miyazato, S.I., Yodsudjai, W. **Influence of recycled aggregate on interfacial transition zone, strength, chloride penetration and carbonation of concrete**, Journal of Materials in Civil Engineering, September-October (2003) 442-451

49. Tam, W.Y.V, Gao, X.F., Tam, C.M., **Microstructure analysis of recycled aggregate concrete produced from two-stage mixing approach**, Cement and concrete research 35 (2005) 1195-1203
50. ACI committee 201.2R-01 Report, **Guide to durable concrete**, September (2000) 201.2R 1-41
51. Speare, P.R., Ben-Othman, B. **Recycled concrete coarse aggregates and their influence on durability**, Concrete 2000; Economic and durable construction through excellence: Proceedings of the international conference held at the University of Dundee, Scotland, UK, September 7-9 (1993) 419-432
52. Salem, M.R., Burdette, E., G., Jackson, M.N., **Resistance to freezing and thawing of recycled concrete**, ACI Materials Journal, May-June (2003) 216-221
53. Barra de Oliviera, M., Vazquez, E., **The influence of retained moisture in aggregates from recycling on the properties of new hardened concrete**, Waste management, vol. 16, No. 1-3 (1996) 113-117
54. Zaharieva, R., Buyle-Bodin, F.,Wirquin, E. **Frost resistance of recycled aggregate concrete**, Cement and Concrete Research 34 (2004) 1927-1932
55. ASTM C 666, **Standard test method for resistance of concrete to rapid freezing and thawing**, published March 1997
56. Gokce, A., Nagataki, S.,Saeki, T., Hisada, M., **Freezing and thawing resistance of air-entrained concrete incorporating recycled coarse aggregate: The role of air content in demolished concrete**, Cement and Concrete Research 34 (2004) 799-806
57. Wang, K., Nelson, E.D., Nixon, A.W., **Damaging effect of de-icing chemicals on concrete materials**, Cement and concrete composites 28 (2006) 173-188
58. ASTM C 672, **Standard test method for scaling resistance of concrete surfaces exposed to de-icing chemicals,** published March 1997
59. Rendell, F., Jauberthine, R., Grantham, M., **Deteriorated concrete inspection and physicochemical analysis**, Thomas Thelford publishing, 2002
60. Gottfredsen, F.R., Thogersen, F., **Recycling of concrete in aggressive Environment,** Demolition and reuse of concrete and masonry , Proceeding of third international RILEM symposium on demolition and reuse of concrete and masonry, Odense, Denmark, 24-27 October (1993) 309-317
61. ACI Committee 222, **Protection of metals in concrete against corrosion (ACI 222R-01)**, American Concrete Institute, Farmington Hills, MI, 2001
62. Hansson, C.M., **Comments on the electrochemical measurements of the rate of the corrosion of steel in concrete**, Cement and concrete research Vol.14, (1984) 574-584
63. Ahmad, S., **Reinforcement corrosion in concrete structures, its monitoring and service life prediction- a review**, Cement and concrete composites, Vol. 25, (2003) 459-471
64. Hootton, R.D., Mesic,T., Beal, D.L., **Sorptivity testing of concrete as an indicator of concrete durability and curing efficiency**, Third Canadian symposium on cement and concrete , Ottawa, Canada, 1993
65. DeSouza, S.J, Hooton, R.D., and Bickley, J.A., **A field test for evaluating high performance concrete covercrete quality**, Canadian Journal of civil engineering vol. 25, 1998

66. Hansson, C.M., Hansson, I.L.H., **Electrochemical extraction of chlorides from concrete , Part 1- A qualitative model of the process**, Cement and concrete research, vol. 23 (1993) 1141-1152
67. Hansson, C.M., Mammoliti, L., Hope, B.B., **Corrosion inhibitors in concrete-Rart1: The principles, Cement and concrete research**, Vol. 28, No. 12 (1998) 1775-1781
68. Andrade, C., **Calculation of chloride diffusion coefficient in concrete from ionic migration measurements**, Cement and concrete research, Vol. 23 (1993) 724-742
69. McGrath, P.F., Hooton, R.D., **Influence of voltage on chloride diffusion coefficient from chloride migration**, Cement and concrete research, Vol. 26, No.8 (1996) 1239-1244
70. Pfeifer, D.W., McDonald, D.B., Krauss, P.D., **The rapid chloride permeability test and its correlation to the 90-day chloride pounding test**, PCI Journal, Vol. 41 (1994) 82-95
71. ASTM C1202, **Standard test method for indication of concrete's ability to resist chloride ion penetration**, published March 1997
72. ASTM C1556, **Standard test method for determining the apparent chloride diffusion coefficient of cementitious mixtures by bulk diffusion**, published February 2003
73. Friedl, L., Volkwein, A., Schiebl, P., **The risk of corrosion of steel in recycled aggregate concrete**, Proceeding of international conference on durability of concrete, Sixth Canmet /ACI, SP-212-65, Greece, (2003) 1055- 1071
74. Tittarelli, F., Moriconi, G., **The effect of fly ash and recycled aggregate on the corrosion resistance of steel in cracked reinforced concrete** , Proceeding of the 9th international conference on " Durability of building materials an components", Brisbane, Queensland, Australia, March 17-20 (2002) paper 70.
75. ASTM C 33, **Standard specification for concrete aggregates**, Published May 1991
76. MTO laboratory testing manual LS-602, Methods of tests for **sieve analysis of aggregates,** Rev. No. 23, Date of latest revision : Feb 2006
77. CSA Standard A23.1, **Clause 12.6.2.2 and table 9**, 2004
78. MTO Material specification for aggregates - concrete, **,** Rev. Date: May 2004 , OPSS 1002
79. CSA A23.2-12A, **Method of test for relative density and absorption of coarse aggregate,** 2004
80. ASTM C127, **Standard test method for specific gravity and absorption of coarse aggregate**, Re-approved date:1993
81. ASTM C114, **Standard test method for chemical analysis of hydraulic cement**, published March 1997
82. ASTM C1152, **Standard test method for acid-soluble chloride in mortar and concrete**, published March 1997
83. Mendoza, A., **Corrosion of reinforcing steel in loaded cracked concretes exposed to de-icing salts**, MA. Sc. Thesis, University of Waterloo, 2003
84. ASTM C39, **Standard test method for compressive strength of cylindrical concrete specimens,** published March 1999

85. CSA A23.2-11C, Method of test for **Water absorption of concrete,** 2004
86. ASTM C 642**, Standard test method for density, absorption, and voids in hardened concrete**, published March 1997
87. Zhang, T., Gjorv, E., O., Effect of chloride source concentration on chloride diffusivity in concrete, ACI Materials Journal, Vol.102, No.5, (2005) 295-298
88. Princeton applied research, **applied instrument group, application note corr 1, basics of corrosion measurements**, pp 1-12
89. Princeton applied research, **applied instrument group, application note corr 4, basics of corrosion measurements**, pp 1-13
90. Kelly, R.G., Scully, J.R., Shoesmith, D.W., Buchheit, R.G., **Electrochemical techniques in corrosion science and engineering,** First Edition, Marcel Dekker Inc., New York, 2003
91. Stearn, M., Geary, A.L., Journal of Electrochemistry Society, Vol 104 (1957) 56-63
92. Andearde, C., Alonso, C., **Corrosion rate monitoring in the laboratory and site,** Construction and building materials, Vol. 10, No.5 (1996) 315-328
93. Andrade, C., Gonzalez, A., **Quantitative measurements of corrosion rate of reinforcing steels embedded in concrete using polarization resistance measurements,** Werkstoffe and Korrosion, Vol 29 (1978) 515-519
94. German instruments A/S., The manual of products, Galvapulse instrument, Catalogue NDT, 2003
95. Montemor, M.F. et al., **Chloride-induced corrosion on reinforcing steel: from the fundamentals to the monitoring techniques**, Cement and concrete composites 25 (2003) 491-502
96. Law, D.W., Millard, S.G., and Bungey, J.H., **Galvanostatic pulse measurements of passive and active reinforcing steel in concrete**, Corrosion, Vol. 56, No. 1, January (2000) 48-56
97. Siverman, D.C., **Primer on the AC impedance technique, Electrochemical techniques for corrosion engineering**, NACE publication, Huston,1986
98. Saremi, M., Mahallati, E., **A study on chloride-induced depassivation of mild steel in simulated concrete pore solution**, Cement and concrete research 32 (2002)1915-1921
99. Otsuki, N. et al , **Evaluation of $AgNO_3$ solution spray method for measurement of chloride penetration into hardened cementitious matrix materials,** ACI Materials Journal, Vol. 89, No.6 (1992) 587-592
100. German instruments, inc. manual book, **Profile grinder PF-1100**, instruction and maintenance manual, PF1113, 2001
101. MTO laboratory testing manual LS-412, **Methods of test for scaling resistance of concrete surfaces exposed to de-icing chemicals,** Rev. No. 23, Date of latest revision : Feb 2006
102. Pigeon, M., Pleau, R., **Durability of concrete in cold climates**, Chapter 4, E & FN SPON, London, 1995
103. Kjellsen, K.O., Monsoy, A., Isachsen, K., Detwiler, R.J., **Preparation of flat-polished specimens for SEM-backscattered electron imaging and X-ray microanalysis- importance of epoxy impregnation**, Cement and concrete research, Vol. 33 (2003) 611-616

104. ASTM C 876, **Standard test method for half-cell potentials of uncoated reinforcing steel in concrete**, published May 1991
105. Novokshchenov, V., **Corrosion surveys of prestressed bridge members using a half-cell potential technique**, Corrosion Vol.53, No.6, June (1997) 489-498
106. Montemor, M.F. et al., **Chloride-induced corrosion on reinforcing steel: from the fundamentals to the monitoring techniques**, Cement and concrete composites 25 (2003) 491-502
107. Sehgal, A., et al., **reproducibility of polarization resistance measurements in steel-in concrete system**, Corrosion vol.48, No. 9, September (1992) 706-714
108. Gonzalez, J.A. et al., **Comparison of rates of general corrosion and maximum pitting penetration on concrete embedded steel reinforcement**, Cement and concrete research, Vol.25, No.2 (1995) 257-264
109. Poulsen, E, **Chloride profiles: analysis and interpretation of observation**, AEC laboratory, Vedbaek, Denmark, 1995

Appendix A

Mix design for the concrete prisms used for corrosion measurements

According to the literature review [8, 9, 16], the average density of concrete made with recycled concrete aggregates was considered 2200 kg/ m^3.

The mass of concrete prisms

The size of each concrete prism was: 0.2 m $\times$ 0.1m $\times$ 0.1m

$\Rightarrow$ Mass of the concrete prism = 2200 kg/ m^3 (concrete density) $\times$ 0.002 m^3
= 4.4 kg

$\Rightarrow$ The total mass of five concrete prisms = 5 $\times$ 4.4 kg
= 22 kg

The mass of concrete cylinders

The volume of each standard concrete cylinder = $(0.05\ m)^2 \times 0.2\ m \times 3.14 = 0.00157\ m^3$

$\Rightarrow$ The mass of each concrete cylinder = 2200 kg/ m^3 (concrete density) $\times$ 0.00157 m^3
= 3.454 kg

$\Rightarrow$ The total mass of five concrete cylinders = 5 $\times$ 3.454 kg
= 17.27 kg

$\Rightarrow$ The total mass of the concrete = 22 kg + 17.27 kg
= 39.27 kg

The mass of concrete constituents

According to the mixture design, the total mass of concrete constituents for 1 M^3 was:

355 kg (Type 10 Portland cement) + 770 kg (sand) + 1070 kg (stone with 19 mm nominal diameter size) + 153 kg (water) = 2348 kg

The mass proportion of each constituent to the total mass of concrete is listed below:

Coarse aggregate, %= $\frac{1070}{2348}$ = 0.456

Sand, %= $\frac{770}{2348}$ = 0.328

Cement, %= $\frac{335}{2348}$ = 0.151

Water, %= $\frac{153}{2348}$ = 0.065

Therefore, the content of each concrete constituent used for mixture should follow the above proportions.

Coarse aggregate mass = 0.456 × 39.27 = 17.907 kg

Coarse aggregates were divided into three different sizes. The mass percentage of each was 10% of 16 mm, 55% of 11.2 mm and 35% of 8.00 mm.

⇒ The mass of each size can be determined as below:

Mass of 16.0 mm coarse aggregates = 17.907 × 0.1= 1.79 kg

Mass of 11.2 mm coarse aggregates =17.907 × 0.55= 9.849 kg

Mass of 8.0 mm coarse aggregates =17.907 × 0.35= 6.268 kg

The mass of other constituents used are:

Sand mass= 0.328× 39.27= 12.88 kg

Cement mass= 0.151×39.27= 5.93 kg

Only the surface moisture content of the aggregate becomes part of the mixing water in concrete and can be determined from the absorbed moisture values (Table 4-1).

The surface moisture content = absorption after immersion - initial moisture content

Where

Absorption after immersion = 100 × (mass of saturated surface-dried aggregates – mass of oven-dried aggregates) / mass of oven-dried aggregates

And

Initial moisture content of aggregates = 100 × (mass of the original aggregates- mass of dried aggregates) / mass of dried aggregates

The total mass of each type of aggregate was 500 gr. Aggregates were graded with the desired proportions mentioned above and dried in oven at 110 ° C for 24 hours.

The mass of dried natural aggregates = 499.38

$\Rightarrow$ The initial moisture content of aggregates, % = $100 \times \frac{(500 - 499.38)}{499.38}$

= 0.12 %

Also 500 grams of dried aggregates were considered for water absorption test and they were immersed in water for 24 hours and the surface moisture of aggregates was removed with a towel and the mass was determined.

The mass of saturated surface-dried natural aggregates = 504.83 g

Absorption after immersion, % =$100 \times \frac{504.830 - 500.00}{500}$ = 0.97 %

$\Rightarrow$ The surface moisture content = absorbed moisture - initial moisture content

= 0.97 - 0.12

= 0.84 %

$\Rightarrow$ The surface moisture content is the required amount of water that should be added to the mix to compensate the water absorption of aggregates.

Thus,

The water content of mixture = (the mass proportion of water $\times$ total mass of concrete) + (the surface moisture content $\times$ Coarse aggregate mass)

The water content should be added to the mixture for concrete made with natural aggregates = (0.0651 $\times$ 39.27) + (0.0084 $\times$ 17.907) = 2.7 litter

The same calculations were applied or concrete made with new clean (NC-RCA) and old contaminated recycled aggregates (OC-RCA):

Total moisture content of NC-RCA, percent = $100 \times \frac{(500 - 488.13)}{488.13}$ = 2.43 %

The mass of saturated surface-dried NC-RCA = 529.08gr

Absorbed moisture content $=100 \times \frac{529.08 - 500.00}{500} = 5.82\%$

$\Rightarrow$ The surface moisture content = absorbed moisture - initial moisture content

$= 5.82 - 2.43$

$= 3.39\%$

$\Rightarrow$ The water content should be added to the mixture for concrete made with NC-RCA =

$(0.0651 \times 39.27) + (0.0339 \times 17.907) = 3.165$ litter

For the concrete made with contaminated recycled aggregates (OC-RCA):

Initial moisture content of OC-RCA , percent $= 100 \times \frac{(500 - 483.50)}{483.50} = 3.41\ \%$

The mass of saturated surface-dried OC-RCA = 509.49gr

Absorbed moisture content $=100 \times \frac{509.49 - 500.00}{500} = 1.90\ \%$

$\Rightarrow$ The surface moisture content = absorbed moisture - initial moisture content

$= 3.41 - 1.90$

$= 1.51\%$

$\Rightarrow$ The water content should be added to the mixture for concrete made with OC-RCA =

$(0.0651 \times 39.27) + (0.01514 \times 17.907) = 2.83$ litter

According to MTO design, the amount of water reducer and air-entrainer for batches were:

Water reducer = 5.93×250 (millilitre) / (100 kg of cement) = 14.82 millilitre

Air entrainer = 5.93×40 (millilitre) / (100 kg of cement) = 2.37 millilitre

All final calculated values for the mixture constituents were multiplied by 1.3 to compensate the probable waste concrete during casting.

Mix design for the concrete slabs used for salt-scaling resistance test

Following the above procedures, the mass of concrete and the qualities of constituents used were:

The mass of concrete slabs and cylinders

The size of each concrete slab was: 0.2667 m $\times$ 0.2667 m $\times$ 0.0762 m

The volume of concrete slabs = 0.2667 m $\times$ 0.2667 m $\times$ 0.0762 m = 0.00542 m^3

$\Rightarrow$ Mass of the concrete slab = 2200 kg/ m^3 $\times$ 0.00542 m^3
= 11.92 kg

3 specimens for each batch were cast.

$\Rightarrow$ The total mass of the concrete slabs = 3 $\times$ 11.92 Kg = 35.77 kg

The volume of each standard concrete cylinder = $(0.05\ m)^2 \times 0.2m \times 3.14 = 0.00157\ m^3$

$\Rightarrow$ The mass of each concrete cylinder = 2200 kg/ m^3 $\times$ 0.00157 m^3 = 3.45 kg

3 concrete cylinders for each batch were cast.

$\Rightarrow$ The total mass of the concrete cylinders = 3 $\times$ 3.45 kg = 10.36 kg

$\Rightarrow$ The total mass of the concrete = 35.77 + 10.36
= 46.13 kg

The mass of concrete constituents

Coarse aggregate mass = 0.456 $\times$ 46.13 = 21.037 kg

Mass of 16.0 mm coarse aggregates = 21.037 $\times$ 0.1= 2.10 kg

Mass of 11.2 mm coarse aggregates = 21.037 $\times$ 0.55 = 11.57 kg

Mass of 8.0 mm coarse aggregates = 21.037 $\times$ 0.35 = 7.36 kg

Sand mass = 0.328 $\times$ 46.13 = 15.1306 kg

Cement mass = 0.151 $\times$ 46.13 = 6.965 kg

The water content should be added to the mixture for concrete made with natural aggregates = (0.0651 × 46.13) + (0.008418 × 21.037) = 3.18 litter

The water content should be added to the mixture for concrete made with NC-RCA = (0.0651 × 46.13) + (0.03386 × 21.037) = 3.716 litter

The water content should be added to the mixture for concrete made with OC-RCA = (0.0651 × 46.13) + (0.01514 × 21.037) = 3.318 litter

Water reducer = 6.965 × 250 (millilitre) / 100 (kg of cement) =17.41 millilitre

Air entrainer = 6.965 × 40 (millilitre) / 100 (kg of cement) = 2.79 millilitre

All final calculated values for the mixture constituents were multiplied by 1.3 to compensate the probable waste concrete during casting.

Appendix B

Density and absorption of coarse aggregates

The mass of different aggregates in various conditions (A, B and C) are listed below:

Where

A = weight of oven-dry test aggregates in air, g

B = weight of saturated-surface-dry test aggregates in air, g

C = weight of saturated-surface-dry test aggregates in water, g

For the natural aggregates:

A= 2991.98 g

B= 3034.37g

A= 1908.42 g

Thus,

Bulk density = $\frac{2991.98}{3034.37-1908.42}$ = 2.66 (kg/m^3)

Bulk density (saturated surface-dry) basis = $\frac{3034.37}{3034.37-1908.42}$ = 2.69 (kg/m^3)

Apparent density = $\frac{2991.98}{2991.98-1908.42}$ =2.76 (kg/m^3)

Absorption, % = $\frac{3034.37-2991.98}{2991.98}$ =1.42 %

For the new clean recycled aggregates:

A= 2939.25 g

B= 3092.85 g

A= 1801.97 g

Thus,

Bulk density = $\frac{2939.25}{3092.85-1801.97}$ = 2.28 (kg/m^3)

Bulk density (saturated surface-dry) basis = $\frac{3092.85}{3092.85-1801.97}$ = 2.40 (kg/m^3)

Apparent density = $\frac{2939.25}{2939.25-1801.97}$ =2.58 (kg/m^3)

Absorption, % = $\frac{3092.85-2939.25}{2939.25}$ = 5.23 %

For the old contaminated recycled aggregate:

A= 2965.25 g
B= 3307.80 g
A= 1858.64 g

Thus,

Bulk density = $\frac{2965.25}{3307.80-1858.64}$ = 2.05 (kg/m^3)

Bulk density (saturated surface-dry) basis = $\frac{3307.80}{3307.80-1858.64}$ = 2.28 (kg/m^3)

Apparent relative density = $\frac{2965.25}{2965.25-1858.64}$ =2.68 (kg/m^3)

Absorption, % = $\frac{3307.80-2965.25}{2965.25}$ = 11.55%

Abrasion resistance of coarse aggregate (Micro-Deval test)

The Micro-Deval abrasion loss for three types of aggregates was determined as below:

% Loss for natural aggregates = $\frac{1500.02-1334.36}{1500.02} \times 100$ = 11.04 %

% Loss for new clean recycled aggregates = $\frac{1500.02-985.76}{1500.02} \times 100$ = 34.28 %

% Loss for old contaminated aggregates = $\frac{1500.06-1341.20}{1500.06} \times 100$ = 10.59 %

Determination of NC-RCA and OC-RCA adhered cement

Both types of aggregates contained 10% of16 mm, 55% of11.2 mm, and 35% of 8mm.

New clean recycled aggregates (NC-RCA):

Original mass of aggregate = 500 g

Dried mass before dissolving = 461.5 g

The mass of residue materials after second drying= 287.9 g

Adhered mortar percent = 100 ×(dried mass before dissolving - the mass of residue materials after second drying) / dried mass before dissolving

$$\Rightarrow \text{Adhered mortar percent of NC-RCA} = \frac{461.5 - 287.9}{461.5} \times 100$$
$$= 37.61\ \%$$

Old contaminated recycled aggregates (OC-RCA):

Original mass of aggregate = 500 g

Dried mass before dissolving = 483.5 g

The mass of residue materials after second drying= 180.76 g

$$\Rightarrow \text{Adhered mortar percent of OC-RCA} = \frac{483.5 - 180.76}{483.5} \times 100$$
$$= 62.61\ \%$$

Density, absorption, and voids in hardened concrete

After following the test procedure, the results were obtained as listed below:

Where

A = mass of oven-dried concrete cylinder in air, g

B = mass of surface-dry concrete cylinder in air after immersion, g

C = mass of surface-dry concrete cylinder in air after immersion and boiling, g

D = apparent mass of concrete cylinder in water after immersion and boiling, g

And, indexes V, R, and C are abbreviated for “concrete cylinder made with virgin, clean recycled and contaminated aggregates”, respectively.

Therefore,

A_v = 3949.10 g
A_R = 3457.82 g
A_C = 3677.67 g

B_v = 4123.00 g
B_R = 3785.71g
B_C = 3865.59 g

C_v = 4128.68 g
C_R = 3804.09 g
C_C = 3873.24 g

D_v = 2436.99 g
D_R = 2113.10 g
D_C = 2203.51 g

Absorption after immersion, (V) %= $\frac{4123.00-3949.10}{3949.10}\times 100 = 4.40$ %

Absorption after immersion, (R) %= $\frac{3785.71-3457.82}{3457.82}\times 100 = 9.48$ %

Absorption after immersion, (C) %= $\frac{3865.59-3677.67}{3677.67}\times 100 = 5.11$ %

Absorption after immersion and boiling, (V) % = $\frac{4128.68-3949.10}{3949.10}\times 100 = 4.55$ %

Absorption after immersion and boiling, (R) % = $\frac{3804.09-3457.82}{3457.82}\times 100 = 10.01$ %

Absorption after immersion and boiling, (C) % = $\frac{3873.24-3677.67}{3677.67}\times 100 = 5.32$ %

Bulk density, dry (V) = $\frac{3.9491}{4.1286-2.4369}\times 100 = 2.33$ (kg/m^3)

Bulk density, dry (R) = $\frac{3.4578}{3.8041-2.1131}\times 100 \times = 2.04$ (kg/m^3)

Bulk density, dry (C) = $\frac{3.6777}{3.8732-2.2035}\times 100 \times 1$(Kg/m^3) = 2.20 (kg/m^3)

Bulk density after immersion (V) = $\frac{4.1230}{4.1286-2.4369}\times 100 = 2.44$ (kg/m^3)

Bulk density after immersion (R) = $\frac{3.7857}{3.8041-2.1131}\times 100$ = 2.24 (kg/m^3)

Bulk density after immersion (C) = $\frac{3.8656}{3.8732-2.2035}\times 100$ = 2.31 (kg/m^3)

Bulk density after immersion and boiling (V) = $\frac{4.1286}{4.1286-2.4369}\times 100$ = 2.44 (kg/m^3)

Bulk density after immersion and boiling (R) = $\frac{3.8041}{3.8041-2.1131}\times 100$ = 2.25 (kg/m^3)

Bulk density after immersion and boiling (C) = $\frac{3.8732}{3.8732-2.2035}\times 100$ = 2.32 (kg/m^3)

Apparent density (V) = $\frac{3.9491}{3.9491-2.4369}$ =2.62 (kg/m^3)

Apparent density (R) = $\frac{3.4578}{3.4578-2.1131}$ = 2.57 (kg/m^3)

Apparent density (C) = $\frac{3.6776}{3.6776-2.2035}$ = 2.49 (kg/m^3)

Volume of permeable pore space (V), %= $\frac{4.1286-3.9491}{4.1286-2.4369}\times 100$ =10.62 %

Volume of permeable pore space (R), %= $\frac{3.8040-3.4578}{3.8040-2.1131}\times 100$ =20.47 %

Volume of permeable pore space (C), %= $\frac{3.8732-3.6776}{3.8732-2.2035}\times 100$ = 11.71 %

Appendix C

Potentiostatic LPR curves using Parstat technique

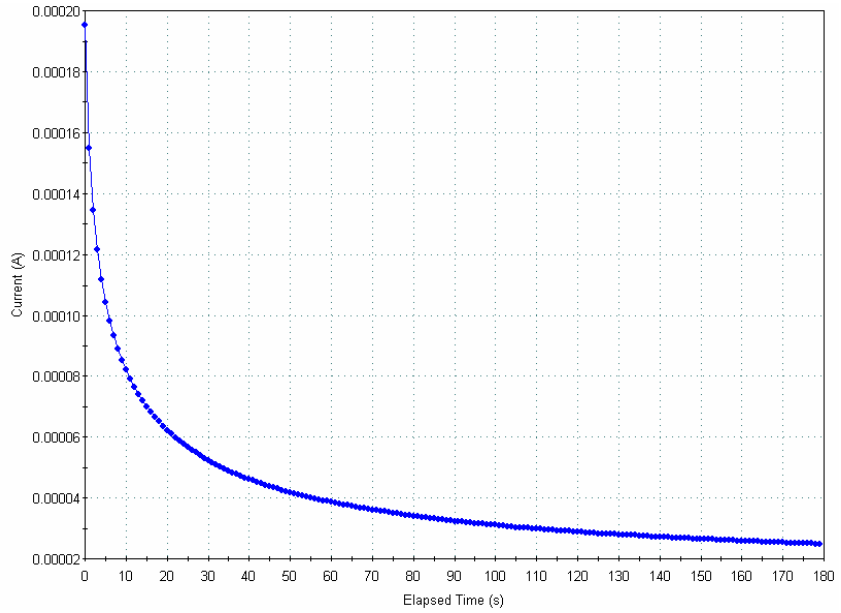

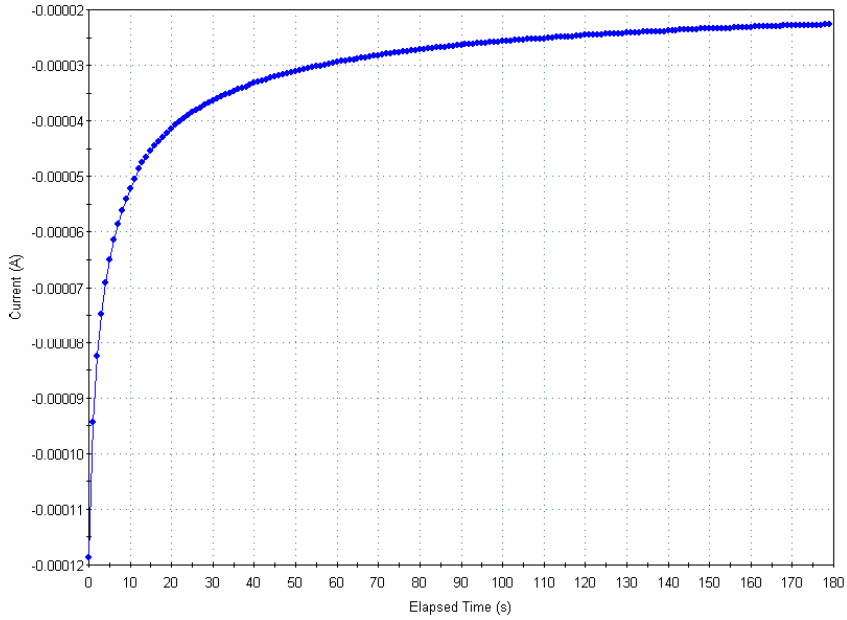

Cyclic polarization curves for O_1, R_1 and C_1 at different times

- before the beginning of the exposure the concrete prisms in saturated salt solution

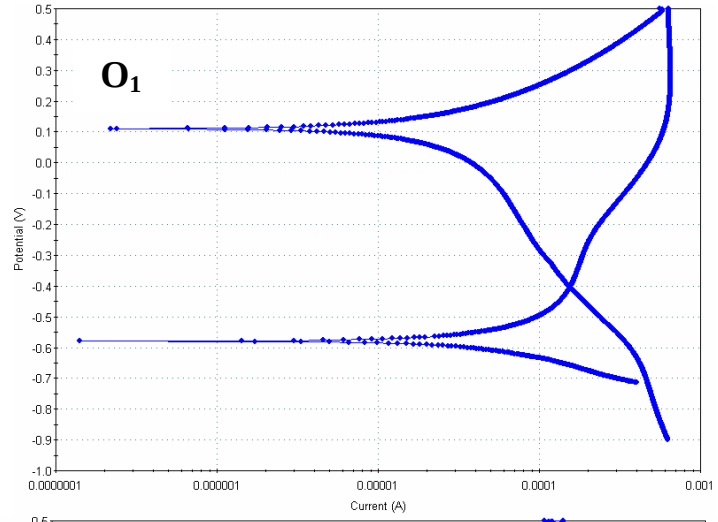

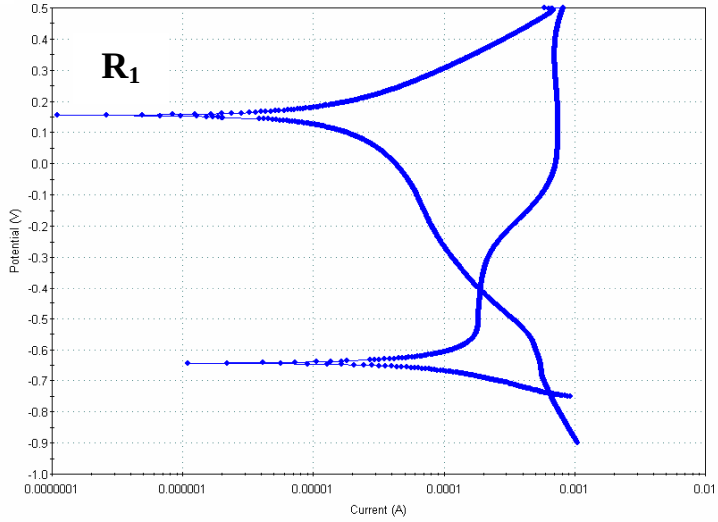

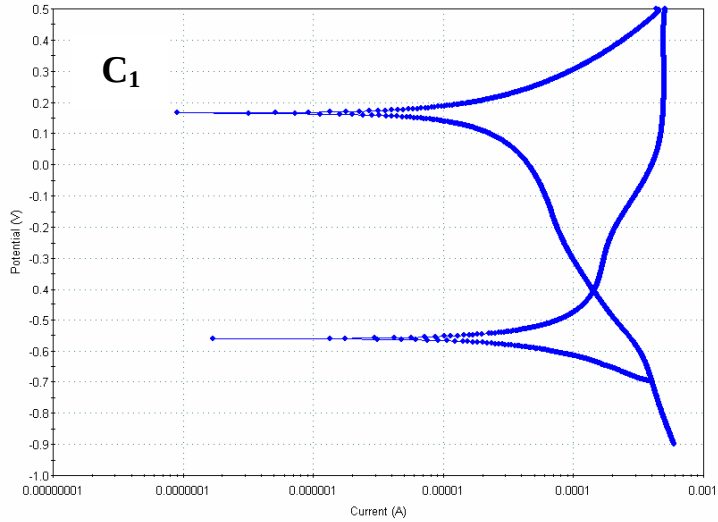

- 290 days after exposure the concrete prisms in saturated salt solution

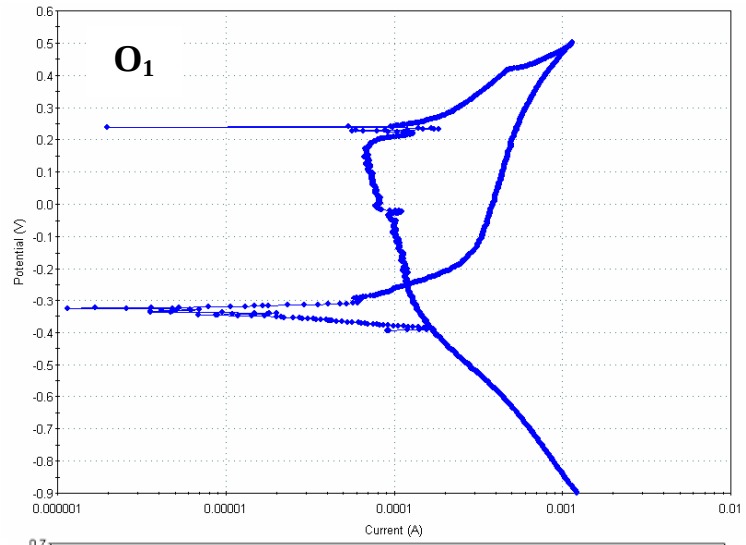

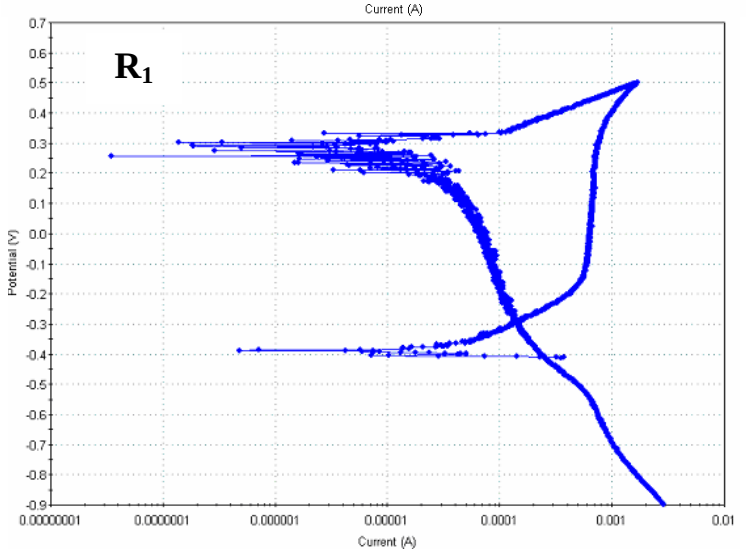

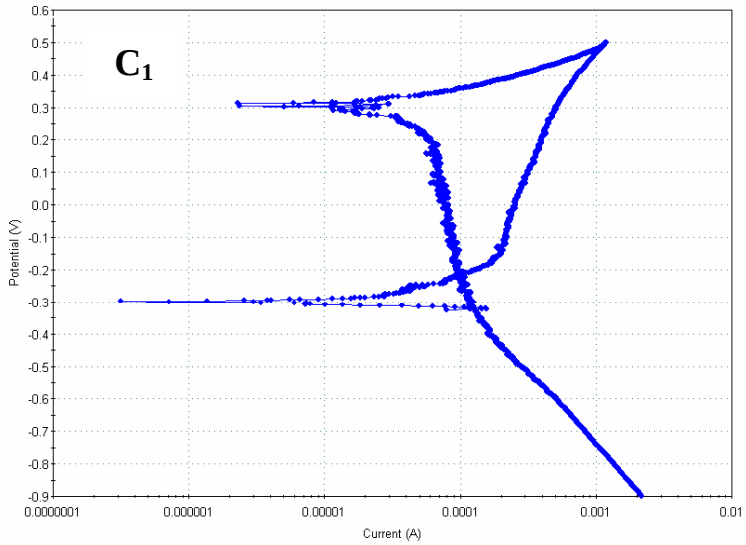

- 335 days after exposure the concrete prisms in saturated salt solution

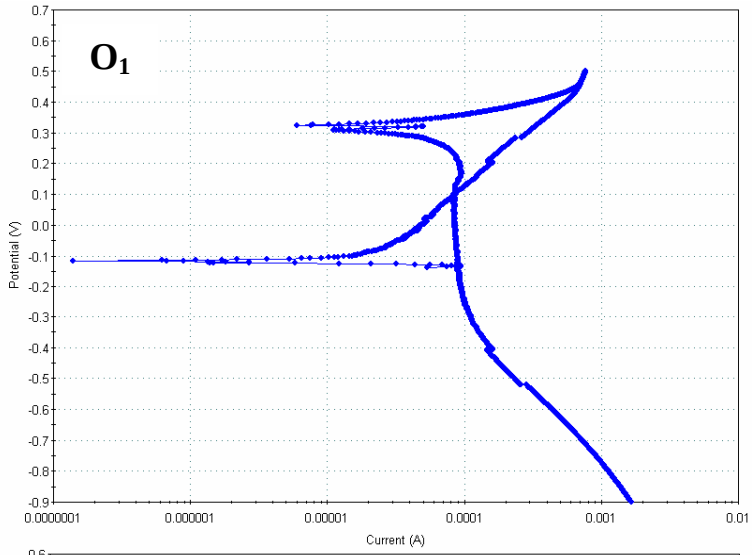

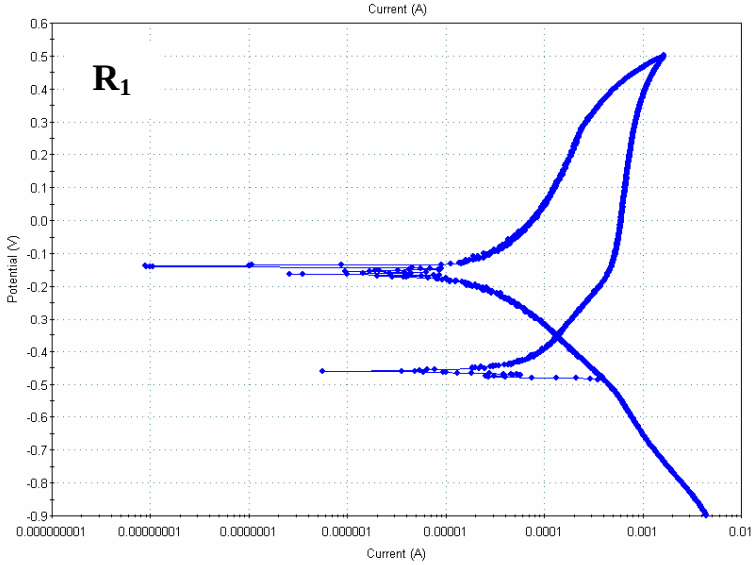

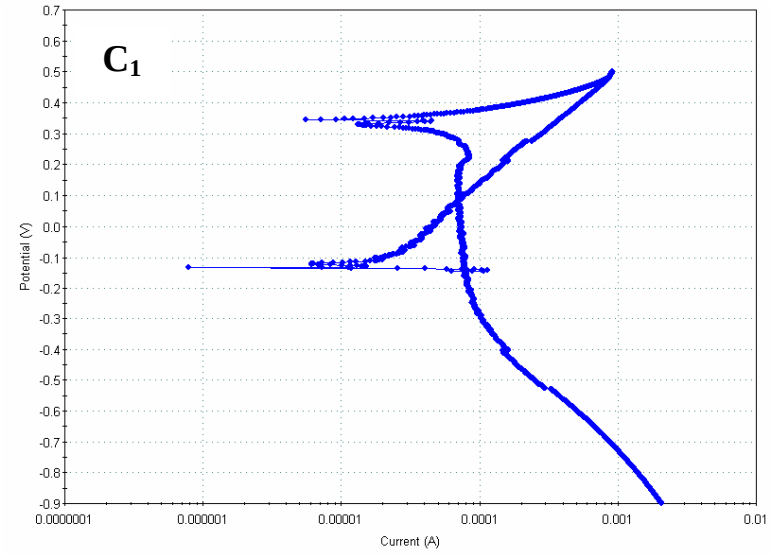

- 380 days after exposure the concrete prisms in saturated salt solution